

**PONTIFÍCIA UNIVERSIDADE CATÓLICA DO PARANÁ**

**CAMILA FERNANDES HIGA**

**SELECTIVE LASER SINTERING OF COPPER-NICKEL AND  
MOLYBDENUM ALLOY TO BE USED AS EDM ELECTRODES**

**MESTRADO EM  
ENGENHARIA MECÂNICA  
PUCPR**

**CURITIBA  
AGOSTO – 2011**

**PONTIFÍCIA UNIVERSIDADE CATÓLICA DO PARANÁ**

**CAMILA FERNANDES HIGA**

**SELECTIVE LASER SINTERING OF COPPER-NICKEL AND  
MOLYBDENUM ALLOY TO BE USED AS EDM ELECTRODES**

Dissertation submitted to the Mechanical Engineering Graduate Program at Pontifical Catholic University of Paraná in partial fulfillment of the Master's Degree.

**Academic Advisor: Prof. Dr. Eng. Fred Lacerda Amorim**

**Academic Co-Advisor: Prof. Dr.-Ing. Irionson A. Bassani**

**CURITIBA**

**AUGUST – 2011**

# **TERMO DE APROVAÇÃO**

**CAMILA FERNANDES HIGA**

## **Selective Laser Sintering of Copper-Nickel and Molybdenum Alloy to be used as EDM Electrodes**

Dissertação aprovada como requisito parcial para obtenção do grau de Mestre no Curso de Mestrado em Engenharia Mecânica, Programa de Pós-Graduação em Engenharia Mecânica, do Centro de Ciências Exatas e de Tecnologia da Pontifícia Universidade Católica do Paraná, pela seguinte banca examinadora:

**Dr.-Ing. Guenter Schaefer**

Technische Universität Clausthal (TU Clausthal)  
Fritz-Süchting-Institut für Maschinenwesen – IMW

**Prof. Dr.-Ing. Walter L. Weingaertner**

Departamento de Engenharia Mecânica (UFSC)

**Prof. Dr.-Ing. Irionson A. Bassani**

Curso de Engenharia Mecânica (PUCPR)

Presidente: **Prof. Dr.Eng. Fred L. Amorim (Orientador)**

Curso de Engenharia Mecânica (PUCPR)

Curitiba, 25 de agosto de 2011

## **TERM OF APPROVAL**

**CAMILA FERNANDES HIGA**

### **Selective Laser Sintering of Copper-Nickel and Molybdenum Alloy to be used as EDM Electrodes**

Dissertation approved as a partial requirement to obtain the Master's Degree in the Master's Course in Mechanical Engineering, in Mechanical Engineering Graduate Program, Center of Exact Sciences and Technology at Pontifical Catholic University of Paraná, by the following examiners:

**Dr.-Ing. Guenter Schaefer**

Technische Universität Clausthal (TU Clausthal)  
Fritz-Süchting-Institut für Maschinenwesen – IMW

**Prof. Dr.-Ing. Walter L. Weingaertner**

Department of Mechanical Engineering (UFSC)

**Prof. Dr.-Ing. Irionson A. Bassani**

Department of Mechanical Engineering (PUCPR)

President: **Prof. Dr.Eng. Fred L. Amorim (Academic Advisor)**

Department of Mechanical Engineering (PUCPR)

Curitiba, August 25<sup>th</sup>, 2011

*This dissertation is dedicated to my family,  
who always supported me in my decisions.*

## ACKNOWLEDGEMENTS

I would like to thank all the people who helped to make this work happen. Thanks to Prof. Fred Amorim and Prof. Irionson Bassani for the help, suggestions and for the opportunity to study abroad. Thanks to Prof. Dr.-Ing. Armin Lohrengel, Dr.-Ing. Günter Schäfer and Prof. Dr.-Ing. Norbert Müller at the Institute of Mechanical Engineering in Germany.

Thanks to Dipl.-Ing. Eric Siemann for all the help during my stay in Germany. Special thanks to Mateus Noronha and Tiago Czelusniak for all the brainstorming, for the help in the experiments and in the characterization tests.

Thanks to Prof. Dr. Volkmar Neubert and his crew at the Institute for materials testing and materials engineering – Dr. Neubert GmbH; to Dipl. –Ing. Joern Fiedler at the Center for Functional Materials; to Dipl.-Phys. Uwe Kahnert at the Institute of Nonmetallic Materials and to Dipl.-Ing. Christian Heet at the Institute of Welding and Machining.

And finally, thanks to CAPES (Coordenação de Aperfeiçoamento de Pessoal de Nível Superior) for the financial support.

## SUMMARY

<b>LIST OF FIGURES</b>	viii
<b>LIST OF TABLES</b>	x
<b>NOMENCLATURE</b>	xi
<b>ABBREVIATIONS</b>	xii
<b>ABSTRACT</b>	xiii
<b>RESUMO</b>	xiv
<b>1 INTRODUCTION.....</b>	<b>1</b>
1.1 OBJECTIVES .....	5
<b>2 ELECTRICAL DISCHARGE MACHINING (EDM).....</b>	<b>6</b>
2.1 INTRODUCTION .....	6
2.2 DIE SINKING EDM AND WIRE EDM.....	8
<b>3 RAPID PROTOTYPING .....</b>	<b>11</b>
3.1 INTRODUCTION .....	11
3.2 RAPID PROTOTYPING APPLICATIONS .....	14
3.2.1 Prototyping .....	14
3.2.2 Rapid Manufacturing .....	14
3.2.3 Rapid Tooling .....	15
3.3 FUNDAMENTALS OF RAPID PROTOTYPING PROCESS.....	16
3.4 SELECTIVE LASER SINTERING (SLS).....	18
3.4.1 Physical Aspects in SLS .....	22
3.4.2 Indirect and Direct Laser Sintering.....	25

3.4.3	Materials used in the Selective Laser Sintering Process.....	27
3.4.4	Factors that influence the Selective Laser Sintering Process.....	27
<b>4</b>	<b>PRODUCTION OF EDM ELECTRODES WITH RP TECHNIQUES .....</b>	<b>33</b>
4.1	MANUFACTURE OF EDM ELECTRODES BY INDIRECT METHODS.....	33
4.2	MANUFACTURE OF EDM ELECTRODES BY DIRECT METHODS .....	36
<b>5</b>	<b>COMMONLY USED MATERIALS FOR EDM ELECTRODES .....</b>	<b>40</b>
5.1	INTRODUCTION .....	40
5.2	BRASS .....	42
5.3	COPPER .....	42
5.4	GRAPHITE .....	43
5.5	COPPER GRAPHITE .....	46
5.6	TELLURIUM-COPPER .....	46
5.7	TUNGSTEN.....	47
5.8	COPPER TUNGSTEN.....	47
5.9	TUNGSTEN CARBIDE .....	48
5.10	SILVER.....	48
5.11	SILVER TUNGSTEN .....	48
5.12	ZINC ALLOYS .....	49
<b>6</b>	<b>SELECTED MATERIALS FOR EDM ELECTRODES.....</b>	<b>50</b>
6.1	INTRODUCTION .....	50
6.2	COPPER-NICKEL .....	51
6.3	MOLYBDENUM.....	52
<b>7</b>	<b>EXPERIMENTAL PROCEDURE .....</b>	<b>54</b>

7.1 MATERIALS .....	54
7.1.1 Powder characteristics .....	55
a) Copper-nickel metal matrix .....	55
b) Molybdenum .....	57
7.2 EQUIPMENT USED IN THE EXPERIMENTS.....	58
7.3 EXPERIMENTAL FLOWCHART.....	58
7.3.1 Influence of the layer thickness on the porosity .....	60
7.3.2 Influence of the laser scan speed on the porosity .....	60
7.3.3 Influence of the hatch distance on the porosity .....	61
7.3.4 Influence of the amount of nickel on the porosity .....	62
7.3.5 Influence of the amount of molybdenum on the porosity .....	62
7.4 CHARACTERIZATION OF THE SINTERED PARTS.....	63
<b>8 RESULTS AND DISCUSSION.....</b>	<b>64</b>
8.1 INFLUENCE OF THE LAYER THICKNESS ON THE POROSITY .....	64
8.2 INFLUENCE OF THE LASER SCAN SPEED ON THE POROSITY.....	66
8.3 INFLUENCE OF THE HATCH DISTANCE ON THE POROSITY.....	70
8.4 SLS PARTS BUILT TO BE USED AS EDM ELECTRODES .....	76
8.5 INFLUENCE OF THE AMOUNT OF MOLYBDENUM ON THE POROSITY .....	78
8.6 INFLUENCE OF THE AMOUNT OF NICKEL ON THE POROSITY .....	82
<b>9 CONCLUSIONS.....</b>	<b>89</b>
9.1 DIRECTIONS FOR FUTURE RESEARCH .....	90
<b>10 REFERENCES .....</b>	<b>92</b>
<b>APPENDIX 1. SELECTIVE LASER SINTERING MACHINE.....</b>	<b>99</b>

## LIST OF FIGURES

Figure 2.1. Concept of EDM (KUNIEDA <i>et al.</i> , 2005).....	6
Figure 2.2. Wire electrical discharge machining (WEDM) (KUNIEDA <i>et al.</i> , 2005).....	9
Figure 2.3. Die Sinking Electrical Discharge Machining (AgieCharmilles).....	9
Figure 3.1. Parts manufactured by RP in the Institute of Mechanical Engineering at TU Clausthal, Germany: a) Selective Laser Sintering (SLS) technique, b) Fused Deposition Modeling (FDM) technique.....	12
Figure 3.2a. Schematic representation of an SLS equipment (KARAPATIS; GRIETHUYSEN; GLARDON, 1998).....	19
Figure 3.2b. Construction process in SLS: 1 – coater, 2 – blade or wiper, 3 – overflow, 4 – support of the building platform, 5 – building platform, 6 – metering platform, A – layer thickness, B – reduction of the metering platform (EOS RP-Tools, 1998).....	21
Figure 3.3. Mechanism of Liquid Phase Sintering (KRUTH <i>et al.</i> , 2005).....	23
Figure 7.1. SEM image of the Cu(90)Ni(10) metal matrix powder: a) Magnification 200x, b) Magnification 500x.....	55
Figure 7.2. Particle size distribution of the Cu(90)Ni(10) powder.....	56
Figure 7.3. Particle size distribution of the Cu(70)Ni(30) powder.....	56
Figure 7.4. SEM image of the molybdenum powder: a) Magnification 1000x, b) Magnification 4000x.....	57
Figure 7.5. SEM image of the Mo 63 wt.% - Cu(90)Ni(10) 37 wt.% powder: a) Magnification 200x, b) Magnification 1000x.....	57
Figure 7.6. Experimental flowchart developed for the SLS experiments.....	59
Figure 7.7. Laser scanning strategy (EOS RP-Tools, 1998).....	60
Figure 8.1. SLS parts after the layer thickness experiments.....	64
Figure 8.2. Micrographs of the SLS parts after the layer thickness experiments (the black spaces represent the pores): a) 250 mm/s, b) 150 mm/s, c) 50 mm/s. Magnification 3,2x.....	65
Figure 8.3. SLS parts produced with laser scan speed of: a) 300, 250, 200 mm/s, b) 150, 100, 50 mm/s.....	67
Figure 8.4. Micrographs of the SLS parts after the laser scan speed experiments (the black spaces represent the pores): a) 300 mm/s, b) 250 mm/s, c) 200 mm/s, d) 150 mm/s, e) 100 mm/s, f) 50 mm/s. Magnification 3,2x.....	69
Figure 8.5. Influence of the laser scan speed on porosity.....	69
Figure 8.6. SLS parts after the hatch distance experiments.....	70

Figure 8.7. Micrographs of the SLS parts after the hatch distance experiments (the black spaces represent the pores): a) 0,4 mm, b) 0,3 mm, c) 0,2 mm, d) 0,1 mm. Magnification 3,2x.....	72
Figure 8.8. Influence of the hatch distance on porosity.....	73
Figure 8.9. Stereomicroscope images of the top of the parts after the hatch distance experiments: a) 0,1 mm, b) 0,2 mm, c) 0,4 mm.....	74
Figure 8.10. Optical micrographs of Mo 63 wt.% - Cu(90)Ni(10) 37 wt.% mixture laser sintered part with the optimized SLS parameters: a) 12,5x, b) 25x, c) 50x.....	75
Figure 8.11. SEM images of the top surface of the laser sintered part with the optimized SLS parameters: a) Magnification 40x, b) Magnification 200x, c) and d) Magnification 800x.....	76
Figure 8.12. SLS parts for EDM experiments.....	77
Figure 8.13. Estimated and measured porosities after the hatch distance experiments.....	77
Figure 8.14. SLS parts: a) Mo 43,3 wt.% - Cu(90)Ni(10) 56,7 wt.% mixture, b) Mo 82 wt.% - Cu(90)Ni(10) 18 wt.% mixture.....	78
Figure 8.15. Micrograph of the SLS parts: a) Mo 43,3 wt.% - Cu(90)Ni(10) 56,7 wt.% mixture, b) Mo 63 wt.% - Cu(90)Ni(10) 37 wt.% mixture, c) Mo 82 wt.% - Cu(90)Ni(10) 18 wt.% mixture. Magnification 3,2x.....	79
Figure 8.16. Influence of the Mo content on porosity.....	80
Figure 8.17. Optical micrographs of Mo 43,3 wt.% - Cu(90)Ni(10) 56,7 wt.% mixture laser sintered part: a) 12,5x, b) 25x, c) 50x.....	81
Figure 8.18. Optical micrographs of Mo 82 wt.% - Cu(90)Ni(10) 18 wt.% mixture laser sintered part: a) 12,5x, b) 25x, c) 50x.....	82
Figure 8.19. SLS parts: a) Mo 63 wt.% - Cu(100) 37 wt.% mixture, b) Mo 63 wt.% - Cu(70)Ni(30) 37 wt.% mixture.....	83
Figure 8.20. Micrograph of the SLS parts: a) Mo 63 wt.% - Cu(100) 37 wt.% mixture, b) Mo 63 wt.% - Cu(90)Ni(10) 37 wt.% mixture, c) Mo 63 wt.% - Cu(70)Ni(30) 37 wt.% mixture. Magnification 3,2x.....	84
Figure 8.21. Influence of the Ni content on porosity.....	84
Figure 8.22. Optical micrographs of Mo 63 wt.% - Cu(100) 37 wt.% mixture laser sintered part: a) 12,5x, b) 25x, c) 50x.....	85
Figure 8.23. Optical micrographs of Mo 63 wt.% - Cu(70)Ni(30) 37 wt.% mixture laser sintered part: a) 12,5x, b) 25x, c) 50x.....	86

## LIST OF TABLES

Table 3.1. Brief description of RP systems.....	13
Table 5.1. Physical properties of some EDM electrode materials (MatWeb).....	41
Table 6.1. Properties of copper and nickel (MatWeb).....	51
Table 6.2. Properties of molybdenum (MatWeb).....	52
Table 7.1. SLS parameters – layer thickness experiments.....	60
Table 7.2. SLS parameters – laser scan speed experiments.....	61
Table 7.3. SLS parameters – hatch distance experiments.....	61

## NOMENCLATURE

Greek Letter:

$\tau$  - duty factor ( $\tau = t_i / t_p$ )

## ABBREVIATIONS

3D - 3-dimensional

3DP - 3D Printing

CAD - Computer-aided design

CNC - Computer Numeric Control

DMLS - Direct Metal Laser Sintering

EDM - Electrical Discharge Machining

EOS - Electro Optical Systems

FDM - Fused Deposition Modeling

LOM - Laminated Object Manufacturing

LPS - Liquid Phase Sintering

RM - Rapid Manufacturing

RP - Rapid Prototyping

RT - Rapid Tooling

SEM - Scanning Electron Microscope

SLA - Stereolithography

SLS - Selective Laser Sintering

## ABSTRACT

This research work carried out an investigation on adequate materials to produce EDM electrodes by Selective Laser Sintering and on the influence of layer thickness, laser scan speed and hatch distance, as well as metallic matrix composition and percentage of structural material in the mixture, on the porosity of laser sintered parts. Pre-alloyed copper-nickel powder material was mixed with molybdenum powder in a specific amount prior to laser sintering. The experiments were performed in a SLS machine EOSINT M 250 X<sup>tended</sup> with a 200 W CO<sub>2</sub> laser and carried out manually. Photo micrographs of the cross-section of all parts were taken with the aid of an optical microscope. It can be said that the porosity decreased with the decreasing of layer thickness and laser scan speed and that increasing the hatch distance, a more porous part was observed. The porosity increased with the increase of the amount of Mo in the mixture and there was an improvement in porosity with the increase of the amount of Ni in the Cu-Ni alloy. It was concluded that the SLS process parameters have a great influence on the densification process and that an adequate combination can produce parts with good quality. The amount of each material in the mixture has a significant influence on the sintered density as well. The energy delivered to the powder bed was enough for liquid phase sintering; still, it was not enough for the melting and connection of all Cu-Ni particles.

*Keywords:* Selective Laser Sintering, EDM electrode.

## RESUMO

Esse trabalho de pesquisa investigou materiais adequados para a produção de eletrodos para Eletroerosão através da Sinterização Seletiva a Laser (SLS) e a influência da espessura de camada, velocidade do laser e distância entre duas linhas de laser consecutivas, assim como a composição da matriz metálica e quantidade de material estrutural na mistura, na porosidade das peças sinterizadas a laser. O pó da pré-liga de cobre-níquel foi misturado com o pó de molibdênio em uma quantidade específica antes da sinterização. Os experimentos foram realizados manualmente na máquina de SLS EOSINT M 250 X<sup>tended</sup> com laser CO<sub>2</sub> de 200 W. Micrografias da seção transversal de todas as peças foram feitas com o auxílio de um microscópio óptico. Pode-se dizer que a porosidade diminuiu com a diminuição da espessura de camada e velocidade do laser e que aumentando a distância entre duas linhas de laser consecutivas, uma peça mais porosa foi observada. A porosidade aumentou com o aumento da quantidade de molibdênio na mistura e houve uma melhora na porosidade com o aumento da quantidade de níquel na pré-liga de cobre-níquel. Concluiu-se que os parâmetros de processo de SLS têm grande influência no processo de densificação e que uma combinação adequada pode produzir peças com boa qualidade. A quantidade de cada material na mistura tem uma influência significativa na densidade também. A energia fornecida às camadas de pó foi suficiente para a sinterização por fase líquida; entretanto, não foi suficiente para a fusão e união de todas as partículas de cobre-níquel Cu-Ni.

*Palavras-chave:* Sinterização Seletiva a Laser, Eletrodo para Eletroerosão.

## CHAPTER 1

### INTRODUCTION

Electrical Discharge Machining (EDM) is one of the most widely used non-conventional material removal processes for the manufacture of complex or hard material parts that are difficult to machine by conventional machining processes, as reported by Kechagias *et al.* (2008). EDM makes use of electrical energy to remove material. Electrical energy is turned into thermal energy through a series of discrete electrical discharges occurring between the electrode and the workpiece immersed in a dielectric fluid.

Because EDM uses thermal energy to machine electrically conductive material parts, the process does not depend on the geometry or hardness of the parts. This has been its distinctive advantage in the manufacture of mold, die, automotive, aerospace and surgical components. In addition, there is no direct contact between the electrode and the workpiece eliminating mechanical stresses, chatter and vibration problems during machining, as stated by Ho & Newman (2003).

Any material demonstrating good electrical conductivity can be used as electrode for EDM. Arthur; Dickens & Cobb (1996) reminded that, traditionally, electrodes have been manufactured from metallic materials including various alloys of copper, tungsten, brass, and also nonmetallic materials (generally graphites). The conventional methods of producing the electrode profiles include stamping, coining, grinding, extrusion/drawing and, more commonly, turning/milling.

The EDM scene has changed dramatically within the last three decades. Speed and finish have all improved at a dramatic rate, making EDM a competitor for production machining where accuracy and finish are vital. Expanding from a targeted portion of the industry to conventional manufacturing, these new capabilities have allowed EDM to cover areas of conductive material machining and beyond, including materials as diverse as ceramics. With the development of newer and more exotic materials with complicated shapes, the limitations of conventional CNC high-speed machining is being

reached at a quicker pace opening the way for non-conventional machining such as EDM (DIMLA; HOPKINSON; ROTHE, 2004).

Electrical-discharge machining (EDM) is used extensively to produce cavities in hardened tool steel for moulding plastics. It is regarded as an essential facility in today's tool room, as die sinking and wire cutting apparatus (ARTHUR; DICKENS; COBB, 1996).

The production of injection mould tool cavities can be a lengthy and time-consuming process. Longer lead-time during the mould making stage can delay the launch of product and can affect the product market. Machining complex features in die and moulds requires multiple electrodes of specific geometry, which are run in sequential order to obtain the desired cavities. This is because of the difficulty in machining large complex electrode profiles. The demand from end users, for a reduction in both lead time and cost has become an important driving force for research (RENNIE; BOCKING; BENNETT, 2001, MEENA; NAGAHANUMAIAH, 2006).

In addition, the reduction in the size of some components is a recent trend. Thus the manufacturing of micro parts is becoming very important. Due to the high precision and good surface quality that it can provide, EDM is potentially an important process for the fabrication of micro-tools, micro-components and parts with micro-features (PHAM *et al.*, 2004). However, the manufacturing of small and micro-EDM electrodes by conventional machining has become even more expensive and time consuming.

Typically, the EDM cycle can account for 25-40% of the tool-room lead time in die and mold production. The major cost and time spent in EDM is electrode production, which can account for over 50% of the total machining costs, as indicated by Arthur; Dickens & Cobb (1996 apud SEMON, 1975). The cost and time of manufacturing electrodes is generally determined by the complexity of the geometry and the accuracy required.

In addition, recently Ozgedik & Cogun (2006) stated that in most of the EDM operations, the contribution of the tool cost to the total operation cost is more than 70%. The cost of a part manufactured by the EDM method is determined mainly by the tool cost, which consists of the raw material cost of the tool, the tool production cost and the number of tools required for operation.

An accurate method of manufacturing electrodes quickly with minimum manual intervention would offer great potential for reducing lead times and tooling costs.

The emerging Rapid Prototyping (RP) technology provides the possibility of the direct fabrication of EDM electrodes from three-dimensional CAD models, especially for complex geometry, to reduce the lead time and processing cost, as stated by Tang *et al.* (2002). RP is a generic term for the generation of 3D models of components directly from a 3D CAD design. The CAD design of the parts is first sliced by software into many thin layers. These layers are then used as templates to build a solid model, layer-by-layer until the object is built.

The first developed RP techniques were mainly used for the production of prototypes in order to make easy the visualization of a product concept. However, RP has evolved to Rapid Tooling (RT), which is the concept of producing tools through the aid of RP. According to Meena & Nagahanumaiah (2006), in recent years, application of RP based techniques for EDM electrode manufacturing has shown promising potential for reducing lead time and minimizing the number of electrodes required for machining of complex cavities.

The production of EDM electrodes is one modern development in the field of the RT. Nowadays, RT represents the most important application of RP. However, according to Dürr; Pilz & Eleser (1999), the difficulty consists of manufacturing a convenient EDM tool with the appropriate material properties.

Tay & Haider (2001) pointed out that the Direct Metal Laser Sintering (DMLS) technique, which is a type of Selective Laser Sintering (SLS), a widely established RP process, could be employed for rapid production of EDM electrodes. DMLS is one of the promising RP techniques that allow manufacturers to produce prototype and production tools directly from metal powders without the use of a polymer binder. During the DMLS process, part of the powder material is melted while other parts remain solid. The material that melts, with low melting point, is called the binder, while the high melting point material is called the structural material.

An electrode made with a material that has high electrical and thermal conductivities, high melting point and low thermal expansion would provide a good combination of properties for use in an EDM process. However, in the case of this work,

the material must be chosen in a suitable way that makes them feasible for both EDM and SLS processes.

Pre-alloyed Cu-Ni and molybdenum powder materials were selected. Copper is usually used as an EDM electrode material for its good electrical and thermal conductivities. However, it has some disadvantages, for instance, it has low melting point which can cause high wear rate in relation to its material removal. Molybdenum is a refractory metal with good thermal conductivity and low thermal expansion coefficient. The mixture of molybdenum and copper would combine properties that are required for good SLS and EDM performances. The addition of nickel was adopted to improve the densification during the SLS process.

Kechagias *et al.* (2008) stated that, since EDM is one of the most extensively used non-conventional material removal processes and RP technology has become well documented, many attempts have been made to manufacture RT electrodes for roughing, semi-roughing and finishing EDM applications. The unlimited theoretical possibilities that RP techniques have in producing complex parts, promote them as the ideal alternative for low cost EDM electrode manufacture rather than multi axis CNC milling which currently exists.

The next chapter presents the Electrical Discharge Machining process. Chapter 3 discusses about Rapid Prototyping and Selective Laser Sintering, which is the RP technique chosen for this project. Previous experimental studies regarding the fabrication of EDM electrodes by different RP techniques are presented in chapter 4. Chapter 5 shows a review on the commonly materials used as EDM electrodes. In chapter 6 the selected materials for EDM electrodes are discussed. Chapter 7 presents the experimental procedure and chapter 8 the results and discussion. Finally, conclusions and directions for future research are found in chapter 9.

## 1.1 OBJECTIVES

This research work is part of the project “Production of EDM Electrodes by Layer Manufacturing Technique (LMT)”, which is into the main focus of BRAGECRIM Program (Brazilian – German Collaborative Research Initiative on Manufacturing Technology), between the Pontifícia Universidade Católica do Paraná – PUCPR and the *Technische Universitaet Clausthal* - TU Clausthal. The main goal of the project is to develop and to improve technologies to produce precision electrodes for Electro Discharge Machining process (EDM) by Layer Manufacturing Techniques (LMT) to machine molding tools and products with complex shapes. The expected outputs of this project include:

- Electrode performance correlating EDMachining and LMT variables;
- The specification of adequate materials and post-processing (e.g. coatings) for EDM electrodes;
- The development of EDM technology tables and procedures for design and fabrication of precision electrodes and an envelope with adequate process EDM parameters settings;
- A real industrial application of a particular electrode geometry;
- EDM procedure to produce complex workpieces of small size.

As part of that project, the main goal of this research work is to investigate the production of EDM electrodes of simple geometry via the Selective Laser Sintering (SLS) technique or, more specifically, the Direct Metal Laser Sintering (DMLS), using the molybdenum and the pre-alloyed copper-nickel powders.

The specific goals can be summarized as follows:

- Determine procedures for fabrication of electrodes, varying the main SLS process parameters: layer thickness, laser scan speed and hatch distance;
- Analyze the influence of the SLS parameters on the porosity of the manufactured parts;
- Analyze different material systems in the SLS process, i.e. different material proportions;
- Analyze the material behavior on the SLS process.

## CHAPTER 2

### ELECTRICAL DISCHARGE MACHINING (EDM)

As stated by Kechagias *et al.* (2008), Electrical Discharge Machining (EDM) is one of the most widely used non-conventional material removal processes for the manufacture of complex or hard material parts that are difficult to machine by conventional machining processes. An introduction to the EDM process is presented in this chapter. A brief description of wire EDM and die sinking EDM are shown as well.

#### 2.1 INTRODUCTION

Electrical Discharge Machining (EDM) is a non-conventional machining process where the material removal process makes use of electrical energy to erode electrically conductive materials. Electrical energy is turned into thermal energy through a series of electrical discharges occurring between an electrode and a workpiece immersed in a dielectric fluid (Figure 2.1). The electrode does not make physical contact with the workpiece for material removal. If the electrode contacts the workpiece, sparking will stop and no material will be removed.

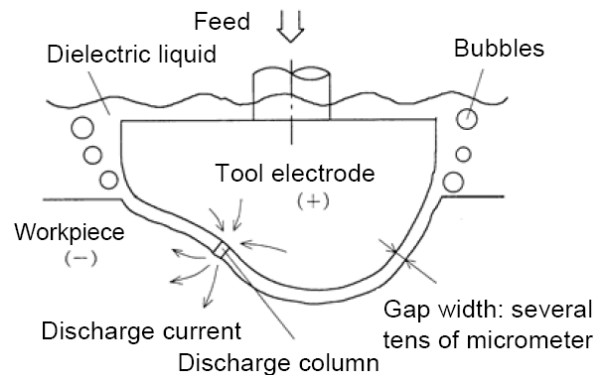


Figure 2.1. Concept of EDM (KUNIEDA *et al.*, 2005).

According to Ho & Newman (2003) EDM is a well-established machining option for manufacturing geometrically complex or hard material parts that are extremely difficult-to-machine by conventional machining processes. Kunieda *et al.* (2005) stated that, since the tool electrode does not need to rotate for material removal like milling or grinding, holes with sharp corners and irregular contours can be machined without difficulty. Reaction forces generated in the EDM gap are insignificant, which also facilitates the machining of thin and flexible parts. Generally, machining accuracy of EDM is very high in the order of several micrometers. On the other hand, the material removal rate of EDM is low compared to other machining processes. Hence EDM is mostly used in die and mold making, where complicated shapes in hard materials and with high precision have to be machined.

EDM has the advantage of allowing tool steel to be treated to full hardness before machining, avoiding the problems of dimensional variability which are characteristic of post treatment. Typically this variability is generally attributed to metallurgical change on quenching to room temperature. Complex geometries or profiles can often be more easily machined on an electrode than in a cavity, making EDM viable in terms of lead time and quality of cut. Many simple geometries such as cubes, spheres and corners with small radii can also be more easily machined by EDM in hardened steel than by conventional material removal techniques (ARTHUR; DICKENS; COBB, 1996).

It is widely applied in hard materials to produce three dimensional details with complex geometrical shapes. According to Amorim; Landiosi & Bassani (2009), the EDM products usually include injection molding tools and forming dies, aerospace prototypes and electronic components, as well as very accurate micro components at any electrical conductive material.

Although EDM is widely used in die and mold making, EDM gap phenomena, which occur between the electrode and the workpiece as shown in Figure 2.1, are very complex and hence not yet fully understood. Electrical discharge phenomena in EDM occur over a very short time period, in a very narrow space filled with liquid, and involve evaporation and melting of the electrodes, thus making both observation and theoretical analysis extremely difficult (KUNIEDA *et al.*, 2005). This confirms what was stated by DiBitonto *et al.* (1989), i.e., since the development of the process of EDM in 1944,

considerable theoretical and experimental research has been performed to identify the basic physical process involved. Although thermal conduction and melting are understood to be dominant mechanisms for electrode erosion, the physics of the plasma bubble is not well understood.

Nowadays the thermoelectric phenomenon is the best supported theory where the material removal in electrical discharge machining is associated with the erosive effect produced when spatially and discrete discharges occur between two electrical conductive materials. Sparks of short duration, ranging from 0,1 to approximately 4.000  $\mu\text{s}$ , are generated in a liquid dielectric gap separating tool and workpiece electrodes. The electrical energy released by the generator is responsible to melt a small quantity of material of both electrodes by conduction heat transfer. Subsequently, at the end of the pulse duration a pause time begins and the melted pools are removed by forces which can be of electric, hydrodynamic and thermodynamic nature (AMORIM; WEINGAERTNER, 2002).

## 2.2 DIE SINKING EDM AND WIRE EDM

The two main types of EDM machines are Wire EDM and Die Sinking EDM.

In Wire EDM complicated shapes can be cut using a wire electrode which is usually a plain brass wire or coated wires, such as zinc coated brass or coated steel wires. Since wire orientation can be changed by controlling the horizontal position of the upper wire guide relative to the lower guide, all types of ruled surfaces can be cut (Figure 2.2). In WEDM, water is most often used as the dielectric liquid (KUNIEDA *et al.*, 2005). Some erosion of the wire is allowable, but high erosion results in wire breakage, the dominant practical and economic problem in WEDM operation (DIBITONTO *et al.*, 1989).

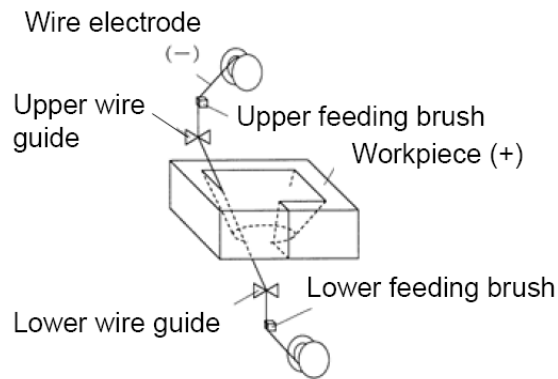


Figure 2.2. Wire electrical discharge machining (WEDM) (KUNIEDA *et al.*, 2005).

In Die Sinking EDM the electrode produces its image on the workpiece. The workpiece can be formed, either by replication of a shaped tool electrode, or by 3D movement of a simple electrode like in milling or a combination of the above (Figure 2.3). The electrode material is normally copper or graphite. The numerical control monitors the gap conditions (voltage and current) and synchronously controls the different axes and the pulse generator. The dielectric liquid, usually a hydrocarbon, is filtrated to remove debris particles and decomposition products (KUNIEDA *et al.*, 2005).

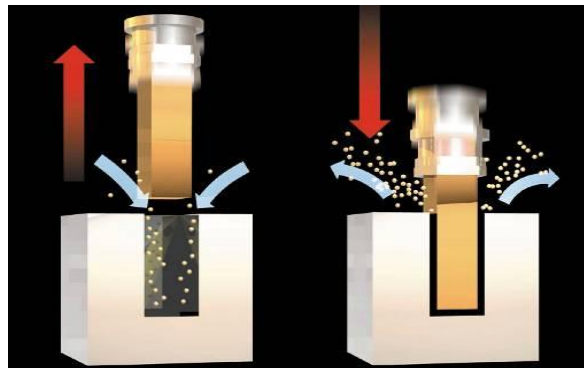


Figure 2.3. Die Sinking Electrical Discharge Machining (AgieCharmilles).

According to Kunieda *et al.* (2005), to obtain stable conditions in EDM, it is essential for the next pulse discharge to occur at a spot distanced sufficiently far from the previous discharge location. Such a spot may be the place where the gap is small or contaminated with debris particles.

When the dielectric strength of the liquid in the gap is exceeded, breakdown occurs and initiates a plasma channel which develops and expands during the following spark on time. In order to prevent arcing between electrodes, the gap, which depends on the power level, is controlled and secured by a servo mechanism (EUBANK *et al.*, 1993).

The interval time between pulse discharges must be long enough so that the plasma generated by the previous discharge can be deionized and the dielectric breakdown strength around the previous discharge location can be recovered by the time the next pulse voltage is applied. Otherwise discharges occur at the same location for every pulse, resulting in thermal overheating and a non uniform erosion of the workpiece (KUNIEDA *et al.*, 2005).

In the EDM process, both the electrode and the workpiece are simultaneously eroded. The aim is to minimize the electrode wear and to maximize the material removal rate with satisfactory surface smoothness.

The interrelationship among the different process parameters is the main factor that contributes to the overall EDM efficiency, regarding the three most important machining characteristics: material removal rate, surface integrity and electrode wear. Besides the appropriate choice of electrical parameters, other parameters have important effects on the EDM results like the polarity of the electrodes, the type and flushing condition, the thermophysical properties of electrode/workpiece materials. According to Amorim & Weingaertner (2002), another EDM variable strictly associated to the electrical parameters and that influences on the machining characteristics is the duty factor  $\tau$ .

A considerable asymmetry in the electrode and the workpiece material removal can be obtained by choosing adequate electrode materials and EDM parameters through experiments.

## CHAPTER 3

### RAPID PROTOTYPING

In this chapter an introduction to the Rapid Prototyping (RP) technology is presented. The RP applications (prototyping, rapid manufacturing and rapid tooling) are briefly described. It is also described the general process for producing rapid prototypes which includes five steps, namely 3D modeling, data conversion and transmission, checking and preparing, building and finally post processing. An introduction to the Selective Laser Sintering (SLS) technique is also presented as well as the indirect and direct laser sintering, materials used in the SLS process and finally the factors that influence the SLS process.

#### 3.1 INTRODUCTION

Rapid prototyping (RP) is the technology that refers to the layer-by-layer fabrication of three-dimensional physical models directly from a computer-aided design (CAD) system. It is a material adding process, in contrast to conventional methods that remove material and, according to Dolenc (1994), the term RP is normally reserved for the technologies that build parts by adding material instead of removing it. The additive approach starts from nothing and builds an object incrementally by adding material.

Charles Hull developed the first RP process in 1986 with the technique called Stereolithography: it builds objects by curing thin consecutive slices of certain ultraviolet light-sensitive liquid resins with a low-power laser. Cooper (2001) reminded that this concept of layer additive construction has been used by various institutions in many different ways, which all have collectively been termed RP. The main advantage of building a part on a layer-by-layer basis is that it makes possible to build complex shapes like intricate internal structures, parts inside of parts and very thin-wall features, as can be seen in Fig 3.1.

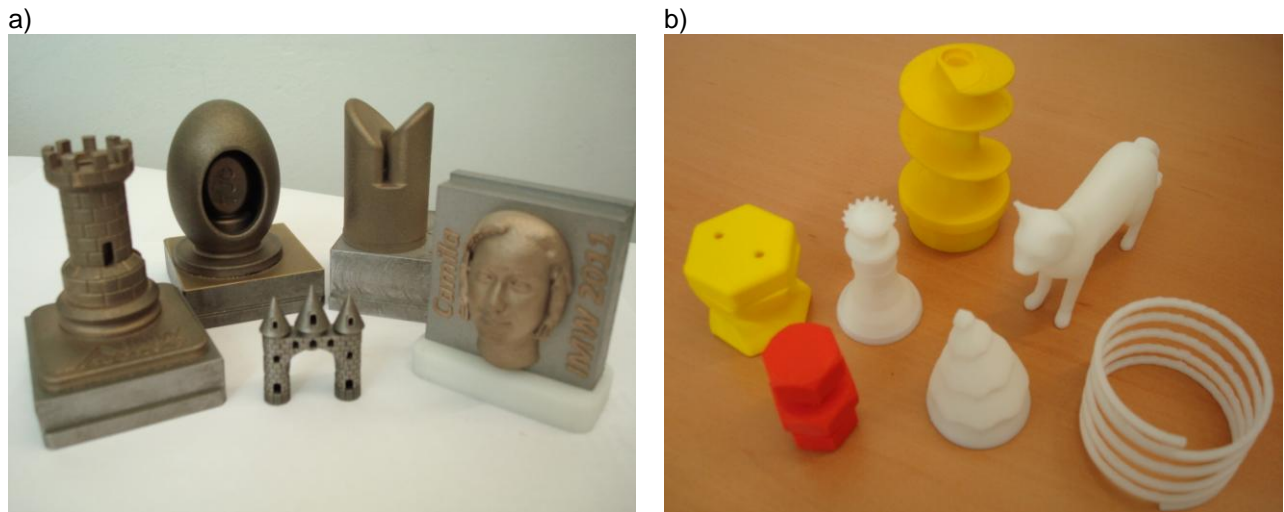


Figure 3.1. Parts manufactured by RP in the Institute of Mechanical Engineering at TU Clausthal, Germany: a) Selective Laser Sintering (SLS) technique, b) Fused Deposition Modeling (FDM) technique.

“Rapid” is a relative term, it can be applied to processes that build prototypes overnight or to those that take a week or more, depending on the size and complexity of the prototype (GRIMM, 2004).

The RP technology decreases the amount of operation time required by humans to build parts. The RP machines, once started, usually run unattended until the part is complete. This comes after the operator spends a small amount of time setting up the control program. Afterwards, some form of clean up operation is usually necessary, generally referred to as post processing. Nonetheless, the user intervention times still remain far less than that for traditional machining processes as stated by Cooper (2001).

Chua; Leong & Lim (2003) reported that maybe because RP is a new technology, a large number of terms is used by the engineering communities around the world. Usually the most used term is Rapid Prototyping, due to its rapid creation of a physical model. A group of terms emphasizes on the unique characteristic of RP – layer-by-layer addition. This group includes Layer Manufacturing, Material Deposit Manufacturing and Material Addition Manufacturing. Another group includes Solid Freeform Manufacturing and Solid Freeform Fabrication. It emphasizes on the words “solid” because while the initial state may be liquid, powder, individual pellets or laminates, the end result is a solid, 3D object and “freeform” because of the ability of RP to build complex shapes with little restriction on its form.

Rapid Prototyping techniques can be classified in three categories according to the initial state of the raw material used. Thus, all RP systems can be classified as liquid-based, solid-based or powder-based (CHUA; LEONG; LIM, 2003).

Liquid-based RP systems have the initial form of its material in liquid state. The liquid is converted into the solid state through a process commonly known as curing. Except for powder, solid-based RP systems include all forms of material in the solid state. In this context, the solid form can include the shape in the form of a wire, a roll, laminates and pellets. In a strict sense, powder is mostly in the solid state. However, it is intentionally created as a category outside the solid-based RP systems to mean powder in grain-like form.

According to Rosochowski & Matuszak (2000) the most popular RP systems in industrial use today are described in Table 3.1.

Table 3.1. Brief description of RP systems.

Stereolithography (SLA)	A method based on photo-polymerization of liquid monomer resin. The surface layer of the resin is cured selectively by the laser beam following the path defined in the slicing model. After this layer has been created, the movable platform is lowered into the vat, a new thin layer of liquid monomer floods the model and the process is repeated.
Selective Laser Sintering (SLS)	A thin layer of finely ground powder is spread onto a working platform. The laser energy is directed onto the powder via a scanning system where it causes the powder to sinter to become a solid. Then the working platform is lowered, a new covering of powder layer is spread and the scanning is repeated.
3D Printing (3DP)	Similar to SLS, in which a binder phase is sprayed selectively onto the powder by means of ink-jet type printing heads.
Fused Deposition Modeling (FDM)	The FDM machine is an XY plotter device which carries an extrusion head. The build material is heated to just above its melting point and extruded in the areas within the bounds of the part. After extrusion the material solidifies immediately and welds to the previous layer.
Laminated Object Manufacturing (LOM)	The build material takes the form of a sheet of paper, metal, plastic or composite. Each layer of the model is profiled from the sheet using a laser. This section is then laid on and bonded to the previous layer using a hot roller which activates a heat sensitive adhesive.

## 3.2 RAPID PROTOTYPING APPLICATIONS

According to Venuvinod & Ma (2004), RP was initially used to help the visualization of design concepts via prototypes produced from wax and other polymers. Additive processes are not exclusively used for prototyping any longer. Nowadays, with the development of new materials and processes, RP is being applied to produce functional prototypes and tooling components (Rapid Tooling - RT). Rapid Tooling can be considered as an evolution of the RP processes. Moreover, RP is being applied to direct manufacture of components in small to medium sized groups (Rapid Manufacturing - RM). The 3 applications of RP are presented as follows.

### 3.2.1 Prototyping

Rapid Prototyping was initially used to help the visualization of design concepts. The primary use of RP is to quickly make prototypes for communication and testing purposes. Prototypes dramatically improve communication because most people, including engineers, find three-dimensional objects easier to understand than two-dimensional drawings. Such improved understanding leads to substantial cost and time savings (PALM, 2002).

### 3.2.2 Rapid Manufacturing

Rapid Manufacturing (RM) is defined as the production of end use parts by the use of layer manufacturing techniques directly, without the need for any tooling. This is already being done with special applications such as, for example, medical implants or plastic aligners for straightening adult teeth, as informed by Gebhardt (2003).

Although currently only a few final products are produced by RP machines, the number will increase as metals and other materials become more widely available. RM will never completely replace other manufacturing techniques, especially in large production runs where mass-production is more economical. For short production runs, however, RM is much cheaper, since it does not require tooling. RM is also ideal for producing custom parts tailored to the user's exact specifications. The other major use of RM is for products that simply cannot be made by subtractive (machining, grinding) or compressive (forging, etc.) processes. This includes objects with complex features, internal voids and layered structures (PALM, 2002).

### **3.2.3 Rapid Tooling**

Rapid Tooling (RT) describes those applications that are aimed at making tools and molds for the production of prototypes and pre-series products by using the same processes as those used in Rapid Prototyping (GEBHARDT, 2003). According to Karapatis; Griethuysen & Glardon (1998), the purpose of RT is not the manufacture of final parts, but the preparation of the means to manufacture final parts: mass production tools such as molds, dies, etc., can be ready in very short times.

The interest in RT is encouraged by the potential to slash both cost and time in the development of tooling and the production of parts. Companies are recognizing opportunities to apply methods of RT to prototype, bridge, short-run and production tooling. Under the right circumstances, some methods of RT work well for some parts. However, developers are faced with a number of problems associated with dimensional accuracy, flatness, surface finish, mold life, size, and even build speed. Unless they can sufficiently address these problems, RT will encounter difficulty in becoming a mainstream alternative to conventional methods of tooling (WOHLERS, 1999).

Rapid Tooling can be divided into indirect or direct tooling. In indirect tooling, a master pattern is created using the RP technology in order to manufacture the final production tool by more classical methods, such as investment casting, resin tooling,

etc. From this master pattern, a mold is made out of a material such as silicone rubber, epoxy resin, etc. This route is called indirect since it includes at least one intermediate step in the tooling process. On the other hand, direct tooling involves no intermediate steps in the manufacture of tools; the tool or the die is created directly by the RP process (CHUA; HONG; HO, 1999).

Shan *et al.* (2003) informed that at present, the indirect tooling processes, i.e. RP parts used as master patterns, have many more applications than direct tooling processes because of their dimensional flexibility, accuracy, strength, and range of materials.

Every industry that makes metal or plastic parts has used RP. Aerospace, automotive, consumer products, electronics, toys, power tools, industrial goods, and durable goods are some of the commonly referenced industries. The technology is now applied to medical modeling, biomedical development (pre-surgical models are one application for rapid prototyping in the field of biomedicine), orthodontics, and custom jewelry manufacturing, as pointed out by Grimm (2004). Also, lately, RP has been used on the development of EDM (Electrical Discharge Machining) electrodes.

### 3.3 FUNDAMENTALS OF RAPID PROTOTYPING PROCESS

As mentioned before, RP transforms digital data into real parts on a layer-by-layer basis. Although each rapid prototyping technology has its own methodology, the general process for producing rapid prototypes has basically the same five steps. Based on Chua; Leong & Lim (2003) and Grimm (2004), they are:

- 1) 3D modeling:

Rapid prototyping requires three-dimensional digital data as its input; the first step is the 3D CAD file creation. Advanced 3D CAD modeling is a general prerequisite in RP processes and, usually is the most time-consuming part of the entire process chain. Examples of considerations that have to be taken into account include orientation of the

part, need for supports, difficult-to-build part structure such as thin walls, small slots or holes and overhanging elements.

Since all rapid prototyping systems construct models layer-by-layer, all prototypes will exhibit some degree of stair stepping unless all features are parallel with the horizontal or vertical planes. As the layer thickness decreases, the stair-stepping effect is minimized, surfaces become smoother, and features become more accurate. Or post treatment can be applied and, in this case, the part can be polished.

CAD data can be created virtually or, as pointed out by Rosochowski and Matuszak (2000), it can come directly from 3D sensors (such as laser, sonic, or optical digitizers), medical imaging data and any other source of 3D point data.

#### 2) Data conversion and transmission:

The 3D CAD model is next converted into a format called the STL file. The STL file approximates the geometry in the CAD file. It uses a simple triangular mesh to approximate the bounding surface of the part. An STL file is a listing of the coordinates of each vertex of the triangles in the mesh. Combined with a surface normal, a vector indicating the outward direction, the listing of all of the triangular elements provides a complete description of the 3D CAD data to be constructed. STL files for curved parts can be very large because the more curved the surfaces the more triangles are needed.

In the transmission step, the STL files, which reside in the workstation, are transferred to the RP system's computer. Data transmission via agreed data formats such as STL may be carried out through a diskette, e-mail or LAN (local area network).

#### 3) Checking and preparing:

Before processing STL files for building, a software verification program analyzes the data. When a bad file is discovered, it is processed with an STL repair program. In most cases, the corruption can be repaired within the STL file. However, in some cases, repairs must be made to the original CAD file and a new STL file exported. The necessity to return to the original CAD file is often the result of poor CAD modeling techniques.

Preparing building parameters for positioning and stepwise manufacturing in the light of many available possibilities can be difficult if not accompanied by proper documentation. These possibilities include determination of the geometrical objects, the

building orientation, spatial assortments, arrangement with other parts, necessary support structures and slice parameters. They also include the determination of technological parameters such as cure depth, laser power and other physical parameters as in the case of SLA.

#### 4) Building:

Once the STL files are verified to be error-free, the RP system's computer analyzes the STL files that define the model to be fabricated and slices the model into cross-sections (at distances equal to the layer thickness). The cross-sections are systematically recreated through the solidification of either liquids or powders, or fusing of solids, layer-by-layer to form a 3D model. For most RP systems, this step is fully automated. Depending on the size and the number of parts required the building process may take several hours.

#### 5) Post processing:

Finally, after the model is built, depending on the system, post processing will be required for cleaning, removal of supports, sanding and painting (primarily to improve the surface finish), post curing, etc.

As previously mentioned, the main goal of this research work is to manufacture EDM electrodes by a Rapid Prototyping technique. In this case, Selective Laser Sintering is the RP method chosen and it will be presented in the following section.

### 3.4 SELECTIVE LASER SINTERING (SLS)

The Selective Laser Sintering (SLS) technique uses a laser beam to selectively sinter metallic or non-metallic powders to produce solid 3D models. It is one of the most rapidly growing RP techniques. This is mainly due to its suitability to process almost any material (powder particles tend to fuse or sinter when heat is applied): polymers, metals, ceramics as well as many types of composites, according to Kruth *et al.* (2003).

The Selective Laser Sintering process represented in Figures 3.2a and 3.2b is described as follows:

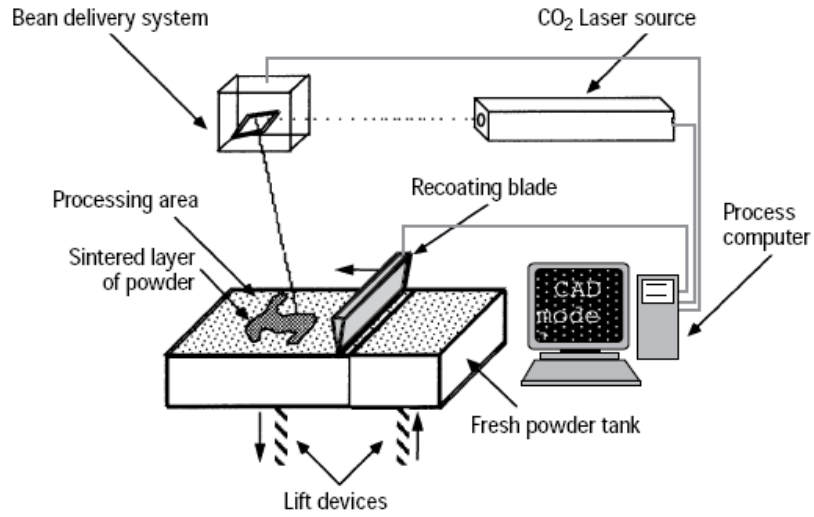
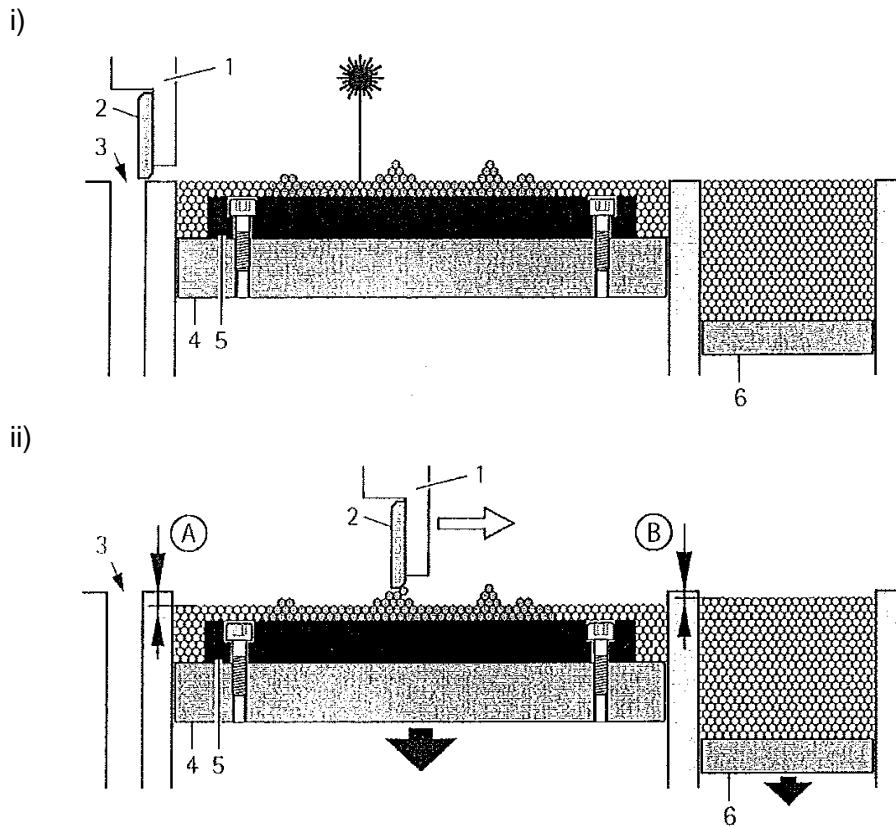
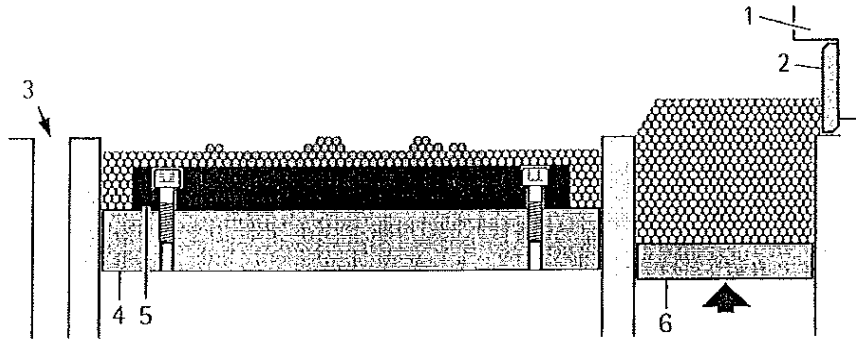


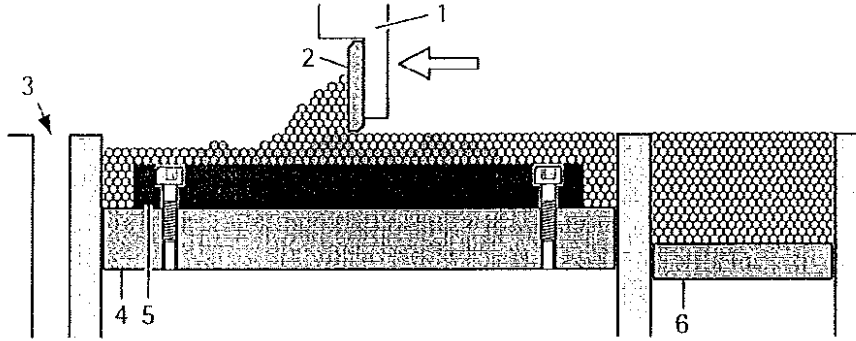
Figure 3.2a. Schematic representation of an SLS equipment (KARAPATIS; GRIETHUYSEN; GLARDON, 1998).



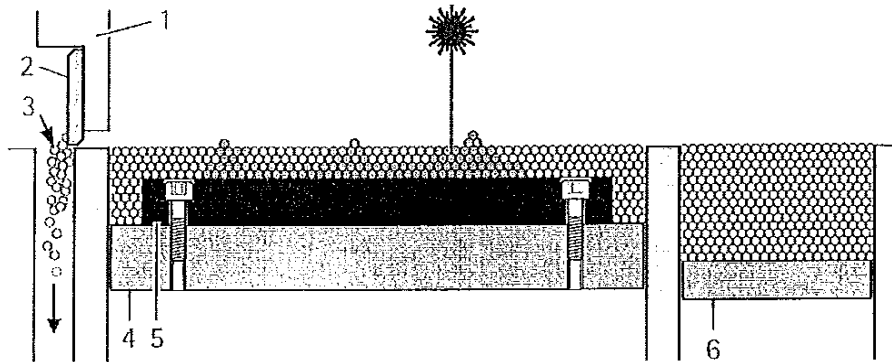
iii)



iv)



v)



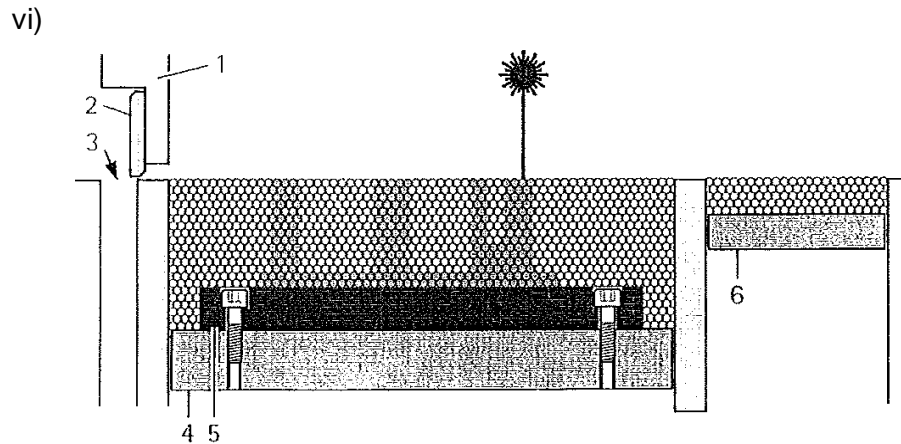


Figure 3.2b. Construction process in SLS: 1 – coater, 2 – blade or wiper, 3 – overflow, 4 – support of the building platform, 5 – building platform, 6 – metering platform, A – layer thickness, B – reduction of the metering platform (EOS RP-Tools, 1998).

- After the laser beam sinters one layer (Fig. 3.2b - i), the blade (or wiper) moves to the right (Fig. 3.2b - ii) while the building platform moves down to a precise depth, i.e. the layer thickness previously specified (letter “A” in Fig. 3.2b) as well as the metering platform.
- The metering platform then moves up (Fig. 3.2b - iii), the blade moves to the left and another layer of powdered material is spread over the surface (Fig. 3.2b - iv). A blade or a roller is used to spread and level the powder.
- The laser beam then selectively scans the layer to fuse those areas defined by the geometry of the cross-section (Fig. 3.2b - v). The power of the beam brings the selected powder areas to a temperature sufficient for the particles in the powder to get attached. The material used to produce one layer provides support to the next and subsequent layers of material. Powder that remains unaffected by the laser beam acts as a support structure for the sintered part, eliminating, occasionally, the need to model and build a support structure.
- After one layer has been formed, the building platform lowers the part by the thickness of the layer, the next layer of powder is deposited and the laser beam solidifies it while it is bonded to the layer beneath at the same time. This procedure is repeated until the whole part is completed (Fig. 3.2b - vi).

When the shape is completely built up, the part is carefully removed from the powder mass. Excess powder is brushed off from the part; the unsintered powder can be reused.

### 3.4.1 Physical Aspects in SLS

In Selective Laser Sintering the densification of the powder layer is achieved by Liquid Phase Sintering (LPS). According to Kruth *et al.* (2007), LPS includes a number of binding mechanisms in which part of the powder material is melted while other parts remain solid. The liquefied material will spread between the solid particles almost instantaneously as it is driven by intense capillary forces. The material that melts, with low melting point, is called the binder, while the high melting point material is called the structural material.

Gibson, Rosen & Stucker (2010) stated that sintering indicates the joining of powder particles without melting (i.e., in their “solid state”) at elevated temperatures. This occurs at temperatures between half of the absolute melting temperature and the melting temperature.

In the classical understanding of sintering under high temperature and high pressure, two neighbouring particles are linked to one another at a contact point first in the form of a neck, which is formed by the mechanism of surface diffusion. With the progression of sintering, over a longer period of time under the combined influence of temperature and pressure, material is transported especially along the particle boundaries and inside the sintering particles (GEBHARDT, 2003).

The laser sintering used as a Rapid Prototyping process does not work under high pressure and over a long period of time. Only a short thermal activation of the particles to be sintered occurs. Because the classical conditions of high pressure and long contact time are, as previously mentioned, not required for laser sintering, it must be assumed, according to Gebhardt (2003), that the laser sintering process is not or is

not dominantly diffusion controlled, but that it is in fact an incipient melting or even a fusion of powder particles.

The Liquid Phase Sintering mechanism is schematically shown in Fig. 3.3. The solid line represents a conventional furnace sintering process. The LPS mechanism, as it occurs in SLS, is represented by the first part of the dashed line, since only the rearrangement phase occurs because of the very short laser-material interaction time. Once the binder is molten and spread out into the solid lattice, the system cools down as the laser beam moves away and the situation is frozen, resulting in a porous green product. A thermal post-treatment in a furnace may be used to complete the cycle (KRUTH *et al.*, 2005).

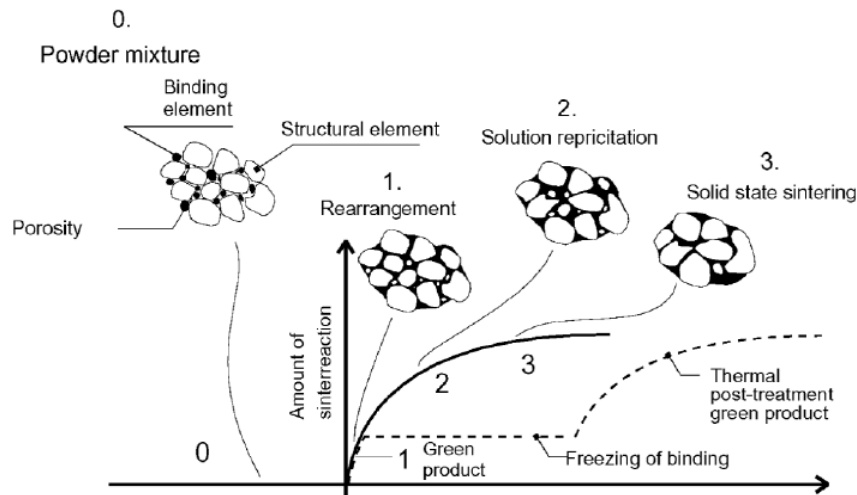


Figure 3.3. Mechanism of Liquid Phase Sintering (KRUTH *et al.*, 2005).

After a liquid is formed between solid particles in the rearrangement step, densification occurs as a result of the rearrangement of solid particles under the influence of capillary forces exerted on them by the wetting liquid. The capillary force exerted on the particles by the liquid, and the wetting of the solid particles by the liquid determines the success of both liquid phase sintering and SLS (AGARWALA *et al.*, 1995).

According to German (1985) when a liquid forms during LPS the microstructure consists of at least three phases: solid, liquid and vapor. Wetting describes the equilibrium between the three phases. The contact angle is a physical characteristic

which represents a balance between the interfacial energies. For a liquid to wet a solid, the total free energy must be decreased.

Agarwala *et al.* (1995) stated that the wetting characteristics of the solid phase by the liquid phase are crucial in successful SLS processing. Wettability can be defined by the contact angle  $\theta$ , the angle measured between the solid surface and the tangent to the surface of the liquid at the point of contact. If the contact angle is greater than  $90^\circ$ , wettability is limited. As the contact angle decreases below  $90^\circ$ , wetting improves and complete wetting occurs as  $\theta$  approaches zero.

A wetting liquid will attempt to occupy the lowest free energy position; thus, it preferentially flows to the smaller capillaries which have the highest energy per unit volume. When there is insufficient liquid to fill all of the pores, the wetting liquid will attempt to pull the particles together to minimize the free energy. Full density (zero porosity) is possible by rearrangement if enough liquid is formed. It is estimated that 35 volume percent liquid is needed to obtain full density by rearrangement processes (GERMAN, 1985).

The amount of liquid phase in the mixture influences the microstructure of the sintered part by changing the thermodynamic and kinetic characteristics, such as solution, viscosity, and wetting. Although the amount of liquid influences the induced energy, which is strongly determined by process parameters, it mainly depends on the volume fraction of binder in the powder mixture (ZHU; LU; FUH, 2004).

According to Tolochko *et al.* (2003) in order to achieve a low porosity, the rearrangement rate (the mobility of the particles) should be increased. They become more mobile with increasing liquid phase acting as a lubricant.

It is necessary for the viscosity of the molten liquid to be low enough such that it successfully surrounds the solid particles (AGARWALA *et al.*, 1995). However, if the viscosity is too low, there will not be enough liquid to cover the solid particles (LÜ; FUH; WONG, 2001).

A very high sintering temperature can lead to a large amount of liquid phase with very low viscosity, which can result in loss of shape. At low sintering temperatures, the amount of liquid phase formed is very small. The high viscosity prevents any significant

densification at the rearrangement stage. The actual level of densification depends on the amount of liquid (LÜ; FUH; WONG, 2001).

Finally, Kruth; Leu & Nakagawa (1998) pointed out that the main advantage of Liquid Phase Sintering is the very fast initial binding, making it applicable with a fast moving laser beam. Full densification and strengthening of the final parts may still require post processing.

### **3.4.2 Indirect and Direct Laser Sintering**

According to Kruth *et al.* (2007), there are different ways to bring different binder and structural materials together: mixture of two-component powder (i.e. separate binder and structural powder particles), using composite powder particles that contain both the binder and the structural material within each individual powder particle, or using coated particles where the binder material is applied as a coating around the structural material, ensuring that the laser radiation hitting the powder particles is preferentially absorbed by the binder material that is to be melted. Moreover, there is a more effective bonding of the structural particles since the binder material already surrounds all structural particles. Coated powders exist both with metal and polymer binder coatings.

Still according to Kruth *et al.* (2007), another possibility is that when there is not a clear distinction between binder and structural phases (even in cases where different powders are mixed). Rather than the distinction between binder and structural material, there is a distinction between molten and non-molten material areas. Therefore 'Partial Melting' is a better name for these technologies than 'Liquid Phase Sintering'. Powders consisting of multiple types of powder particles can be classified in this group when they are only partially molten.

Depending on how those materials are processed, there are two basic types of SLS: indirect and direct.

According to Venuvinod & Ma (2004) in indirect SLS, metal powders are mixed with a small amount of polymer binder. Alternatively, metallic and ceramic powders are

coated with polymer. Particle binding occurs essentially through polymer-polymer bonds. For instance, during SLS of a steel powder, the polymer melts and forms necks between adjacent particles. The resulting part is called green part. Owing to melting of polymer, the green part is usually highly porous. Hence, it cannot be used without some post processing. The green part is then post processed in a furnace, where the polymer binder is burned out, and the metal powders are bonded together through traditional sintering mechanics.

However, Koenig (1997) stated that the drawback to this indirect method is that it takes a long time to burn out the polymer and the dimensional and shape accuracy of the part can deteriorate during the subsequent post processing operation. For this reason, another approach, known as direct sintering, has been developed and deployed in some areas of industry.

Direct laser sintering is one of the promising Rapid Prototyping (RP) processes due to its ability to fabricate three-dimensional metal parts directly, known also as direct metal laser sintering (DMLS). That makes this process more attractive to the industrial community, because it eliminates the expensive and time-consuming pre-processing and post-processing steps as compared to indirect laser sintering or other conventional processes (ZHU; LU; FUH, 2004).

Direct Metal Laser Sintering (DMLS) is a technique that allows manufacturers to produce prototype and production tools directly from metal powders without the use of a polymer binder. The first DMLS machine was developed in 1995 by Electro Optical Systems (EOS) of Munich, Germany (VENUVINOD; MA, 2004).

Initially, the DMLS process used a bronze powder mix (known as 'DirectMetal') that was useful for short runs of plastic injection molded products. A steel powder (known as 'DirectSteel') was introduced that builds parts in layers of 50 micrometers – this material was meant to be more robust than the bronze material and was intended for extended tool life. However, the surface finish is relatively poor and requires fairly extensive hand-finishing to make it usable. More recently a powder has been introduced that allows parts to be built in layers of just 20 micrometers for plastic injection molding, studies have shown that minimal finishing is required of these tools (HAGUE, 2003).

Direct SLS is also possible with high performance materials such as nickel and cobalt base superalloys, cermets, titanium base alloys and monolithic high temperature metals such as molybdenum. These materials are used for high performance components that typically experience high operating temperatures, high stress, and severe oxidizing or corrosive environments (LÜ; FUH; WONG, 2001).

### **3.4.3 Materials used in the Selective Laser Sintering Process**

In theory, all materials that can be melted and, after cooling, solidify again can be used for the sinter process (GEBHARDT, 2003). Moreover, Venuvinod & Ma (2004) stated that virtually any material that softens/melts and has decreased viscosity upon heating can be used.

In the case of a mixture of two-component powder, the two materials may differ considerably: polymer binder vs. metallic structural material, metallic binder vs. ceramic structural material, low-melting metal vs. high melting metal. The structural material (a metal, alternatively a ceramic) should generally have a higher melting point than the (metallic) binder material (KRUTH *et al.*, 2007).

Several thermoplastic materials such as nylon, glass filled nylon, and polystyrene suitable for SLS are commercially available. The process has also been applied successfully to powders made up of steels, Ni-based super alloys, Ti and its alloys, cermets, and refractory bronze-Ni (perhaps the most effective combination) (VENUVINOD; MA, 2004).

### **3.4.4 Factors that influence the Selective Laser Sintering Process**

Numerous factors influence the densification of powders during SLS process. The SLS parameters that most influence the intensity of the energy delivered to the powder

bed by the laser beam are laser wavelength (type of laser), laser power, laser scan speed, layer thickness, hatch distance, laser beam spot size, powder bed temperature, geometrical scanning strategy including the length of scan vector and the method of irradiation between each successive layers. Important powder material properties include particle size, size distribution and shape, powder composition, laser absorptance and melting point.

#### **3.4.4.1 Selective Laser Sintering Parameters**

Powder bed temperature, laser power, laser beam spot size, laser scan speed, layer thickness, hatch distance and scanning strategy must be combined in a way that the best exchange between dimensional accuracy, surface finish, build rate and mechanical properties are achieved.

The powder bed temperature should be kept uniform and constant to achieve repeatable results. In general, high-laser-power/high-bed-temperature combinations produce dense parts, but can result in part growth. On the other hand, low-laser-power/low-bed-temperature combinations produce better dimensional accuracy, but result in lower density parts and a higher tendency for layer delamination. High-laser-power combined with low-part-bed-temperatures result in an increased tendency for non-uniform shrinkage and the build-up of residual stresses; leading to curling of parts (GIBSON; ROSEN; STUCKER, 2010).

The longer the laser stays in a particular location, the deeper the fusion depth and the larger the melt pool diameter. Operating at lower laser powers requires the use of lower scan speeds in order to ensure proper particle fusion. Melt pool size is highly dependent upon settings of laser power, scan speed, spot size and bed temperature. Hatch distance should be selected to ensure a sufficient degree of melt pool overlap between adjacent lines of fused material to ensure robust mechanical properties (GIBSON; ROSEN; STUCKER, 2010).

The minimum layer thickness that can be successfully employed is determined most importantly by the maximum particle size. Below a certain layer thickness, the roller or blade mechanism tend to displace the previously sintered layers from their predetermined position, thus disturbing the geometry of the part. This problem is particularly serious during the early build up of the part (AGARWALA *et al.*, 1995). Higher SLS part densities are most obtained by using lower layer thickness. However, if it is possible to have good results working with thicker layers, the production time will be reduced. That is why it is important to investigate this parameter.

Simchi (2006) stated that the laser scanning strategy can influence the densification. The sintered density might decrease as the vector length increases. As the vector length increases, the higher delay period between successive irradiation leads to a decrease in the amount of energy stored on the surface. Consequently, less densification is expected during the laser sintering. Another consequence of applying higher vector length is related to the development of thermal stresses. It is known that an increase in the scan length results in development of higher thermal stresses in the sintered parts. These stresses are responsible for part cracking, warpage and Christmas tree defects.

In direct SLS of metals, the impact of sintering atmosphere on the densification could be related to the amount of oxygen present during sintering. The presence of oxygen allows surface oxides to form as the powder particles are heated and melted by the scanning laser beam. The formation of oxide layer on the surface of powder particles significantly increases the absorption rate of CO<sub>2</sub> laser radiation. This changes the temperature-time history of sintering and increases the melt volume (SIMCHI, 2006).

According to Das (2003) since SLS is a layer-by-layer additive process, oxidation of laser processed powder is a severe impediment to interlayer bonding and causes defects such as balling. Balling occurs when the laser melted metal powder layer does not wet the underlying substrate due to a contamination layer of oxide being present on the substrate and on the surface of the melt. Oxidation also causes delamination induced by poor interlayer bonding in combination with thermal stresses. These phenomena severely degrade material properties and part geometry. In order to diminish oxidation as well as to ensure good wetting and successful layer-by-layer

consolidation in direct SLS of metals, processing must be conducted in a vacuum or protective atmosphere using high purity inert gases.

Therefore the atmosphere must be controlled. Depending on the material system, nitrogen, argon, nitrogen-hydrogen mixture and hydrogen have been used as protective/reducing atmospheres. By using different protection gases, the wetting can also be enhanced (LÜ; FUH; WONG, 2001). If the oxygen potential of the sintering atmosphere is kept constant, the role of protective atmosphere on the densification is not very pronounced (SIMCHI, 2006).

#### **3.4.4.2 Material Properties**

The density of SLS processed parts can be increased by using a mixture of powders with different sizes. Finer particles provide larger surface area to absorb more laser energy, which increases the working temperature and thus the sintering kinetics (SIMCHI, 2006).

Usually the binder particles are smaller than the structural particles, in order to facilitate their preferential melting. However, for instance, preferential binder melting may be neutralized by the higher reflectivity or lower laser absorption of a metallic binder material (typically Cu or Co) as compared to the structural material (metal or ceramic). The combination of small binder particles and larger structural particles has the additional benefit of better packing with small pores, favoring fast spreading of the molten binder by capillary forces and fast rearrangement of the particles (KRUTH *et al.*, 2007).

The density of a SLS processed part is also affected by its initial packing density. In a high starting density part, the rigid network of high melting point solid particles restricts the flow of the low melting point component and prevents their rearrangement. In a lower starting density part, the liquid is freer to flow and rearrange the solid particles to cause densification (LÜ; FUH; WONG, 2001).

The particle size determines the minimum thickness of the laser sintered layer that controls the accuracy of the SLS parts. Therefore, a smaller particle size is preferred. However, fine powder particles are easily oxidized during the SLS process due to the presence of more surface area compared to larger particles (LÜ; FUH; WONG, 2001).

It is especially important to take into account the powder absorptance during SLS of two-component powder mixtures (TOLOCHKO *et al.*, 2003). The absorptance of a material is defined as the ratio of the absorbed radiation to the incident radiation. Only part of the incident radiation is absorbed by the outer surface of the particles in a loose powder. Another part of the radiation penetrates through the inter-particle spaces (pores) into the depth of the loose powder interacting with the underlying particles (TOLOCHKO *et al.*, 2000).

Laser absorption in powders is usually higher than in solid material. This is due to multiple reflection and absorption of the laser beam trapped in the pores of the powder (KRUTH *et al.*, 2003). Multiple reflections effect between the powder particles leads to higher optical penetration depths compared to bulk materials (SIMCHI, 2006).

Usually infrared CO<sub>2</sub> or Nd:YAG lasers are used as energy sources. The type of laser has a large influence on the consolidation of powder particles, because laser absorption of various materials greatly depends on the laser wavelength. According to Kruth *et al.* (2003), CO<sub>2</sub> lasers with wavelength of 10,6 µm are well suited for sintering polymer powders, as polymers depict high absorption at far infrared or long wavelength. The same is true for oxide ceramics, but no longer for carbide ceramics that better absorb at Nd:YAG wavelength of 1,06 µm. It is also well known that metals absorb much better at short wavelength. This is why Nd:YAG lasers may outperform CO<sub>2</sub> lasers for metallic materials.

According to Lü, Fuh & Wong (2001) the reflectivity of a material is most dependent on its electrical conductivity. A metal with high electrical conductivity has the highest reflectivity; for example copper. Hence, a high energy density is required to sinter a material like copper. In addition, a material with high thermal diffusivity will normally allow a greater depth of fusion penetration with no thermal shock or cracking.

Finally, the quality of laser sintered parts greatly depends on proper selection of the processing parameters. The latter not only includes the adjustable machine parameters (laser power, laser beam spot size, laser scan speed, etc.), but also the type of laser (wavelength) and the powder composition (materials, mixture ratios, grain sizes, etc.). This is because the SLS process is not only controlled by the amount and speed of energy supply, but to a great extent by the basic laser-material interaction (KRUTH *et al.*, 2003).

It is important to point out that SLS is not without its share of disadvantages. Venuvinod & Ma (2004) reported that compared to most other RP equipment (e.g. SLA), an SLS system is mechanically more complex. As with parts produced by any layered manufacturing technique, SLS parts also suffer from the stair stepping problem. Surface finish and accuracy are not quite as good as with SLA. SLS parts exhibit powdery, porous surfaces that are absorbent and mark easily. The porosity and, hence, the density can vary across the part. However, part finish can be improved by applying a sealant. A sealant also strengthens parts. Also, infiltrating the part with some other material can solve some of the problems arising from part porosity.

## CHAPTER 4

### PRODUCTION OF EDM ELECTRODES WITH RP TECHNIQUES

A number of research works have explored the application of Rapid Prototyping techniques in the production of EDM electrodes. The previous experimental studies are divided into indirect and direct methods. Electroforming is the indirect method most studied to manufacture EDM electrodes whereas Selective Laser Sintering (SLS), previously described, is the direct one.

#### 4.1 MANUFACTURE OF EDM ELECTRODES BY INDIRECT METHODS

Indirect techniques follow the pattern-based approach in which the 3D physical model produced from RP technique is used as pattern in other manufacturing processes such as investment casting, slip casting, etc. Whereas, in direct techniques, the 3D model generated can be directly used as production tool, e.g. EDM electrodes, moulds, etc (MEENA; NAGAHANUMAI AH, 2006).

Electroforming is the use of electrodeposition of metal over a model or mandrel which is subsequently separated from the deposit to produce a metal shell. Electrodeposition, or electroplating, is the process of producing a coating on a surface by the action of electric current. The deposition of a metallic coating onto an object is achieved by putting a negative charge on the object to be coated and immersing it into a solution which contains a salt of the metal to be deposited. The metallic ions of the salt carry a positive charge and are thus attracted to the object (SCHLESINGER, 2002).

The mandrels or models used for producing electroforms can be metals or non-metals. Non-metal mandrels require metalizing prior to use to make them electrically conductive, for instance the use of a conductive metal loaded paint, which may be brushed, sprayed or dipped (RENNIE; BOCKING; BENNETT, 2001).

Thin coated stereolithography (SL) models have been used as EDM electrodes with simple geometry to erode 4 mm deep cavities in hardened tool steel. Using silver

paint as an interface, epoxy SL models have been electroplated with copper to a thickness of 180  $\mu\text{m}$ . The authors concluded that it is possible to make limited use of thin coated SL models as electrodes for EDM primarily for re-cutting or finish cutting of cavities. Copper electroformed electrodes from SL cavities were also produced. Electroforming copper into SL cavities shows potential for manufacture of electrodes for use in roughing or semi-roughing, with efficient machining rates. Limitations to the geometry that can be electroformed and separation of the shell from master (with the SL master being sacrificial) need to be examined (ARTHUR; DICKENS; COBB, 1996).

The viability of using an electroformed shell of copper as an EDM electrode was studied again. The model, a square cavity with a variety of features on the bottom face, was made on the stereolithography apparatus (SLA). Using silicone RTV rubber and vacuum casting, a flexible silicone cavity was produced. The cured silicone casting was then detached from the SL core and was then sent for the electroforming of the cavity. The electroformed copper shell obtained was then backed with zinc. Hardened steel was selected as the workpiece material. The authors concluded that electroformed tools are not recommended for rough machining because it can deform the tool. Semi-roughing to finishing machining operations may be undertaken using these tools. Distortion in the tools is an inevitable side effect. The use of more than one tool to perform a single operation may be imperative (YARLAGADDA; CHRISTODOULOU; SUBRAMANIAN, 1999).

Once again rapid prototyping combined with electroforming for the generation of EDM electrodes was studied. The negative geometry of the EDM electrode was prototyped by stereolithography for use as the master. Before electroforming, the SL parts were metalized using electroless plating. The metalized SL parts were then electroplated with copper to the required thickness, in this case 1 mm and 2 mm. Incineration was used to remove the SL master from the electroformed copper shell. The copper shell was backed with a tin-lead alloy. The electrodes were used to machine a hard steel workpiece using the machining settings typically used for EDM roughing. The main sources of tooling inaccuracy are thermal deformations caused by burning out the SL master and by backfilling the electroformed metal shell with a molten metal.

According to the authors, the integration of electroforming with RP is a viable way for rapid tooling of EDM electrodes (YANG; LEU, 1999).

A study of the use of electroforming for the production of EDM electrodes was also conducted by Rennie, Bocking & Bennett (2001). Two RP systems, Stereolithography (SL) and ThermoJet (THJ), were examined. The initial work for this study used SL models for electroforming of copper shells. The model was sprayed with a layer of silver paint and, after metallization, the models were placed into the electroforming tank. A range of shell thickness between 0,6 and 3,0 mm was produced. Two methods of back-filling the electrodes were used: polyurethane with Fillite sand mixed and tin/bismuth alloy. The electroform was removed from the SL mandrel after filling with the respective material. In order to reduce the time taken to produce the mandrels by the SL process, the ThermoJet (THJ) technique was employed in the creation of these patterns. Preparation of these mandrels was similar to the SL models. It has been found that thin walled ( $\leq 1,5$  mm) copper electroforms backed up with suitable filler materials are optimal for use as EDM electrodes.

A research was performed to assess the suitability of electrodes created by electroplating copper onto SL model with a complex geometry. The process chain for manufacturing the SL based electrode was: build an SL model, support removal and finishing of SL model, spray conductive silver paint on the SL model and electroplate the silver coated SL model with copper. The amount of copper deposited on the electrode models proved problematic as the electroplating process was unable to deposit enough copper in the inner cavities of the electrodes, with very gradual reduction in copper layer thickness from the outer faces/surface to virtually no deposition in the inner walls and bottom face. Consequently, the electrodes were found to be unsuitable for EDM process due to variations in coating thickness (DIMLA; HOPKINSON; ROTHE, 2004).

The study of Hsu *et al.* (2008) investigated an effective method for manufacturing electrical discharge machining (EDM) electrodes with complex geometry using the rapid prototyping (RP) system based on electroless plating and electroforming. This investigation used the Zcorp 3D Printing RP system and the material used was gypsum powder. Electroless plating of nickel was then performed to introduce electric conductivity onto the gypsum electrode surface, followed by copper electroforming of the

thickness about 1 mm to obtain the EDM electrode. Finally, die-sinking electric discharge machining was performed. No remarkable damages were observed in the electrode after die-sinking EDM tests. The authors concluded that it is feasible to manufacture EDM electrodes using rapid prototyping gypsum powder associated with electroless plating and electroforming of copper.

## 4.2 MANUFACTURE OF EDM ELECTRODES BY DIRECT METHODS

The development of non-erodible electrodes that could be fabricated into complex shapes of various sizes by both Selective Laser Sintering (SLS) and conventional methods for Metal-Matrix-Ceramic (MMC) was the goal of Eubank *et al.* (1998). The authors have developed a new MMC material,  $ZrB_2/Cu$ , to be used as electrodes. First, raw  $ZrB_2$  powders were coated with a polymer optimized for use in a SLS machine. Then these powders were processed using SLS to tack together the  $ZrB_2$  powders by actually sintering their respective polymer coatings, creating a  $ZrB_2$  part in the desired shape. After that, a high-temperature furnace was used to both vaporize the polymer coating and sinter the  $ZrB_2$  powder. Finally, the 35-70% dense network of  $ZrB_2$  was infiltrated with an appropriate copper alloy. The authors have improved the process for making electrodes of  $ZrB_2/Cu$ , a MMC, to the point where their electrodes were much superior to pure copper and various graphite's, the most common electrode materials, and somewhat better than W-Cu, a more expensive MMC.

An investigation on the EDM electrode production using Direct Metal Laser Sintering (DMLS) technique was carried out by Dürr, Pilz & Eleser (1999). The SLS system EOSINT-M 160 was used for the investigations and the metallic powder used was a bronze nickel mixture. The influence of the DMLS process parameters (scan rate, sinter strategy, hatch distance and laser power) on the porosity of the manufactured electrodes was investigated. After EDM tests, it was found out that a decrease in the electrode porosity led to a decrease in the relative electrode wear. Regarding the erosion rate, a decrease in the electrode porosity led to an increase of the material

removal rate. The porosity of the electrodes could be reduced after the SLS process by infiltration with tin and be almost completely eliminated by infiltration in vacuum with silver-containing brazing metal. The infiltration with tin led to an increase of the relative wear with the increase of the pulse time compared to the untreated SLS electrode. The infiltration with silver-containing brazing metal brought an improvement of the wear values related to the untreated electrode.

Tay & Haider (2001) also investigated about the EDM electrode production using the DMLS technique. The metal powder used was a mixture of copper, tin, nickel and phosphorus and an infra-red 200 W CO<sub>2</sub> laser was used. Four types of electrodes were chosen for the performance test: a solid copper electrode, a copper electroplated DMLS electrode, an electroless copper plated DMLS electrode and an untreated DMLS electrode. The investigation of the machining performance of the selected electrodes under roughing, semi-roughing and finishing operations was carried out. It was concluded that an untreated DMLS electrode could be considered for both roughing and semi-roughing, especially where minimal material removal is required; an electroless copper plated electrode was appropriate for both roughing and semi-roughing operations where dimensional accuracy and moderate material removal are essential; the electroless copper plated electrode and the untreated DMLS electrode were found to be unsuitable for finishing operations, as the sintered material was porous and soft; surface finish was almost the same for all the electrodes for each condition; the copper electroplated EDM electrode was good for EDM roughing; although the performances of the copper electroplated electrode were very similar to those of the solid copper electrode, the dimensional accuracy could not be maintained, especially at the sharp edges and corners during electroplating.

Analysis of the wear characteristics of an EDM electrode made by selective laser sintering was made by Zhao *et al.* (2003). The material used consisted of steel, polyester and phosphate in different proportions. Post-treatment was used to improve the strength and density of the SLS metal prototype. The last step was infiltration with copper. The manufactured electrode was not full-dense, but its density was close to that of solid copper. The main EDM parameters were researched, i.e., applied current, pulse duration and pulse interval. The electrode with higher content of steel presented the

lowest wear rate due to its higher density and the best surface finish of eroded cavity. The authors concluded that the electrode made by SLS can be used as an EDM electrode. A parametric experiment proved that the wear rate of the electrode approaches to that of a general electrode and the surface roughness of the cavity is acceptable at the same machining conditions. The preferable surface finish of cavity could be obtained using rough or semi-finish machining parameters with that kind of electrode.

An investigation of complex EDM electrodes production by DMLS was carried out by Dimla, Hopkinson & Rothe (2004). The design of the electrode included deep slots, which have been identified as problematic for milling, along with surfaces at various angles. The DMLS model was built using nickel based bronze powder on a standard DMLS machine. The electroplating of the DMLS electrode was a straightforward procedure as the bronze content facilitated electroplating. The electroplating process was unable to deposit enough copper in the inner cavities of the electrodes, with very gradual reduction in copper layer thickness from the outer faces to virtually no deposition in the inner walls and bottom face being a big concern. Without a sufficient layer of copper, the electrode would just burn out immediately when erosion begins. The electrode was found to be unsuitable for EDMing due to variations in coating thickness.

The research work of Meena & Nagahanumaiah (2006) was to optimize the EDM parameters and investigate the feasibility of using DMLS parts as EDM electrodes. The material used was composed by Cu, Ni, Sn and P and the EOSINT M 250 machine with a 200W CO<sub>2</sub> laser and spot size of 0,3 mm was used. Experimental results showed that the performance characteristics of the EDM process (TWR, MRR and surface roughness) using DMLS electrode could be quantified and controlled effectively by grey relational approach presented in the study. Current was found to be the most affective parameter in EDM machining using DMLS electrode. Excessive DMLS electrode wear was also reported, especially at corners, which limits the use of DMLS tool for EDM machining and it was found out that porosity was one of the primary cause. This could be improved by secondary operations like post sintering, infiltration and coating. According to the authors, the DMLS material showed huge potential to be used as EDM electrode.

In general, the results have been unsatisfactory until now for the production of EDM electrodes by SLS. With better material powder systems and the improvement of the SLS parameters, it might be possible to overcome porosity, the major problem in the production of the electrodes. Therefore this research work carried out experiments with a new material, i.e. Cu-Ni and Mo mixture, in order to investigate the production of EDM electrodes by Selective Laser Sintering.

## CHAPTER 5

### COMMONLY USED MATERIALS FOR EDM ELECTRODES

This chapter presents the materials that are commonly used for the manufacture of EDM electrodes (brass, copper, graphite, copper graphite, tellurium-copper, tungsten, copper tungsten, tungsten carbide, silver, silver tungsten and zinc alloys) and their properties.

#### 5.1 INTRODUCTION

Any material demonstrating good electrical conductivity can be used as EDM electrode. Because EDM is a thermal process, the influence of thermal properties of electrode materials on the removal volume is significant. Materials with higher thermal conductivity are suitable as tool electrodes as well as materials with higher melting point and boiling point (KUNIEDA *et al.*, 2005). Moreover, due to the high pressure and temperature present on the electrode during EDM machining, the electrode material must have acceptable mechanical strength and melting point to reduce tool wear and edge weakness. Furthermore, since the shaped electrode defines the area in which spark erosion will occur, the dimensional accuracy of the produced part depends on the dimensional accuracy and the surface texture of the electrode (KECHAGIAS *et al.*, 2008).

The purpose of an electrode is to transmit the electrical charges and to erode the workpiece to a desired shape. Different electrode materials greatly affect machining. Some will remove material efficiently but have great wear; other electrode materials will have slight wear but remove material slowly (SOMMER, 2001).

Thus, the electrode material properties that effect the EDM process are electrical conductivity; melting point temperature; structural integrity - how well the material responds to hundreds of thousands of sparks on its surface will be a significant factor in determining the electrode material's performance regarding wear, surface finish, and

ability to withstand poor flushing conditions; mechanical properties - tensile strength, grain size (if applicable) and hardness will affect both the fabrication of the electrode, and its performance in the EDM process; manufacturability - the usefulness of an electrode material is somewhat determined by the difficulty of manufacturing electrodes from it, such factors may include machinability, stability and burr formation and removal; and finally cost (KERN, 2008).

It can be said that materials having good electrical and thermal conductivity and high melting point are adequate to be used as EDM electrodes.

Common EDM electrode materials include brass, copper, graphite, copper graphite, tellurium-copper, tungsten, copper tungsten, tungsten carbide, silver, silver tungsten and zinc alloys. Table 5.1 shows some of their physical properties.

Table 5.1. Physical properties of some EDM electrode materials (MatWeb).

<i>Properties</i> <i>Materials</i>	Electrical resistivity	Thermal conductivity	Melting point	Density	Thermal expansion coefficient	Specific heat capacity
	$\mu\Omega \cdot \text{cm}$	W/m.K	$^{\circ}\text{C}$	$\text{g}/\text{cm}^3$	$\mu\text{m}/\text{m} \cdot ^{\circ}\text{C}$	$\text{J}/\text{g} \cdot ^{\circ}\text{C}$
Brass	4,70 – 28,0	26,0 - 159	820 - 1030	7,60 – 8,75	18,7 - 21,2	0,375 - 0,380
Copper	1,70	357 (727 $^{\circ}\text{C}$ ) 401 (0 $^{\circ}\text{C}$ )	1083,2 - 1083,6	8,93	16,4 (20,0 - 100 $^{\circ}\text{C}$ ) 24,8 (925 $^{\circ}\text{C}$ )	0,385
Graphite	6000,0	24,0	-	2,25	0,600 - 4,30 (20,0 $^{\circ}\text{C}$ )	0,70768
Copper Graphite	4,36	200, z direction 300, x-y directions	-	6,80	7,40 (20,0 $^{\circ}\text{C}$ )	-
Tellurium 0.50 % Copper 99.5 %	-	392	1083	8,91	17,7 (-4,00 - 149 $^{\circ}\text{C}$ )	-
Tungsten	5,65	163,3	3370	19,3	4,40 (20,0 - 100 $^{\circ}\text{C}$ )	0,134
Copper 25.0 % Tungsten 75.0 %	3,83	220	1085 - 3410	14,84	-	-
Tungsten Carbide	53,0 – 80,0	-	2800 - 2870	15,7	5,20	-
Silver	1,55	419	961,93	10,49	19,9 (0 - 250 $^{\circ}\text{C}$ ) 22,4 (0 - 900 $^{\circ}\text{C}$ )	0,234
Silver 30.0 % Tungsten 70.0 %	3,45	160	$\geq 980$	15,28	-	-
Zinc Alloys	6,20	105	410 - 420	7,00	30,0 (20,0 - 100 $^{\circ}\text{C}$ )	0,420

Materials typically used for electrodes in die-sinking EDM are presented as follows.

## 5.2 BRASS

Brass, a copper and zinc alloy, was one of the first EDM electrode materials used. It is inexpensive and easy to machine. Nowadays, however, brass is rarely used as an electrode material due to its high wear rate (KERN, 2008).

The grade used is normally specified as free-machining brass. It has a fairly good wear ratio when machining steel, and a very high wear ratio when machining tungsten carbide (JAMESON, 2001).

It is often used for tubular electrodes in specialized applications like drilling of small holes where high electrode wear is acceptable. Brass has shown itself to be a good electrode material for some alloys of titanium under poor material removal conditions (RAO, 2009).

## 5.3 COPPER

Many shops in both Europe and Japan still prefer to use copper as the primary electrode material, due to their tool-making culture that is averse to the untidiness of working with graphite (KERN, 2008).

Pure copper or electrolytic grade copper is extensively used as an electrode material. It has good electrical and thermal conductivity and it is most often used when fine surface finishes are required in the workpiece. Machining of copper is a major problem because of its poor machinability (RAO, 2009). Moreover, copper electrodes will generally burn only half as fast as graphite electrodes and copper is an extraordinarily difficult material to deburr. It can take longer to deburr a copper electrode than to manufacture it (KERN, 2008).

Although the combination of copper and certain power supply settings enables low wear burning (KERN, 2008), another problem with copper is that its melting point is approximately 1.085°C; whereas the spark temperature in the gap exceeds 3.800°C.

Copper's low melting point often causes too high a wear rate in relation to its material removal (SOMMER, 2001).

Copper electrodes are the preferred material for all High Speed Small Hole applications involving aerospace alloys as well as carbide (KERN, 2008).

#### 5.4 GRAPHITE

Graphite is the preferred electrode material for 90% of all die-sinking EDM applications (KERN, 2008). In North America, approximately 85% of the electrodes used are graphite (SOMMER, 2001).

Graphite is made from powdered carbon which is mixed with a petroleum based binder material and then compacted. After compacting, the compacted material undergoes a series of thermal treatments that convert the carbon to graphite (KERN, 2008).

Graphite is maybe the most widely used EDM electrode material because of good machinability and wear characteristics. It permits fast material removal rates and has good wear ratio (RAO, 2009). Graphite machines and grinds easily compared to metal electrodes and burrs are absent when machining it (SOMMER, 2001).

Graphite has an extremely high melting point. In fact, graphite does not melt, but sublimates directly from a solid to a gas at a temperature thousands of degrees higher than the melting point of copper. This resistance to temperature makes graphite an optimal electrode material (KERN, 2008).

Due to the significant differences between metallic electrodes and graphite, there are certain properties unique to graphite that are commonly specified and controlled such as particle size and density. Since graphite is a porous material, density must be closely controlled and usually higher density is preferable (KERN, 2008). Because graphite is porous, liquids can penetrate and introduce impurities. The larger graphite grain structure, the greater the risk for impurities. However, dense graphite, even after being soaked in fluid for several hours, shows little fluid penetration (SOMMER, 2001).

When a graphite electrode is attacked by an EDM spark, a particle will often be displaced. Particle size is the best predictor of the level of detail achievable, strength, corner wear, and surface finish. Graphite is available in particle sizes ranging from less than one micrometer up to particle sizes in excess of 20 micrometers. Graphite featuring a particle size of less than one micrometer is the most expensive of the graphite grades, and will hold sharp corners and reproduce extremely fine detail (KERN, 2008). Coarse particle graphite is normally used for large volume EDM work, where there is little or no fine detail to be produced. Coarse particles have more porosity and produce rougher finishes. Medium grade graphite usually works well when machining through holes in steels (RAO, 2009).

Generally, the smaller the particle size, the better the mechanical properties of the graphite, which result in finer detail, better wear, and better workpiece surface finish (KERN, 2008). It can be said that finer grain size graphite is used for fine detail, good finish and high-wear resistance and coarser (less costly) electrode when there is no concern for small detail or fine finish (SOMMER, 2001).

Graphite is widely used due to its significant production advantages over metallic electrode materials: graphite is faster than copper in both roughing and finishing; graphite usually wears less than copper; with advances in dielectric, power supply electronics, and orbiting, achievable graphite finishes match those previously only possible with copper; graphite machines and grinds an order of magnitude faster than copper, and can also have more detail easily machined into it. Graphite doesn't have to be de-burred like any metallic does, further reducing electrode fabrication costs (KERN, 2008). In addition, graphite produces high material removal rates and has a wear ratio equivalent to that of copper-tungsten alloy (RAO, 2009).

Graphite has lower thermal expansion than copper, with almost no deformation during the process. In particular, during EDM of deep cavities under roughing conditions, the volumetric thermal expansion of copper is considerably high, which usually compromises the flushing condition of the debris. Graphite, which has lower thermal expansion, is widely used in roughing conditions, with bigger particle size grades (10 to 20  $\mu\text{m}$ ) which have more accessible prices (AMORIM, 2002).

However, when compared to metallic electrode materials, graphite has some limitations like the fact that machining operations on graphite will produce great amounts of graphite dust which, unless efficiently controlled, gets on everything, even on mechanical components of machines, which can be fatal. In addition, burning with graphite also results in the production of significantly more debris that has to be filtered out of the dielectric oil (KERN, 2008).

Care should be taken when machining tungsten carbide because if the material removal conditions are not good, cutting surface will become carbonized and it may result in uncontrolled arcing or dc arcing. The dc arcing is caused by the carbon deposited on the work surface which is heated to the point that deionization of the dielectric fluid does not take place. Without deionization, current flows across the same point between electrode and workpiece, causing excessive heating. It is generally recommended that only fine particle and high density graphite be used (RAO, 2009).

With the proper tooling, graphite can be machined by all the conventional material removal processes, including milling, drilling, and most types of grinding. Cutting tool life expectancy can be considerably shorter when machining graphite instead of conventional metals. Since the material is abrasive, the rules that apply for cutting metal do not apply for graphite. Because high-speed steel would wear too rapidly for most applications, tungsten carbide or diamond-coated cutters are most commonly used (FREDERICKSON, 2002).

The easiest way to initiate or upgrade a shop's ability to machine EDM graphite electrodes is to buy a specialized CNC machining center developed for the purpose. These machines often come equipped with high-speed electric spindle systems, as well as the necessary dust evacuation system and other refinements (FREDERICKSON, 2002).

## 5.5 COPPER GRAPHITE

Copper graphite is graphite manufactured with a controlled amount of interconnected porosity which is then infiltrated with copper by capillary action in a furnace. The resulting material has increased electrical conductivity and mechanical strength. Copper graphite has shown particular advantage when applied to aerospace applications such as titanium, Inconel, and other high temperature aerospace alloys (KERN, 2008).

However, it is more expensive than graphite. Although it has better electrical conductivity than graphite, corner wear is not as good as that of pure graphite. It works well under poor flushing conditions and for machining tungsten carbides (RAO, 2009).

## 5.6 TELLURIUM-COPPER

The addition of 1-3% tellurium to copper improves its machinability to a level similar to brass, eliminating the gummy properties normally exhibited by copper when it is machined or ground. However, the EDM performance of copper is somewhat compromised by the addition of the tellurium. Compared to electrolytic copper, tellurium copper exhibits 15-25% higher wear and 10% decreased metal removal rate. Nevertheless, because of the ease of machining this material, most shops are willing to accept this trade-off (KERN, 2008). Another disadvantage of tellurium-copper is its scarcity (RAO, 2009).

## 5.7 TUNGSTEN

Due to the combination of its high density, tensile strength, and melting point, tungsten had been the electrode material of choice for limited EDM applications. Due to its relatively poor electrical conductivity, tungsten cuts much slower than brass or copper. In addition, tungsten is seldom used due to its high cost and very low machinability (KERN, 2008). Tungsten has good wear ratio and is used for making small holes that are less than 0,2 mm for which electrodes with small flush holes are not available (RAO, 2009).

## 5.8 COPPER TUNGSTEN

Copper tungsten is manufactured by the powder metallurgy process. Copper and tungsten powder are pressed into a pre-form and then sintered. During sintering, the material shrinks by approximately 25% and care must be taken to avoid porosity (KERN, 2008).

Copper tungsten combines the high electrical conductivity of copper with the high melting point of tungsten. The mixture of these two metals creates an electrode material with very good wear properties. Copper tungsten has good wear resistance, holds up very well in sharp corners, and is readily machined and ground without the burr issues associated with copper. Copper tungsten is also the preferred material for EDMing carbide (KERN, 2008).

Copper tungsten is usually sold in the 70W:30Cu grade, but it is possible to obtain copper tungsten with different ratios. Higher tungsten content would improve the corner wear at the expense of lower cutting stability and higher cost. Lower tungsten content would increase corner wear, but enable smoother burning in addition to reducing the cost of the material, since copper is cheaper than tungsten. Moreover, copper tungsten typically cuts only half as fast as copper (KERN, 2008).

Copper tungsten is used for close tolerances, fine detail and low wear. It has good thermal and electrical conductivity as well as good strength and tends less to breakage or fracture when machined into thin sections and fine details (RAO, 2009).

## 5.9 TUNGSTEN CARBIDE

Due to its high stiffness and low wear properties, tungsten carbide is often the preferred electrode material for applications requiring very small holes. However, tungsten carbide is very brittle (KERN, 2008).

## 5.10 SILVER

Silver is occasionally used as an electrode material, due to its superior electrical conductivity, purity, and structural integrity. The use of silver electrodes and fine finish power supplies can produce very good fine finishes. However, due to the high cost, silver is rarely used (KERN, 2008).

## 5.11 SILVER TUNGSTEN

Silver tungsten is a powder metallurgy product which combines the wear resistance of tungsten with the high conductivity of silver, resulting in low wear and fine surface finish for EDM applications with fine detail. Silver tungsten is made by the same process as copper tungsten. Due to its high cost and limited availability, silver tungsten has a very limited range of applications (KERN, 2008). For instance, silver tungsten is

used for making deep slots under poor flushing conditions, especially in tungsten carbides (EL-HOFY, 2007).

## 5.12 ZINC ALLOYS

The main application of zinc alloys is for high production when a large number of identical electrodes are required which can be mass produced by pressure diecasting or can be coined. Complex shapes of electrodes can be easily diecast compared to machining used with other electrodes. The main disadvantage with zinc alloys is their rapid corner wear and very poor wear ratio (RAO, 2009).

## CHAPTER 6

### SELECTED MATERIALS FOR EDM ELECTRODES

This chapter presents the materials that were selected to be evaluated in the SLS machine and then to be used as EDM electrodes: pre-alloyed copper-nickel and molybdenum powders, and the reasons those materials are interesting choices.

#### 6.1 INTRODUCTION

As previously mentioned, in the research work of Eubank *et al.* (1998), the authors have improved the process for making electrodes of  $ZrB_2/Cu$ , to the point where their electrodes were superior to pure copper and various graphite's and somewhat better than  $W-Cu$ , a more expensive MMC. They concluded that the ideal non-eroding electrode is understood to be of a material with both high melting point and high thermal conductivity. N. Mohri & T. Tani (2006) also state that the machining rate or electrode wear under certain conditions depends on thermal properties peculiar to each material. According to them, experimental data reveal that in EDM, materials with large product of thermal conductivity and melting temperature have small wear.

As the main goal of this research work is to manufacture EDM electrodes by means of Selective Laser Sintering (SLS), the materials must be chosen in a suitable way for both processes. This characteristic can be achieved by mixing a high melting point and high temperature resistance material with materials that have good thermal and electrical conductivity. The difficulty is in finding materials with suitable properties that make them feasible for both EDM and SLS processes.

Materials with high melting point and high thermal conductivity were investigated. Studying what both processes require, the following powder materials were selected: pre-alloyed Cu-Ni and molybdenum. The Cu-Ni alloy represented the binder in the SLS process and the electrical and thermal conductor in the EDM process, while

molybdenum was acting as a structural material in the SLS process and improving the wear properties of the electrode in the EDM process. The properties and the features that make those materials interesting for the use as EDM electrodes are presented as follows.

## 6.2 COPPER-NICKEL

As previously mentioned in section 5.2, copper is widely used as an EDM electrode material; it has good electrical and thermal conductivity and it is most frequently used when fine surface finishes are required in the workpiece. Table 6.1 shows some properties of copper material.

Table 6.1. Properties of copper and nickel (MatWeb).

<i>Properties</i> <i>Materials</i>	Electrical resistivity	Thermal conductivity	Melting point	Density	Thermal expansion coefficient	Specific heat capacity
	$\mu\Omega\cdot\text{cm}$	W/m.K	$^{\circ}\text{C}$	$\text{g}/\text{cm}^3$	$\mu\text{m}/\text{m}\cdot^{\circ}\text{C}$	J/g. $^{\circ}\text{C}$
Copper	1,70	357 (727 $^{\circ}\text{C}$ ) 401 (0 $^{\circ}\text{C}$ )	1083,2 - 1083,6	8,93	16,4 (20,0 - 100 $^{\circ}\text{C}$ ) 24,8 (925 $^{\circ}\text{C}$ )	0,385
Nickel	6,40	60,7	1455	8,88	13,1 (20,0 $^{\circ}\text{C}$ )	0,460

Nevertheless, copper material has some disadvantages for instance it has poor machinability, it is a difficult material to deburr, it has low melting point often causing high wear rate in relation to its material removal. In particular, during the EDM of deep cavities under roughing conditions, the volumetric thermal expansion of copper is considerably high, which usually compromises the flushing conditions of the debris (AMORIM, 2002).

Regarding the SLS process, the work of Leong *et al.* (2002) investigated the laser sintering process of the Ti-B<sub>4</sub>C-Cu and Ti-B<sub>4</sub>C-Cu-Ni powder systems. Some porosity was observed in the Ti-B<sub>4</sub>C-Cu system. To enhance wettability as well as energy absorption of Cu from laser beam, addition of Ni was adopted to improve the liquid phase sintering and hence to decrease the porosity. As a result, adding Ni (varying from

6,7 to 30,4 wt.%) to the Ti-B<sub>4</sub>C-Cu powder system, the degree of porosity in the samples was dramatically reduced (almost full dense parts could be obtained due to improvement of wetting). Some properties of nickel material are presented in Table 6.1.

### 6.3 MOLYBDENUM

Molybdenum is a refractory metal and has good thermal conductivity and low coefficient of thermal expansion. These properties make molybdenum an interesting material to be used as an EDM electrode. Table 6.2 shows some properties of molybdenum.

Table 6.2. Properties of molybdenum (MatWeb).

<i>Properties</i> <i>Materials</i>	Electrical resistivity	Thermal conductivity	Melting point	Density	Thermal expansion coefficient	Specific heat capacity
	$\mu\Omega\cdot\text{cm}$	W/m.K	$^{\circ}\text{C}$	$\text{g}/\text{cm}^3$	$\mu\text{m}/\text{m}\cdot^{\circ}\text{C}$	J/g. $^{\circ}\text{C}$
Molybdenum	5,70	138	2617	10,22	5,35 (20,0 $^{\circ}\text{C}$ )	0,255

Molybdenum has many unusual and useful properties. The vast majority of engineering applications utilize this metal's high melting temperature, high strength and stiffness especially at elevated temperatures, resistance to chemical corrosion in many media, and its excellent thermal and electrical properties. This combination of properties makes available new design concepts for higher operating efficiency and improved service performance than are possible with other more common materials (BURMAN, 1984).

Molybdenum is a rare, silvery white metal with an extremely high melting point. It is commonly used in wire supports holding the glowing filament in light bulbs (the main use of molybdenum is in heat-resistant components of light bulbs). Molybdenum is also an element in some stainless steels and in superalloys for jet and rocket engines. Chemicals containing molybdenum are used in some paints and dyes and for making fireproof materials (LEPORA, 2007).

An electrode made with a material that has high electrical and thermal conductivities, high melting point and low thermal expansion would provide a good combination of properties for use in an EDM process. The addition of molybdenum to copper would combine properties that are required for a good EDM performance.

In the work of Yih & Chung (1997), copper-matrix composites were fabricated by solid state sintering using the admixture method, a conventional powder metallurgy process using a mixture of reinforcement and matrix metal powder, in this case the reinforcement was molybdenum particles. Compaction was conducted by cold pressing in a graphite die followed by hot pressing. The authors discovered that 60 vol.% Mo for the Cu/Mo particle composite system corresponds to the limitation of the reinforcement content, i.e. critical volume fraction above which gives composites of high porosity.

## CHAPTER 7

### EXPERIMENTAL PROCEDURE

This chapter presents the experimental procedure used during the experimental part. The first step was the selection of the materials to be manufactured by the Selective Laser Sintering process and to be used as Electrical Discharge Machining electrodes afterwards and it was discussed in chapter 6. The materials used for the SLS experiments as well as their characterization, the SLS machine used to carry out the experiments, the experimental flowchart developed, the description of the experimental strategy and finally the equipment used for the characterization of the SLS parts are presented in this chapter.

#### 7.1 MATERIALS

The pre-alloyed copper-nickel powder material was obtained using an ALD VIGA 5S8 Gas Atomizer at the Zentrum für Funktionswerkstoffe gGmbH and the molybdenum powder material was purchased from H.C. Starck in Germany. The pre-alloyed Cu-Ni with 90 wt.% of copper and 10 wt.% of nickel (this mixture will be referred to as Cu(90)Ni(10) from now on) was chosen to be used as the first metallic matrix to be examined.

Prior to laser sintering, the metallic matrix was mixed with molybdenum powder in a specific amount selected based on previous research works (see section 6.2). The composition of the mixture was Mo 63 wt.% - Cu(90)Ni(10) 37 wt.%. The powders were mixed for 45 minutes using a WAB Turbula T2C mixer at the *Institut für Schweißtechnik und Trennende Fertigungsverfahren* (Institute of Welding and Machining).

The amount of nickel in the pre-alloyed Cu-Ni powder material, as well as the amount of molybdenum in the mixture, was varied in order to evaluate their influence on the densification process. Details of the material amounts will be presented later in sections 7.3.4 and 7.3.5.

### 7.1.1 Powder characteristics

The density of the powder materials was measured with a Porotec Helium pycnometer at the *Institut für Nichtmetallische Werkstoffe* (Institute of Nonmetallic Materials). It was also used a Scanning Electron Microscope (SEM) at the same institute for photos of the powder materials. The particle size distribution analysis was made with a Sympatec Helos (H0353) Particle Size Analysis machine at the *Zentrum für Funktionswerkstoffe gGmbH* (Center for Functional Materials).

#### a) Copper-nickel metal matrix

The copper-nickel metal matrix powder, i.e., Cu(90)Ni(10), has spherical particles (Fig. 7.1) and their size have a Gaussian distribution with the mean value near 33  $\mu\text{m}$  (Fig. 7.2). Its density is 8,925  $\text{g}/\text{cm}^3$ .

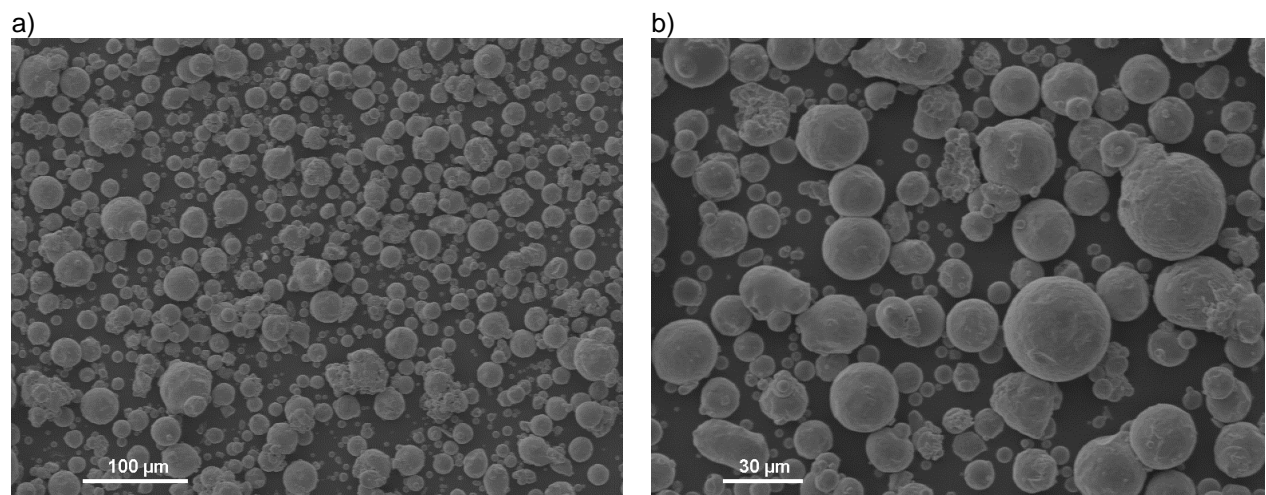


Figure 7.1. SEM image of the Cu(90)Ni(10) metal matrix powder: a) Magnification 200x, b) Magnification 500x.

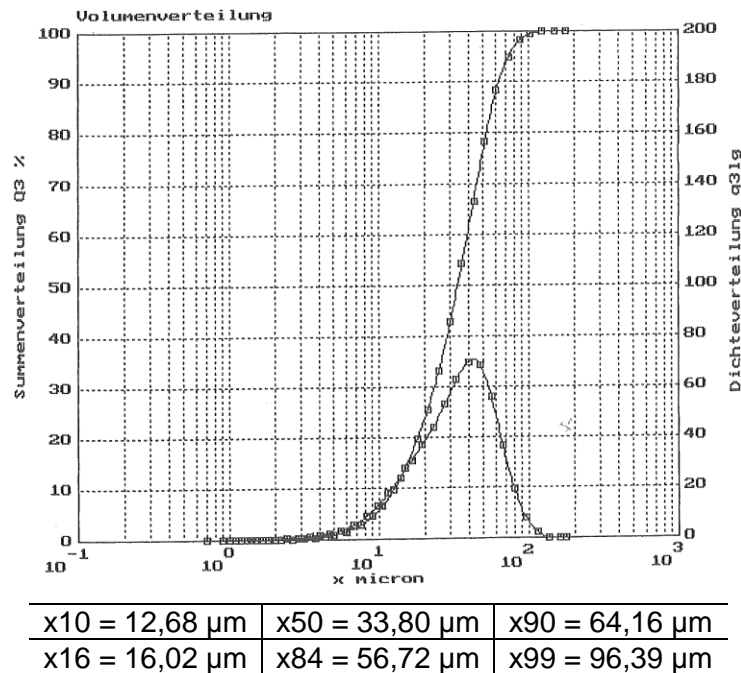


Figure 7.2. Particle size distribution of the Cu(90)Ni(10) powder.

A particle size distribution analysis was also made with the other copper-nickel metal matrix powder, i.e., Cu(70)Ni(30), which was investigated later. Its particle size has a Gaussian distribution with the mean value near 34  $\mu\text{m}$  (Fig. 7.3). Its density is 8,915  $\text{g}/\text{cm}^3$ .

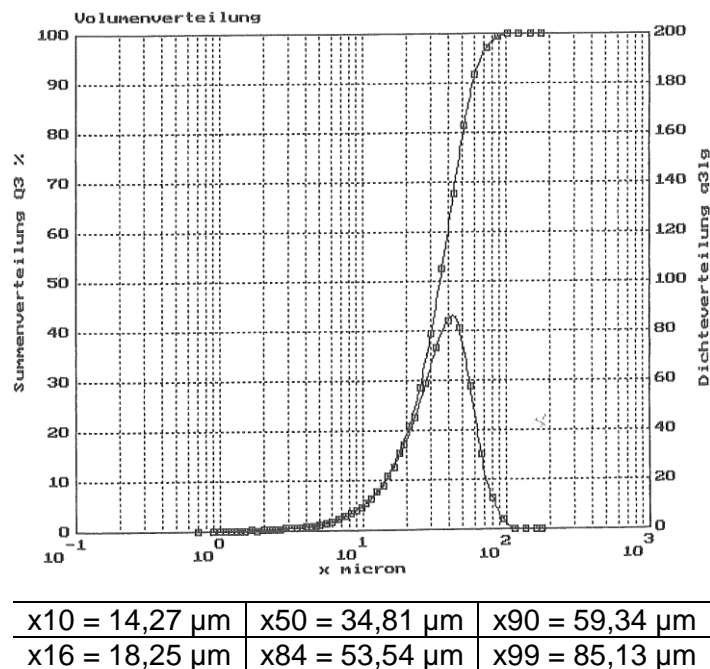


Figure 7.3. Particle size distribution of the Cu(70)Ni(30) powder.

## b) Molybdenum

The molybdenum powder presents Mo particle agglomerates (Fig. 7.4) and, according to the manufacturer H. C. Starck, it has particle size of 3-5  $\mu\text{m}$ . Its density is 10,22  $\text{g}/\text{cm}^3$ .

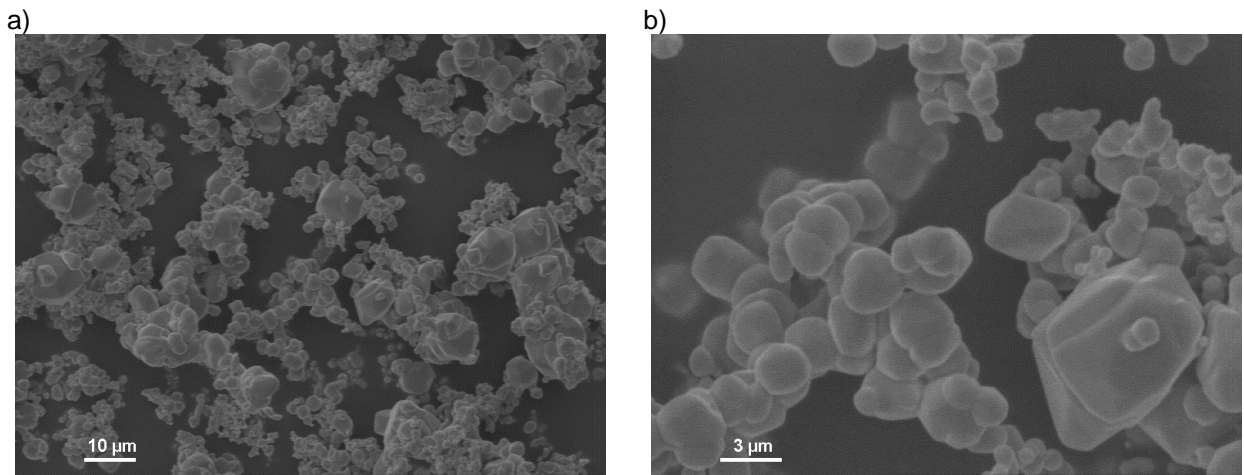


Figure 7.4. SEM image of the molybdenum powder: a) Magnification 1000x, b) Magnification 4000x.

The SEM image of the copper-nickel metal matrix, Cu(90)Ni(10), mixed with the molybdenum powder mixture, i.e., Mo 63 wt.% - Cu(90)Ni(10) 37 wt.%, is shown in Fig. 7.5. The density of the mixture was measured using a Porotec Helium Picnometer and it is 9,708  $\text{g}/\text{cm}^3$ .

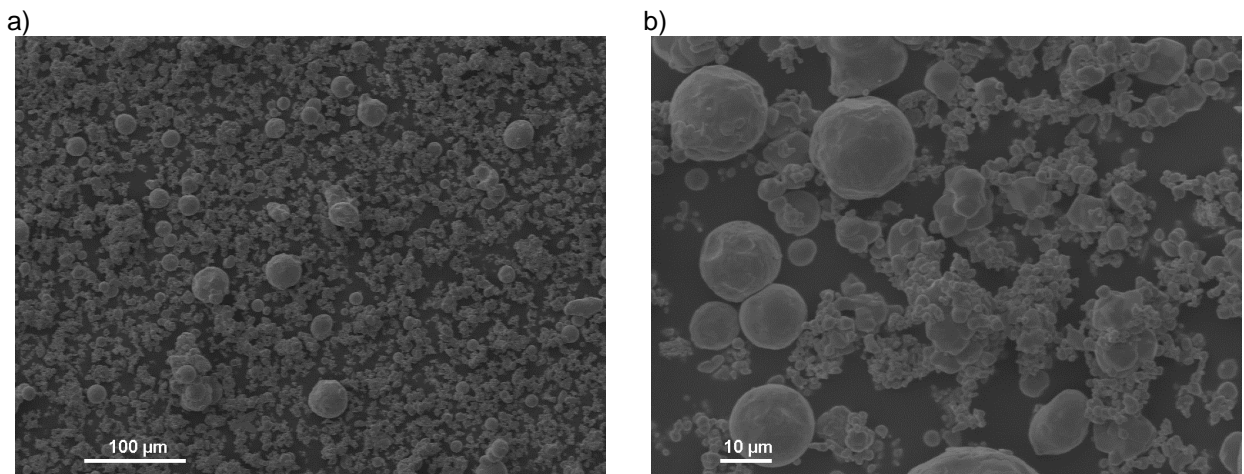


Figure 7.5. SEM image of the Mo 63 wt.% - Cu(90)Ni(10) 37 wt.% powder: a) Magnification 200x, b) Magnification 1000x.

## 7.2 EQUIPMENT USED IN THE EXPERIMENTS

The electrodes were manufactured in the *Technische Universität Clausthal* (TUC) in Germany at the *Institut für Maschinenwesen* (Institute of Mechanical Engineering). The SLS machine EOSINT M 250 X<sup>tended</sup> with a 200 W CO<sub>2</sub> laser and nitrogen atmosphere was used. The specifications and features of the SLS machine are presented in Appendix 1. The experiments were carried out manually for it was needed only a small amount of powder material. Unlike the automatic mode described in Fig. 3.2b, the manual method means that every step was controlled by an operator, i.e., the sintering by the laser beam, the movements of the blade and the building platform, as well as the deposition of the powder on the building platform.

## 7.3 EXPERIMENTAL FLOWCHART

In order to manufacture the electrodes and evaluate the influence of the main SLS parameters on the building process, an experimental strategy was developed and the flowchart is presented in Fig. 7.6.

Three SLS process parameters were chosen to be varied because of their importance in the laser energy delivery to the powder bed in the following order:

- 1) layer thickness,
- 2) laser scan speed and
- 3) hatch distance (the distance between two consecutive laser lines).

Specimens of simple geometry (10 x 10 x 3 mm) were manufactured in order to evaluate the influence of the SLS process parameters. The laser scanning strategy adopted was the stripes mode (Fig. 7.7). After the laser scans the contour of the part, it fills the respective cross-sectional area on the powder surface in which one layer is exposed in *x*-direction and the following layer in *y*-direction, i.e. a 90° rotation of the scan direction at every other layer.

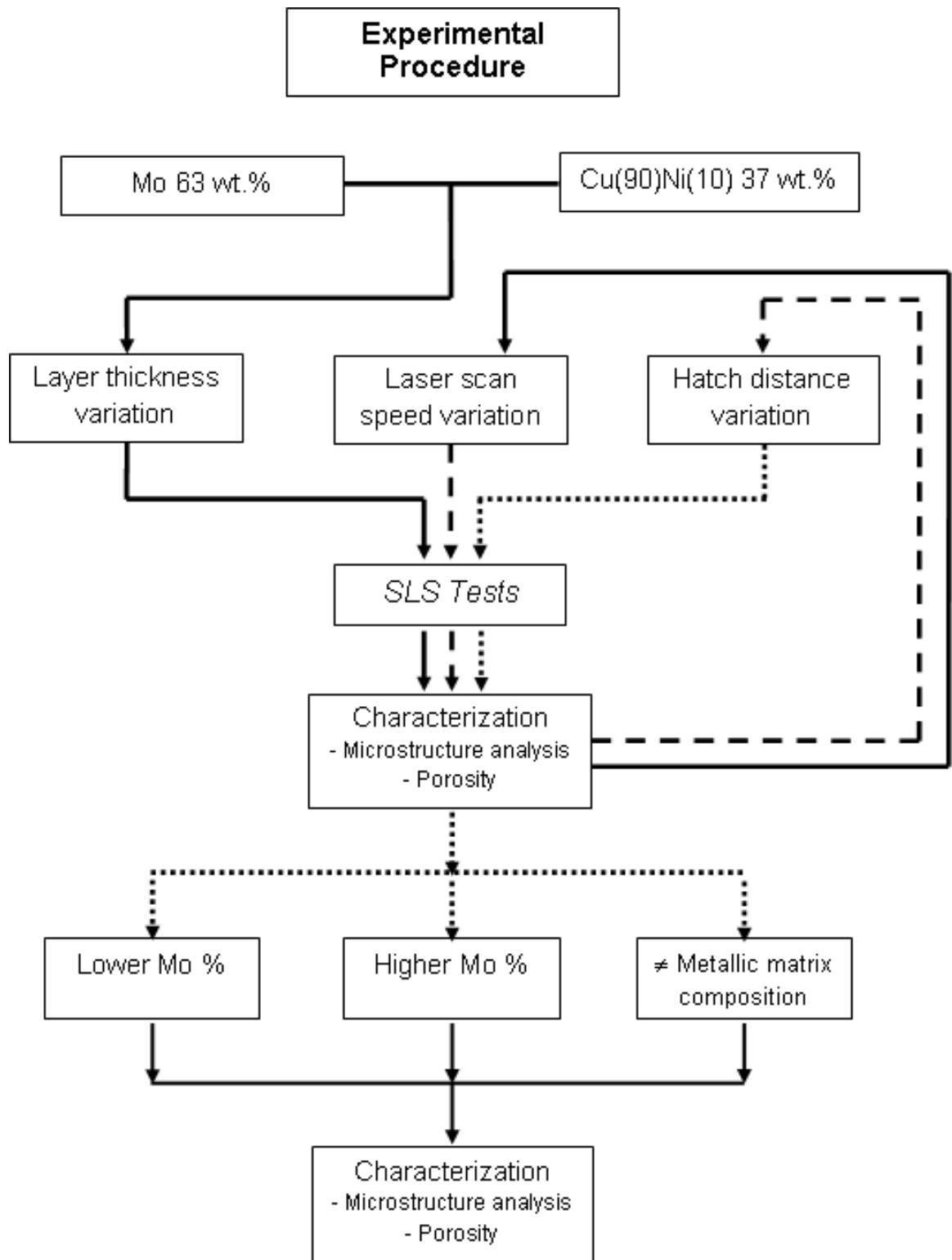


Figure 7.6. Experimental flowchart developed for the SLS experiments.

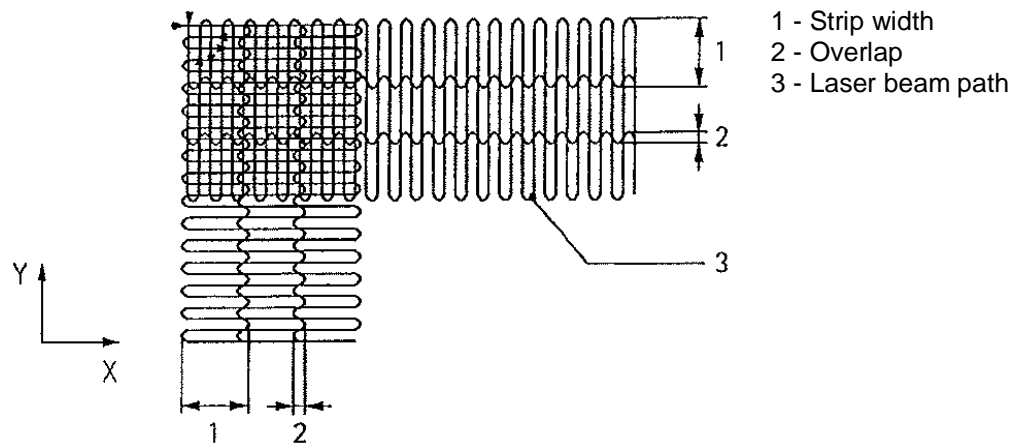


Figure 7.7. Laser scanning strategy (EOS RP-Tools, 1998).

### 7.3.1 Influence of the layer thickness on the porosity

The layer thickness was the first parameter to be used and its variation was made so that the minimum layer thickness was achieved, while maintaining good process conditions. The values of the SLS parameters, i.e., layer thickness, laser scan speed and hatch distance, are presented in Tab. 7.1. Each layer thickness was sintered 15 times, starting from 0,06 to 0,01 mm.

Table 7.1. SLS parameters – layer thickness experiments.

Layer thickness (mm)	Laser scan speed (mm/s)	Hatch distance (mm)
0,06 - 0,01	250	0,3
	150	
	50	

### 7.3.2 Influence of the laser scan speed on the porosity

After finding the most adequate layer thickness, the next step was to vary the laser scan rate. Six values were chosen from higher laser scan speed (low energy) to

lower laser scan speed (high energy). The values of the SLS parameters in this step are presented in Tab. 7.2.

Table 7.2. SLS parameters – laser scan speed experiments.

Layer thickness (mm)	Laser scan speed (mm/s)	Hatch distance (mm)
Most adequate	300	0,3
	250	
	200	
	150	
	100	
	50	

### 7.3.3 Influence of the hatch distance on the porosity

With the most adequate layer thickness and laser scan speed, the hatch distance parameter was varied. Three hatch distance values were chosen, also according to the energy delivered from the laser to the powder bed. Higher values mean less energy and vice-versa. The values of the SLS parameters are presented in Tab. 7.3. After this last step, it was considered that the main SLS parameters were investigated and the most adequate parameters were found.

Table 7.3. SLS parameters – hatch distance experiments.

Layer thickness (mm)	Laser scan speed (mm/s)	Hatch distance (mm)
Most adequate	Most adequate	0,4
		0,2
		0,1

The best combination of parameters used for the powder composition of Mo 63 wt.% - Cu(90)Ni(10) 37 wt.% was then applied to evaluate the influence of the amount of nickel in the metallic matrix on the densification process and the influence of the structural material quantity, by varying its amount, described next.

### **7.3.4 Influence of the amount of nickel on the porosity**

As previously mentioned, the nickel amount first used to discover the most adequate SLS parameters was 10 wt.% in the copper-nickel pre-alloy, i.e., Cu 90 wt.% + Ni 10 wt.% or Cu(90)Ni(10). Once the most adequate SLS parameters were found, i.e., layer thickness, laser scan speed and hatch distance, the next quantities to be studied were 0 wt.% and 30 wt.% of nickel or Cu(100) and Cu(70)Ni(30), respectively.

### **7.3.5 Influence of the amount of molybdenum on the porosity**

The first composition of the mixture, Mo 63 wt.% - Cu(90)Ni(10) 37 wt.% or Mo 60 vol.% - Cu(90)Ni(10) 40 vol.%, was used during the experiments for the most adequate SLS parameters. In order to evaluate the influence of molybdenum, the composition was varied to more molybdenum amount, i.e., Mo 82,08 wt.% - Cu(90)Ni(10) 17,92 wt.% or Mo 80 vol.% - Cu(90)Ni(10) 20 vol.% as well as to less molybdenum amount, i.e., Mo 43,29 wt.% - Cu(90)Ni(10) 56,71 wt.% or Mo 40 vol.% - Cu(90)Ni(10) 60 vol.%.

The strategy described was adopted to reduce the number of experiments, while making possible to analyze the influence of the main SLS parameters as well as the influence of nickel and structural material amount on the densification process. By using the best layer thickness to vary the speed rate and using the best speed rate to vary the hatch distance, the number of experiments was greatly reduced if compared to a strategy where a complete investigation of each parameter is carried out, i.e., for each parameter, all other parameters are investigated.

#### 7.4 CHARACTERIZATION OF THE SINTERED PARTS

After sectioning, mounting, grinding and polishing the sintered parts, microstructure analysis was made using a Light Optical Microscope (LOM) at the *Institut für Materialprüfung und Werkstofftechnik* (Institute for materials testing and materials engineering) - Dr. Neubert GmbH.

The samples were cut from the sintered specimens and mounted in a cold curing resin for metallographic testing. The grinding was performed with SiC sand paper, starting from 120 to 1200 grit finish. After grinding the samples were rough and finish polished. For rough polishing a diamond suspension of 6  $\mu\text{m}$  was used. The samples from the hatch distance tests and the different amount of nickel and molybdenum tests were covered with wax and, after that, polished by colloidal silica emulsion polishing (OPS) for a better picture quality (without scratches). Between each grinding and polishing process the specimens were cleaned with an ultrasonic ethanol bath using a Bandelin Sonorex RK 52 H Ultrasonic Cleaner, in order to remove impurities. The sintered samples were porous, facilitating the access of water inside the pores. Therefore the use of water was restrained during the process, to improve the quality of the micrographs. The samples were not etched.

Micrographs of the cross-sectioned parts were taken using a Jenavert microscope fitted with an Olympus DP10 camera and Photoimpact 10 Software. The porosity of the cross-section of the parts was estimated with the aid of the GNU Image Manipulation Program software.

After the last step of the experimental strategy, i.e., the hatch distance experiments, a CamScan Scanning Electron Microscope and a Zeiss Stereomicroscope at the *Institut für Nichtmetallische Werkstoffe* (Institute of Nonmetallic Materials) were used for the characterization of the top surface of the parts.

After the most adequate SLS parameters were found, the final parts were built to be used as EDM electrodes and the porosity of the sintered parts was measured using a Micromeritics' GeoPyc 1360 Density Analyzer at the *Institut für Nichtmetallische Werkstoffe* (Institute of Nonmetallic Materials).

## CHAPTER 8

### RESULTS AND DISCUSSION

For the Selective Laser Sintering of the parts, a thin layer of powdered material was spread over the surface of a building platform and leveled by a wiper (blade). The laser beam then selectively scanned the powder bed according to the CAD data and this process was repeated layer-by-layer until the part was built. This chapter will present the results achieved after the layer thickness, laser scan speed and hatch distance experiments. The results of the different amount of nickel and molybdenum in the mixtures are also presented.

#### 8.1 INFLUENCE OF THE LAYER THICKNESS ON THE POROSITY

With the Mo 63 wt.% - Cu(90)Ni(10) 37 wt.% mixture, the SLS parts manufactured with laser scan speed of 250, 150 and 50 mm/s for the layer thickness experiments are shown in Fig. 8.1.

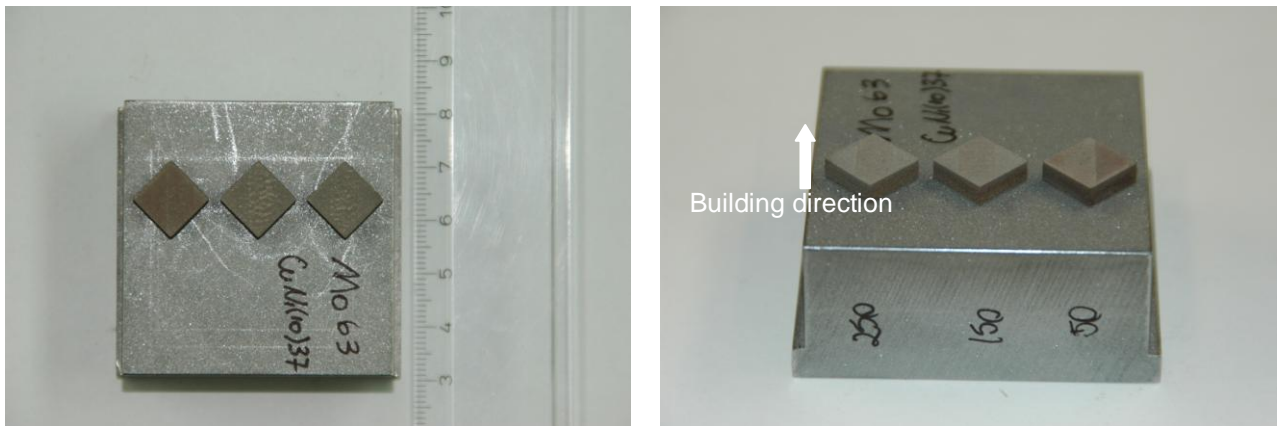


Figure 8.1. SLS parts after the layer thickness experiments.

The SLS process worked well for all layers and for the three velocities as well. The parts had good adhesion to the building platform. The part with 50 mm/s (more energy) presented darker colour compared to the other parts. Visually, it appeared that

with the decreasing of the layer thickness, the surface finish became smoother. The micrographs of the cross-section of the parts produced with each velocity are shown in Fig. 8.2.

a)



b)



c)

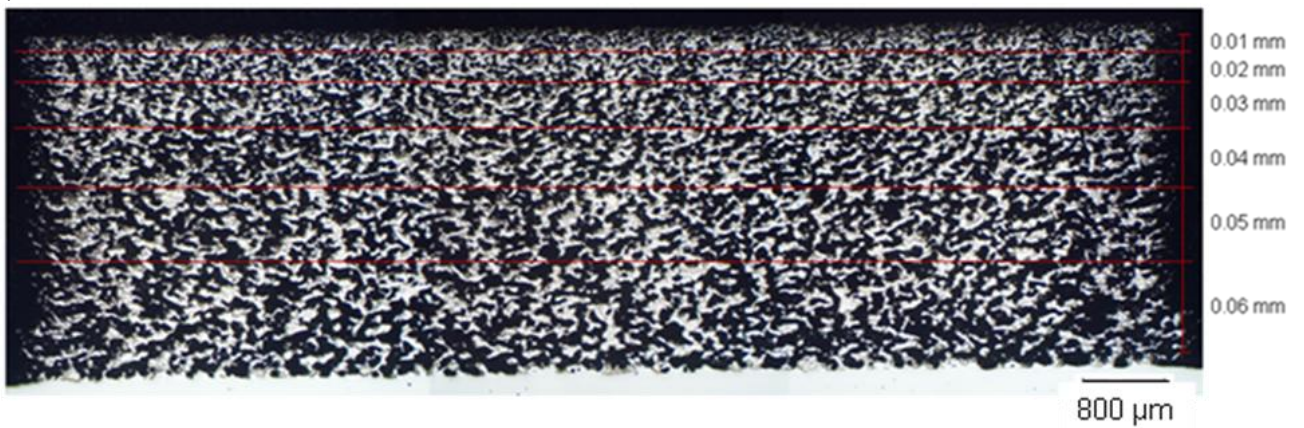


Figure 8.2. Micrographs of the SLS parts after the layer thickness experiments (the black spaces represent the pores): a) 250 mm/s, b) 150 mm/s, c) 50 mm/s. Magnification 3,2x.

It can be seen that the smaller the layer thickness, less porosity is observed; higher layer thickness might provide insufficient laser penetration depth resulting in poor adhesion between the sintered layers. Decreasing the layer thickness, the bonding ability between sintered layers was improved. The most adequate layer thickness was chosen to be 0,02 mm, for it presented less porosity than the thicker layers.

The minimum layer thickness that can be effectively used is determined mostly by the maximum particle size. Under a certain layer thickness, the wiper can drag non-melted big particles or chunks of melted particles, displacing the previously sintered layers from their position. However, the process worked well for the layer thickness of 0,02 mm, below the particle size of the larger particle of the mixture, Cu-Ni (~ 30  $\mu\text{m}$ ).

When the laser beam scans over the powder layer, the laser energy is absorbed in a narrow layer of individual powder particles inducing a high temperature of the particle surface. The heat generated during laser–powder interaction is difficult to conduct and transfer into the interior of the powder layer, especially for a thicker layer. In this case, interconnected pore channels between adjacent layers would be formed, since the powder layer has not been completely melted down due to the insufficient energy penetration of the laser beam. For a thinner layer, the laser energy can not only completely penetrate the current layer, but also remelt the surface of the previously sintered layer, thus obtaining bonded layers (GU; SHEN, 2009).

## 8.2 INFLUENCE OF THE LASER SCAN SPEED ON THE POROSITY

Using layer thickness of 0,02 mm and hatch distance of 0,3 mm, the SLS parts were manufactured with laser scan speed of 300, 250, 200, 150, 100 and 50 mm/s for the laser scan speed experiments and they are shown in Fig. 8.3.

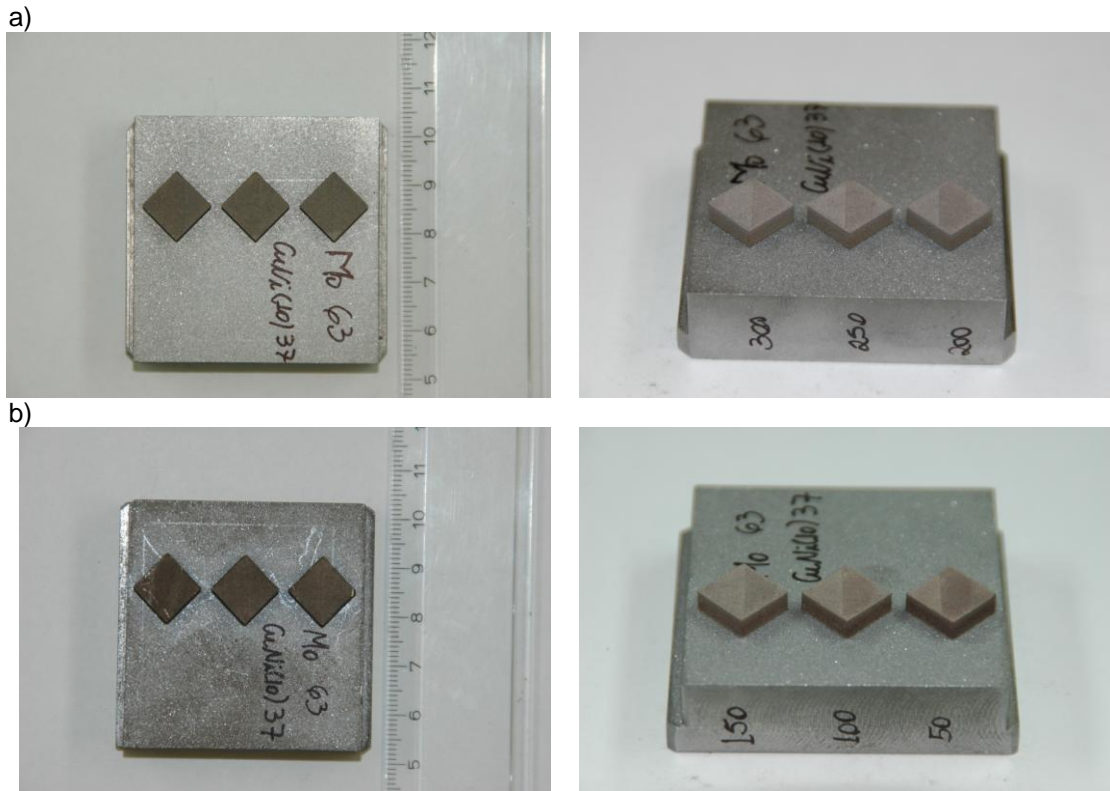
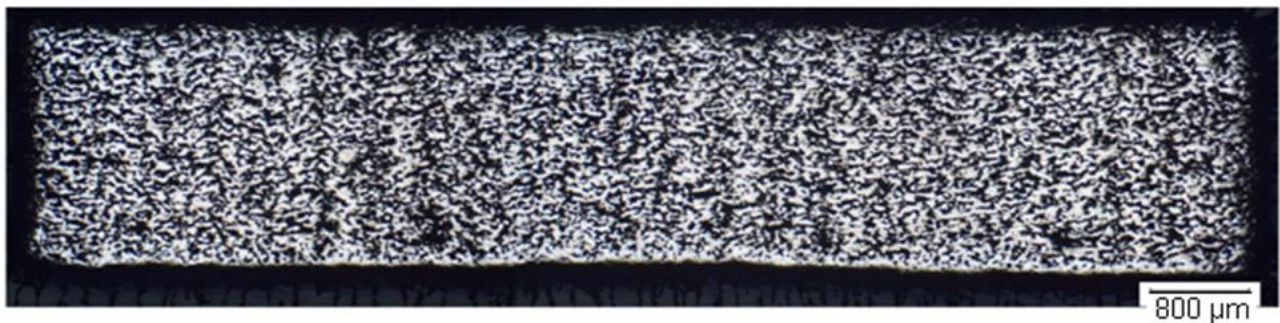


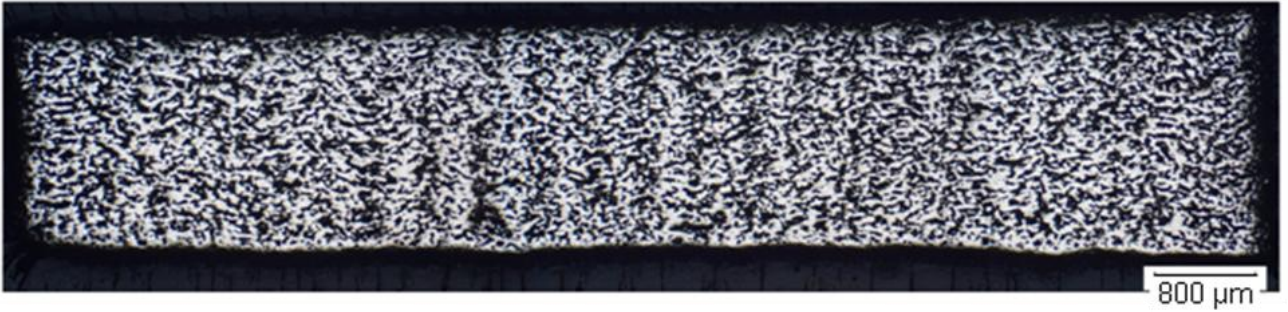
Figure 8.3. SLS parts produced with laser scan speed of: a) 300, 250, 200 mm/s, b) 150, 100, 50 mm/s.

The SLS process worked well for the six different laser scan speeds. Variation in colour could be seen; decreasing the laser scan speed a darker colour could be observed (piece with 50 mm/s was darker on the surface) and it might be due to the higher delivered energy. The micrographs of the cross-section of the parts produced with each laser scan speed are shown in Fig. 8.4.

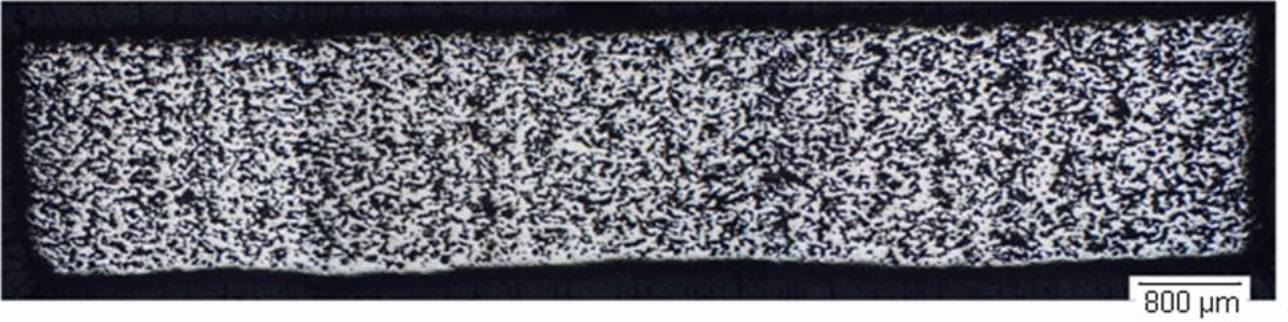
a)



b)



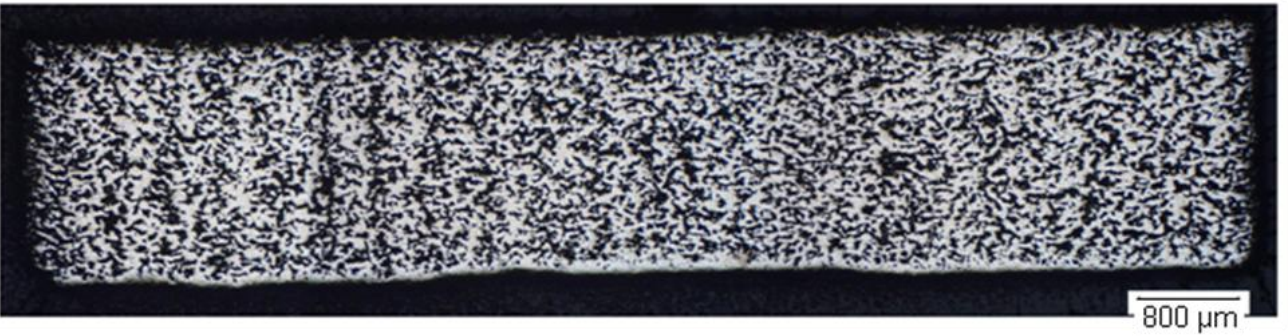
c)



d)



e)



f)



Figure 8.4. Micrographs of the SLS parts after the laser scan speed experiments (the black spaces represent the pores): a) 300 mm/s, b) 250 mm/s, c) 200 mm/s, d) 150 mm/s, e) 100 mm/s, f) 50 mm/s. Magnification 3,2x.

The micrographs show that there is no apparent difference in porosity of the parts between the different laser scan speeds. The porosity of the cross-section of the parts was estimated with the aid of the GNU Image Manipulation Program software, and the result is showed in Fig. 8.5. It can be said that decreasing the laser scan speed increases the energy delivered to the powder bed due to the longer interaction time of the laser beam with the powder and thus can lead to less porosity. Because the laser scan speed of 50 mm/s slightly presented less porosity, it was the scan speed chosen to build the next parts, i. e., varying the hatch distance.

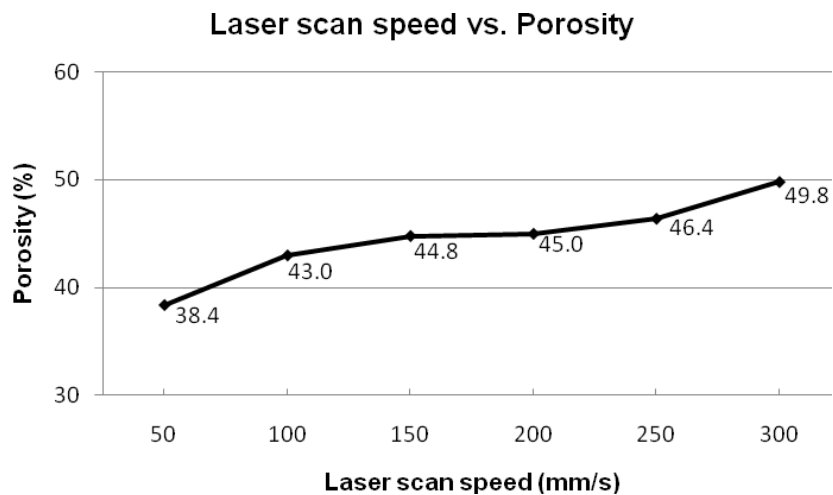


Figure 8.5. Influence of the laser scan speed on porosity.

Laser sintering of the CuNi-Mo system starts with the selective melting of Cu-Ni component by the laser beam to form liquid phase, due to a significant difference in the melting temperatures of Cu-Ni and Mo (1.083 against 2.617°C). As the laser beam moves away, the solid-liquid mixture undergoes a rapid solidification process as a result of the rearrangement of the solid particles under the influence of capillary forces exerted on them by the liquid.

With lower energy (higher laser scan speed), the part presented low amount of liquid formation due to an insufficient melting of the low melting point Cu-Ni system, which resulted in more amount of porosity after laser sintering.

With more energy (lower laser scan speed), there was a better melting of the Cu-Ni system, thus producing a more sufficient amount of liquid phase. More molten liquid is likely to flow and infiltrate into the voids between the Mo particles, resulting in a slightly denser structure.

### 8.3 INFLUENCE OF THE HATCH DISTANCE ON THE POROSITY

With the most adequate layer thickness and laser scan speed found, the next step was to find the most adequate hatch distance, the distance between two laser lines. The SLS parts manufactured with hatch distance of 0,4, 0,2 and 0,1 mm are shown in Fig. 8.6.

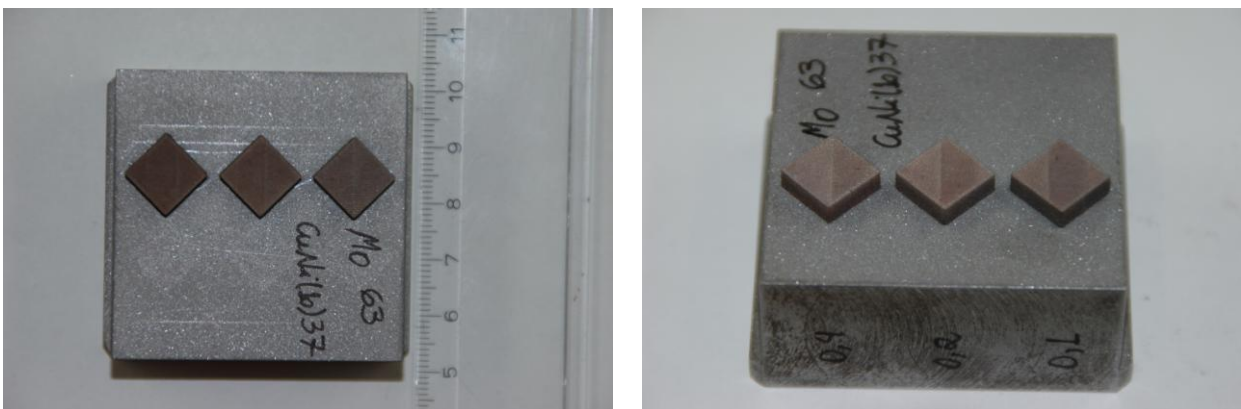
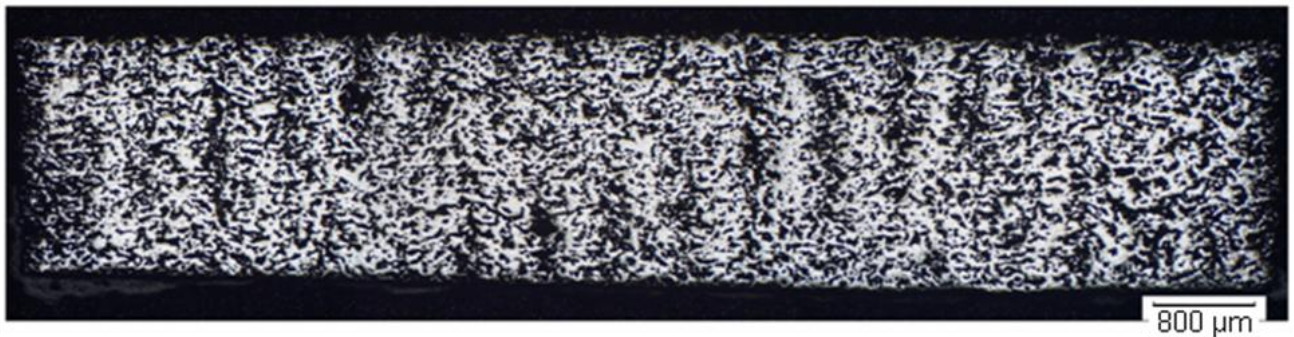


Figure 8.6. SLS parts after the hatch distance experiments.

The SLS process worked well for the three hatch distances. Regarding the color of the parts, it can be said that the smaller the hatch distance, the darker was the part probably due to the higher delivered energy as a result of the overlapping between the adjacent laser lines.

The micrographs of the cross-section of the parts produced with each hatch distance are presented in Fig. 8.7, including the one with 0,3 mm from the laser scan speed experiments for comparison.

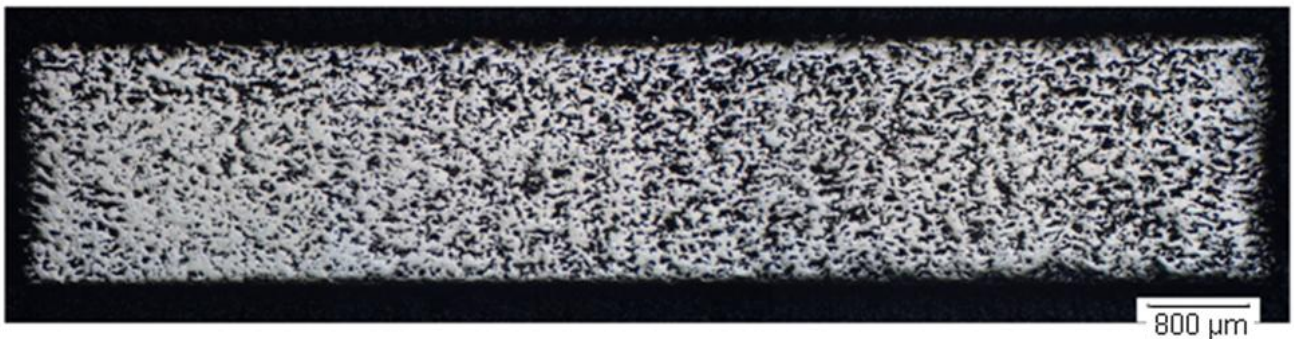
a)



b)



c)



d)

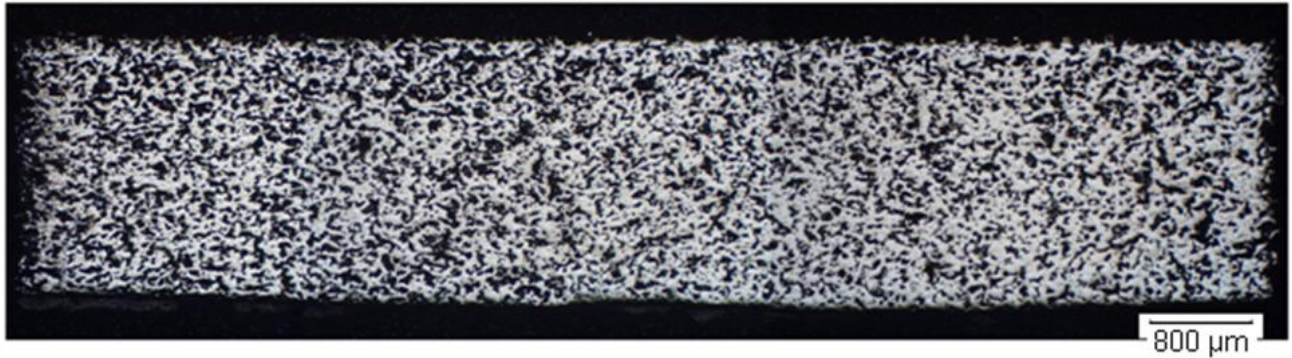


Figure 8.7. Micrographs of the SLS parts after the hatch distance experiments (the black spaces represent the pores): a) 0,4 mm, b) 0,3 mm, c) 0,2 mm, d) 0,1 mm. Magnification 3,2x.

The micrographs show that there is no apparent difference in terms of porosity between the hatch distances of 0,3, 0,2 and 0,1 mm. In the case of the hatch distance of 0,4 mm, as the laser beam spot size is 0,4 mm, probably there was not enough overlapping between the adjacent laser lines, resulting in a porous part (Fig. 8.7-a).

Decreasing the hatch distance brings the scan lines closer to each other until they overlap. With the overlapping of the adjacent lines a large part of the laser spot would scan over the previously scanned line and, therefore, remelt the previously sintered materials. This helps the flow and spreading of liquid between adjacent scan lines, leading to the enhancement of the inter-line bonding and the reduction in the sintered porosity (GU; SHEN, 2009).

The result of the estimation of the porosity of the cross-section of the parts with the aid of the GNU Image Manipulation Program software is presented in Fig. 8.8. It shows a decrease of porosity from hatch distance of 0,1 to 0,2 mm followed by an increase of porosity from 0,2 to 0,4 mm.

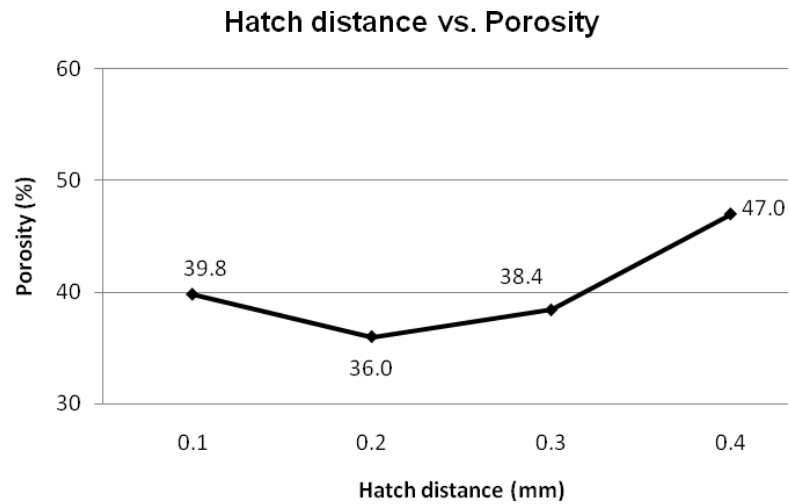


Figure 8.8. Influence of the hatch distance on porosity.

Because the hatch distance of 0,2 mm slightly presented less porosity, it was the hatch distance selected and with that it can be said that the most adequate SLS parameters were found.

Images from a stereomicroscope were taken from the top surface of the parts (Fig. 8.9). There is not a big variation between the hatch distances of 0,1 and 0,2 mm. However it is possible to see the laser lines on the part manufactured with hatch distance of 0,4 mm.

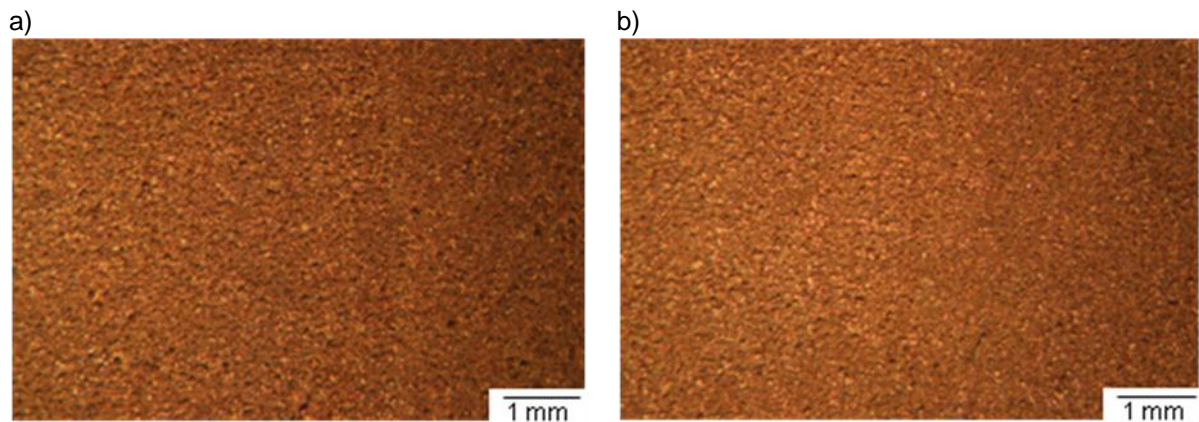
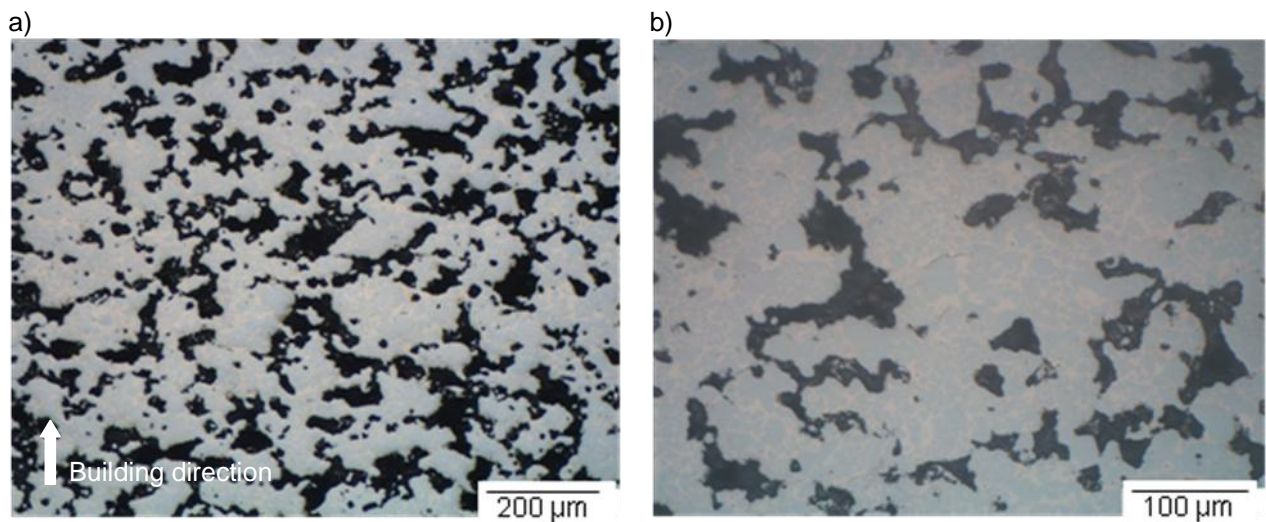




Figure 8.9. Stereomicroscope images of the top of the parts after the hatch distance experiments: a) 0,1 mm, b) 0,2 mm, c) 0,4 mm.

Through a series of laser sintering experiments, the following optimized processing parameters were chosen for the Mo 63 wt.% - Cu(90)Ni(10) 37 wt.% mixture: layer thickness of 0,02 mm, laser scan speed of 50 mm/s and hatch distance of 0,2 mm.

Figure 8.10 shows the optical micrographs of polished section of the Mo 63 wt.% - Cu(90)Ni(10) 37 wt.% mixture laser sintered part with the optimized parameters in higher magnification. The black spaces represent the pores.



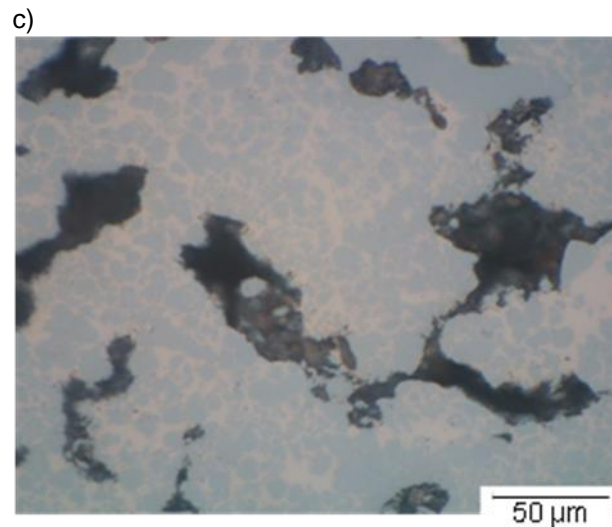


Figure 8.10. Optical micrographs of Mo 63 wt.% - Cu(90)Ni(10) 37 wt.% mixture laser sintered part with the optimized SLS parameters: a) 12,5x, b) 25x, c) 50x.

In the SLS process, the laser temperature ranges from 800 – 1.200°C. The melting point of copper (1.083°C) is in between those values, which means that the copper-nickel particles melted by the laser beam while the molybdenum particles (melting point of 2.617°C) were dispersed in the metallic matrix. It is possible to see in Fig. 8.10 separated Mo particles in the Cu-Ni matrix as well as Mo particles contacting each other to form Mo particle clusters, with a poor densification. Discontinuous agglomerates were formed, separated by large and interconnected pore channels.

In addition, SEM images were taken from the top of the parts (the surface was not polished neither etched). Figure 8.11 shows the SEM images of the part that was manufactured with the most adequate SLS parameters found, i.e., layer thickness of 0,02 mm, laser scan speed of 50 mm/s and hatch distance of 0,2 mm. It is possible to see a porous sintered surface containing melted areas as well some unsintered copper-nickel and molybdenum powder particles. It can be said that the energy delivered to the powder bed was enough for liquid phase sintering; however, it was not enough for the melting and connection of all Cu-Ni particles.

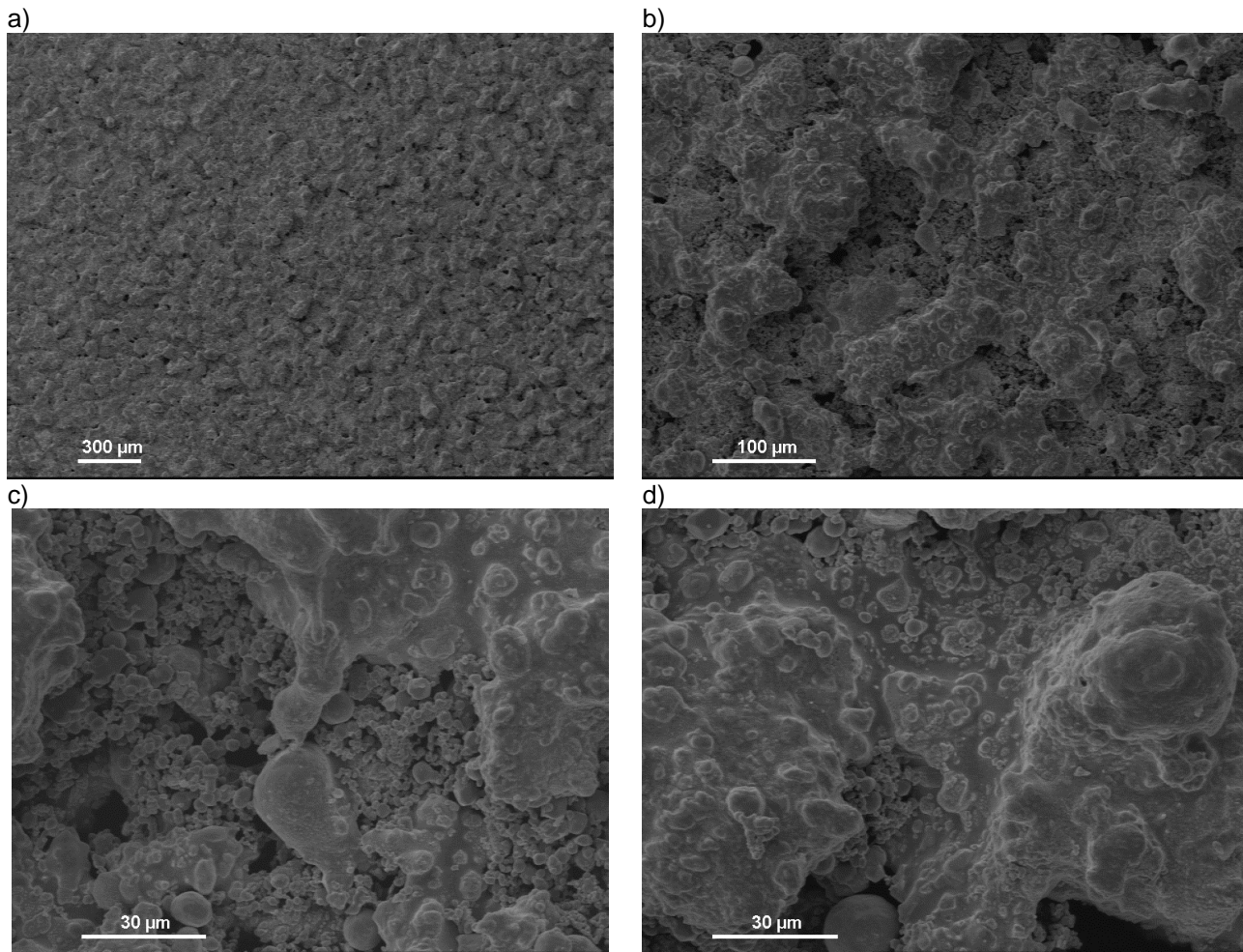


Figure 8.11. SEM images of the top surface of the laser sintered part with the optimized SLS parameters: a) Magnification 40x, b) Magnification 200x, c) and d) Magnification 800x.

#### 8.4 SLS PARTS BUILT TO BE USED AS EDM ELECTRODES

After the most adequate SLS parameters were found, i.e., layer thickness of 0,02 mm, laser scan speed of 50 mm/s and hatch distance of 0,2 mm, final parts with 10x10x10 mm were built to be used as EDM electrodes. For porosity measurements, a rounded shape is most adequate, so parts with different geometries were built: a cylinder shape with 0,2 mm hatch distance and the three others (barrel shape) with 0,1, 0,2 and 0,3 mm (Fig. 8.12). The final parts were built manually and it took 27 hours.



Figure 8.12. SLS parts for EDM experiments.

The porosity measurements of the barrel shaped parts are presented in Fig. 8.13. The porosity measurement of the cylinder shaped part with hatch distance of 0,2 mm is not presented in Fig. 8.13; it corresponds to 29,2 %. It can be seen that there is not a big difference in the porosity values of the parts for both estimated and measured values. However, there is a significant difference when one compares the estimated porosity and the measured porosity. This might be because of the method that the samples were prepared for the microstructure analysis, as described in section 7.4.

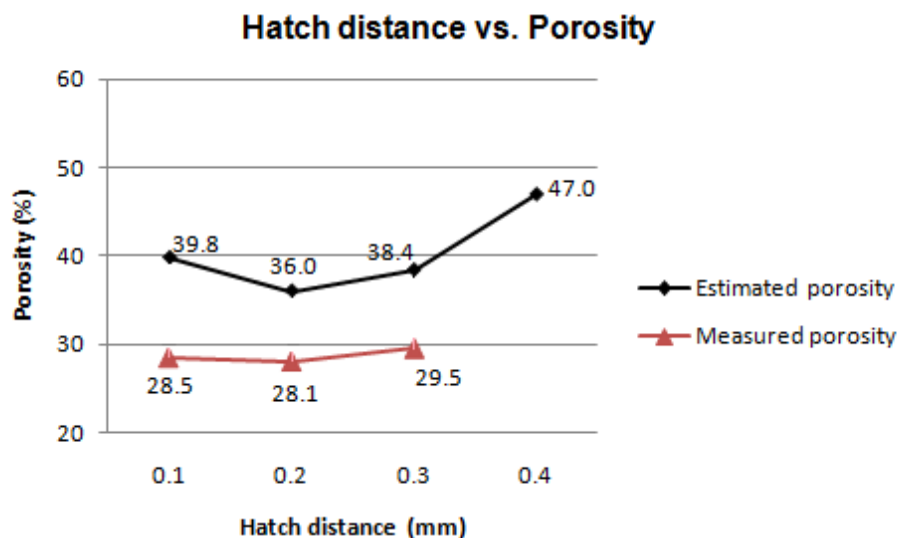


Figure 8.13. Estimated and measured porosities after the hatch distance experiments.

## 8.5 INFLUENCE OF THE AMOUNT OF MOLYBDENUM ON THE POROSITY

In order to investigate the influence of the molybdenum amount in the mixture on the densification process, its amount was varied to more and less than the current amount (63 wt.%) in the mixture, using the most adequate SLS parameters found previously, i.e., layer thickness of 0,02 mm, laser scan speed of 50 mm/s and hatch distance of 0,2 mm.

The SLS parts manufactured with the Mo 43,3 wt.% - Cu(90)Ni(10) 56,7 wt.% mixture and with the Mo 82 wt.% - Cu(90)Ni(10) 18 wt.% mixture are shown in Fig. 8.14.

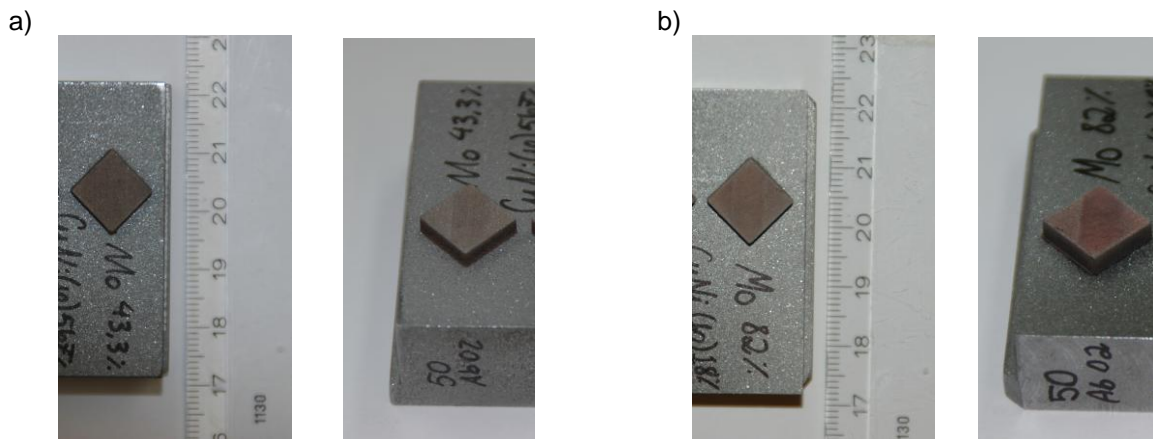


Figure 8.14. SLS parts: a) Mo 43,3 wt.% - Cu(90)Ni(10) 56,7 wt.% mixture, b) Mo 82 wt.% - Cu(90)Ni(10) 18 wt.% mixture.

The micrographs of the cross-section of the parts are shown in Fig. 8.15 as well as the micrograph of Mo 63 wt.% - Cu(90)Ni(10) 37 wt.% mixture for comparison.

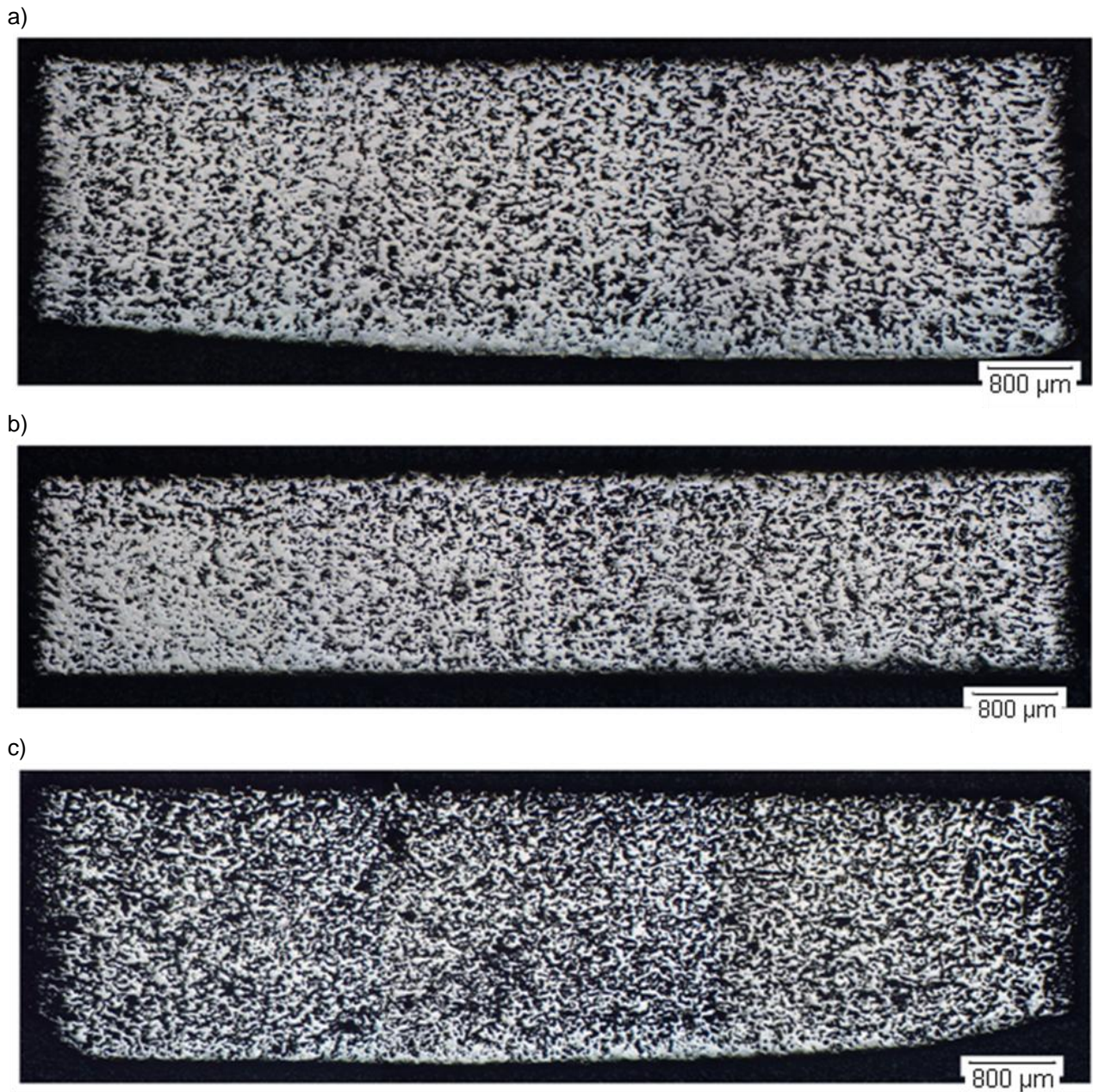


Figure 8.15. Micrograph of the SLS parts: a) Mo 43,3 wt.% - Cu(90)Ni(10) 56,7 wt.% mixture, b) Mo 63 wt.% - Cu(90)Ni(10) 37 wt.% mixture, c) Mo 82 wt.% - Cu(90)Ni(10) 18 wt.% mixture. Magnification 3,2x.

Figure 8.15 shows that at Mo contents of 43,3 wt.% and 63 wt.% the parts presented similar level of porosity and that it increased when the Mo content increased to 82 wt.%. The porosity of the cross-section of the parts was estimated with the aid of the GNU Image Manipulation Program software, and the result is showed in Fig. 8.16.

At a high Mo content, the higher porosity could be due to the small amount of Cu-Ni particles, which could not flow through the Mo particles to fill up the interstices. The liquid phase was only enough to bind the neighboring Mo particles, forming discontinuous agglomerates with large interconnected pores. At Mo content of 43,3 wt.%, there was a sufficient amount of Cu-Ni particles to surround the Mo particles, so the porosity was lower.

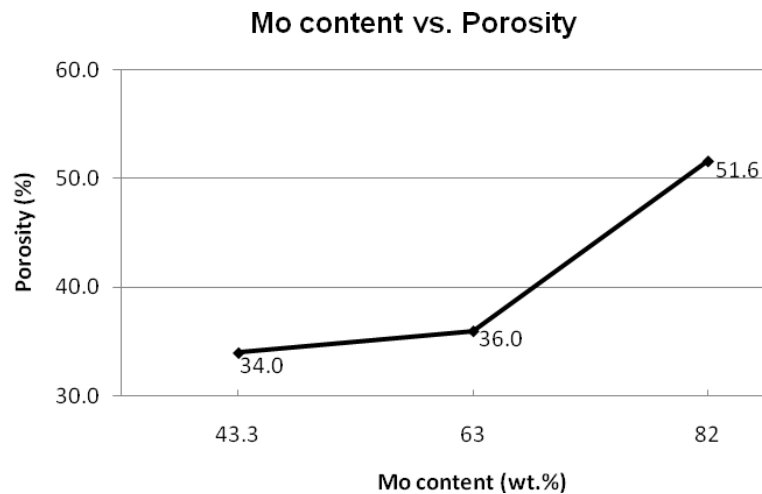
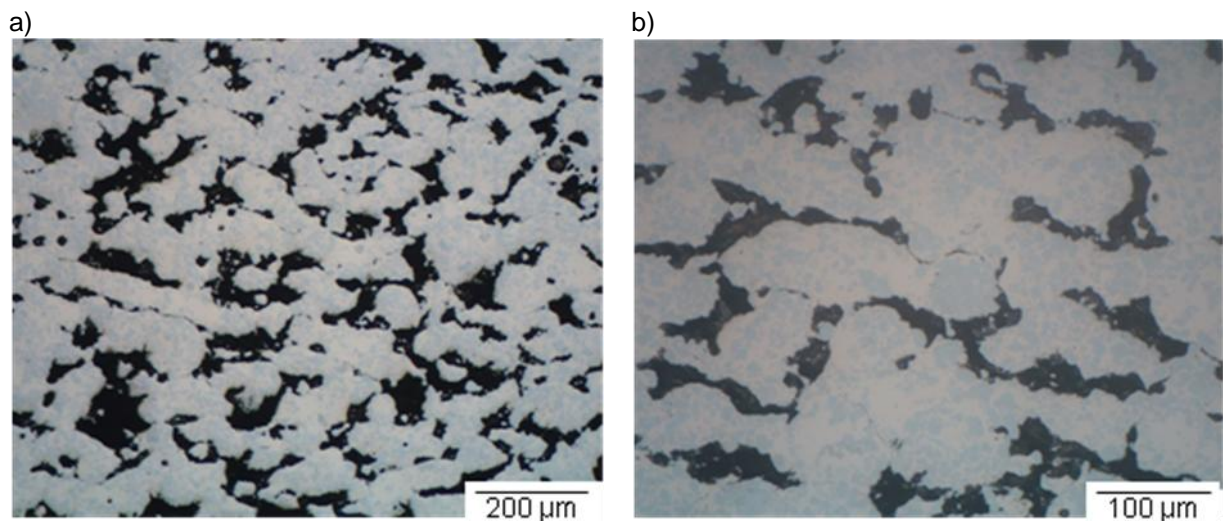


Figure 8.16. Influence of the Mo content on porosity.

Figure 8.17 shows the optical micrographs of polished section of the Mo 43,3 wt.% - Cu(90)Ni(10) 56,7 wt.% mixture laser sintered part with the optimized parameters in higher magnification.



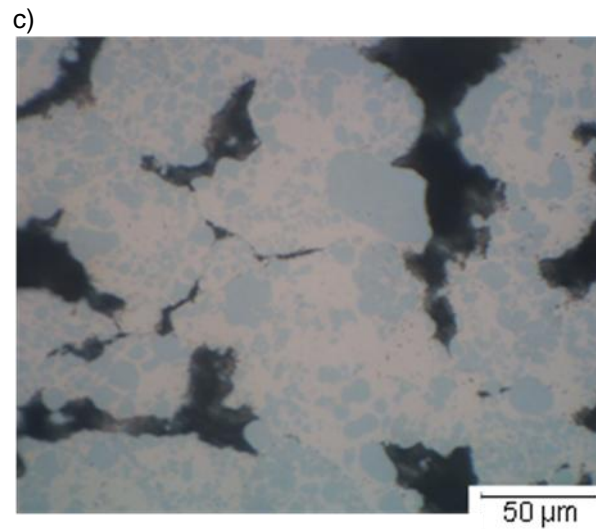
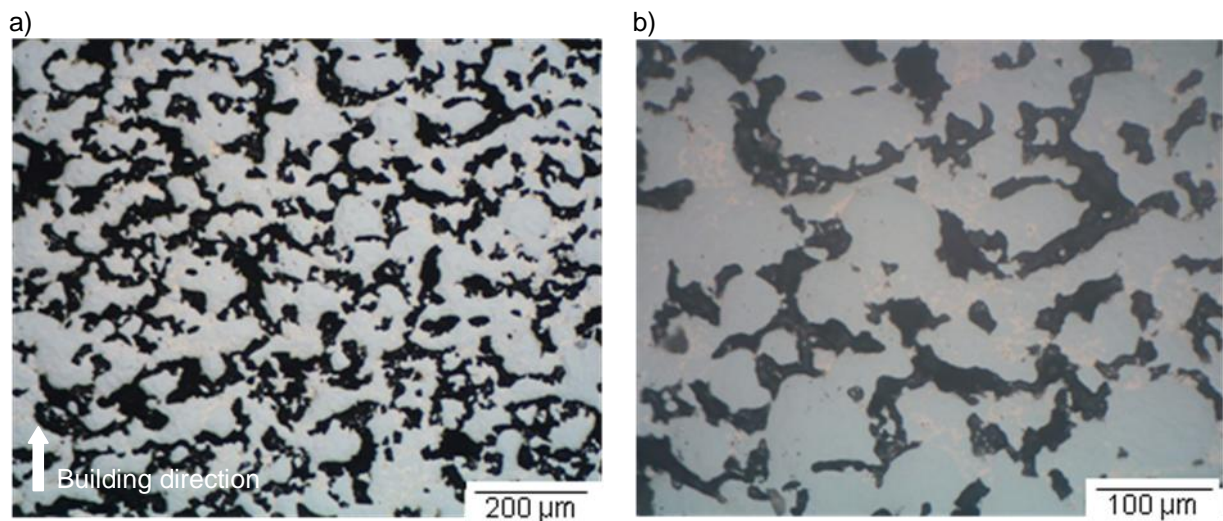


Figure 8.17. Optical micrographs of Mo 43,3 wt.% - Cu(90)Ni(10) 56,7 wt.% mixture laser sintered part: a) 12,5x, b) 25x, c) 50x.

Figure 8.18 shows the optical micrographs of polished section of the Mo 82 wt.% - Cu(90)Ni(10) 18 wt.% mixture laser sintered part with the optimized parameters in higher magnification.



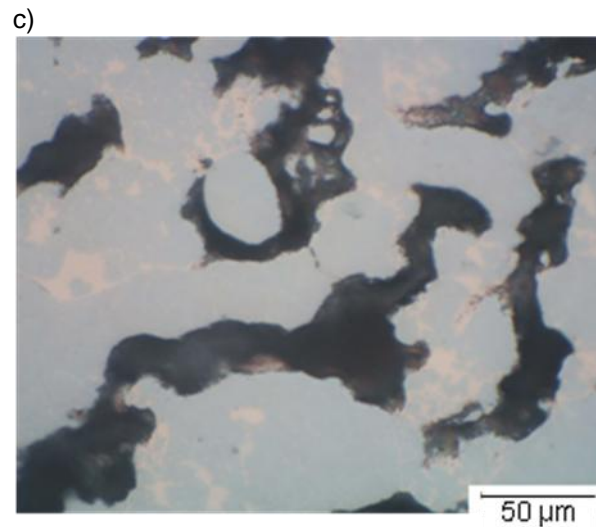


Figure 8.18. Optical micrographs of Mo 82 wt.% - Cu(90)Ni(10) 18 wt.% mixture laser sintered part: a) 12,5x, b) 25x, c) 50x.

When 82 wt.% Mo was used, a poor sinterability with significant agglomeration of Mo particles was obtained (Fig. 8.18) and a large amount of pores. The degree of Mo particle contact increased with increasing Mo content, since it was difficult for the small amount of melted Cu-Ni particles to flow through the contacted Mo particles.

## 8.6 INFLUENCE OF THE AMOUNT OF NICKEL ON THE POROSITY

In order to investigate the influence of the nickel amount in the mixture on the densification process, its amount was varied to more and less than the current amount (10 wt.%) in the mixture, using the most adequate SLS parameters found previously, i.e., layer thickness of 0,02 mm, laser scan speed of 50 mm/s and hatch distance of 0,2 mm.

The SLS parts manufactured with the Mo 63 wt.% - Cu(100) 37 wt.% mixture and with the Mo 63 wt.% - Cu(70)Ni(30) 37 wt.% mixture are shown in Fig. 8.19.

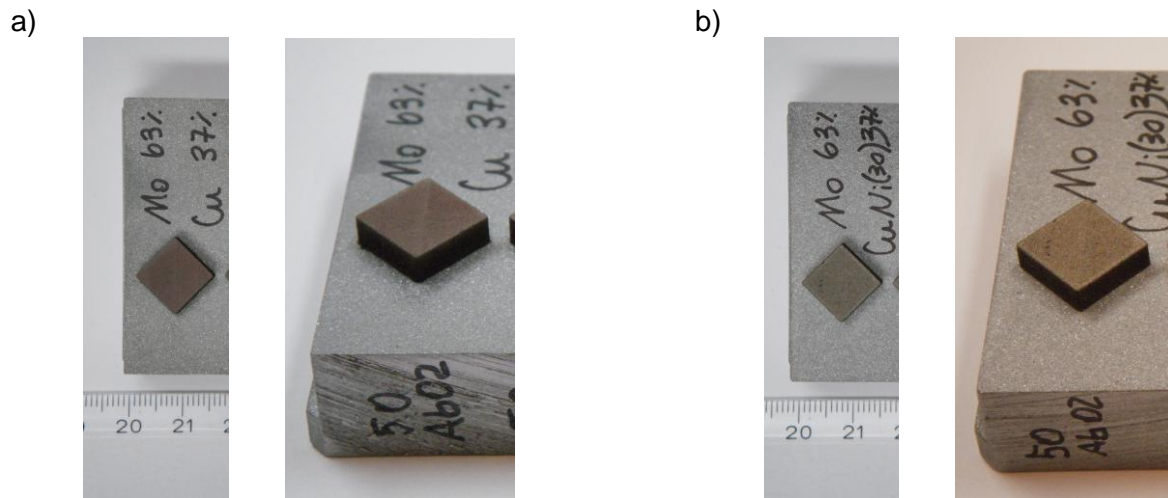
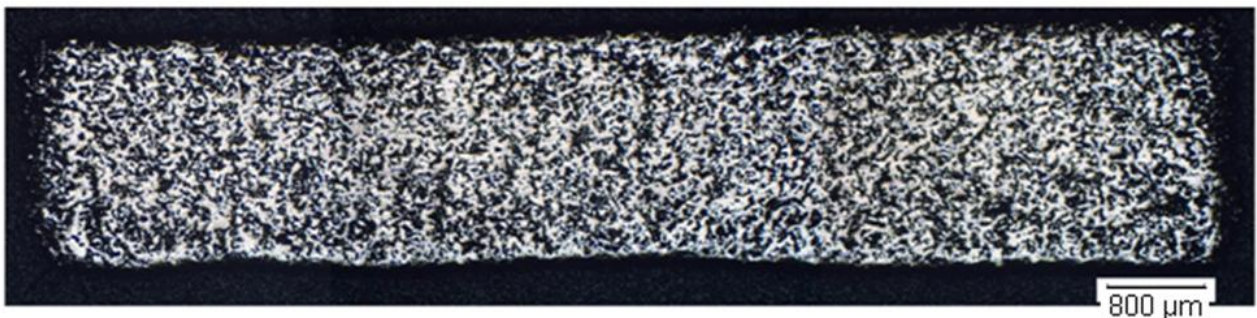


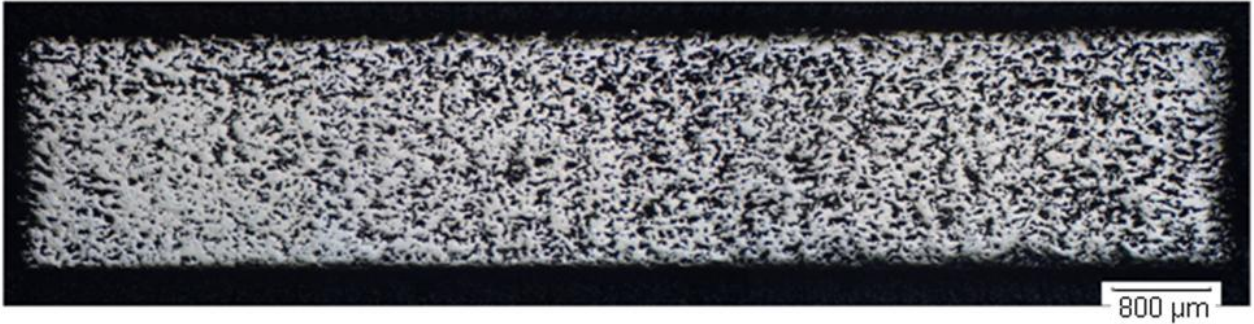
Figure 8.19. SLS parts: a) Mo 63 wt.% - Cu(100) 37 wt.% mixture, b) Mo 63 wt.% - Cu(70)Ni(30) 37 wt.% mixture.

The micrographs of the cross-section of the parts are shown in Fig. 8.20 as well as the micrograph of Mo 63 wt.% - Cu(90)Ni(10) 37 wt.% mixture for comparison. The addition of Ni was suggested in order to enhance the wettability as well as energy absorption of Cu from the laser beam, improving the liquid phase sintering and therefore decreasing the porosity. This can be seen in Fig. 8.20 that shows that there is an improvement in terms of porosity with the increase of the amount of Ni in the Cu-Ni alloy and in Fig. 8.21 that presents the result of the estimated porosity of the cross-section of the parts with the aid of the software.

a)



b)



c)



Figure 8.20. Micrograph of the SLS parts: a) Mo 63 wt.% - Cu(100) 37 wt.% mixture, b) Mo 63 wt.% - Cu(90)Ni(10) 37 wt.% mixture, c) Mo 63 wt.% - Cu(70)Ni(30) 37 wt.% mixture. Magnification 3,2x.

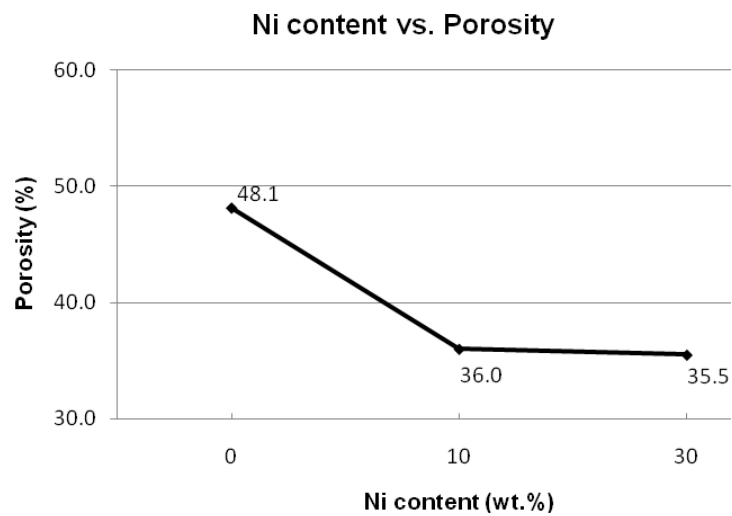


Figure 8.21. Influence of the Ni content on porosity.

Figure 8.22 shows the optical micrographs of polished section of the Mo 63 wt.% - Cu(100) 37 wt.% mixture laser sintered part with the optimized parameters in higher magnification.

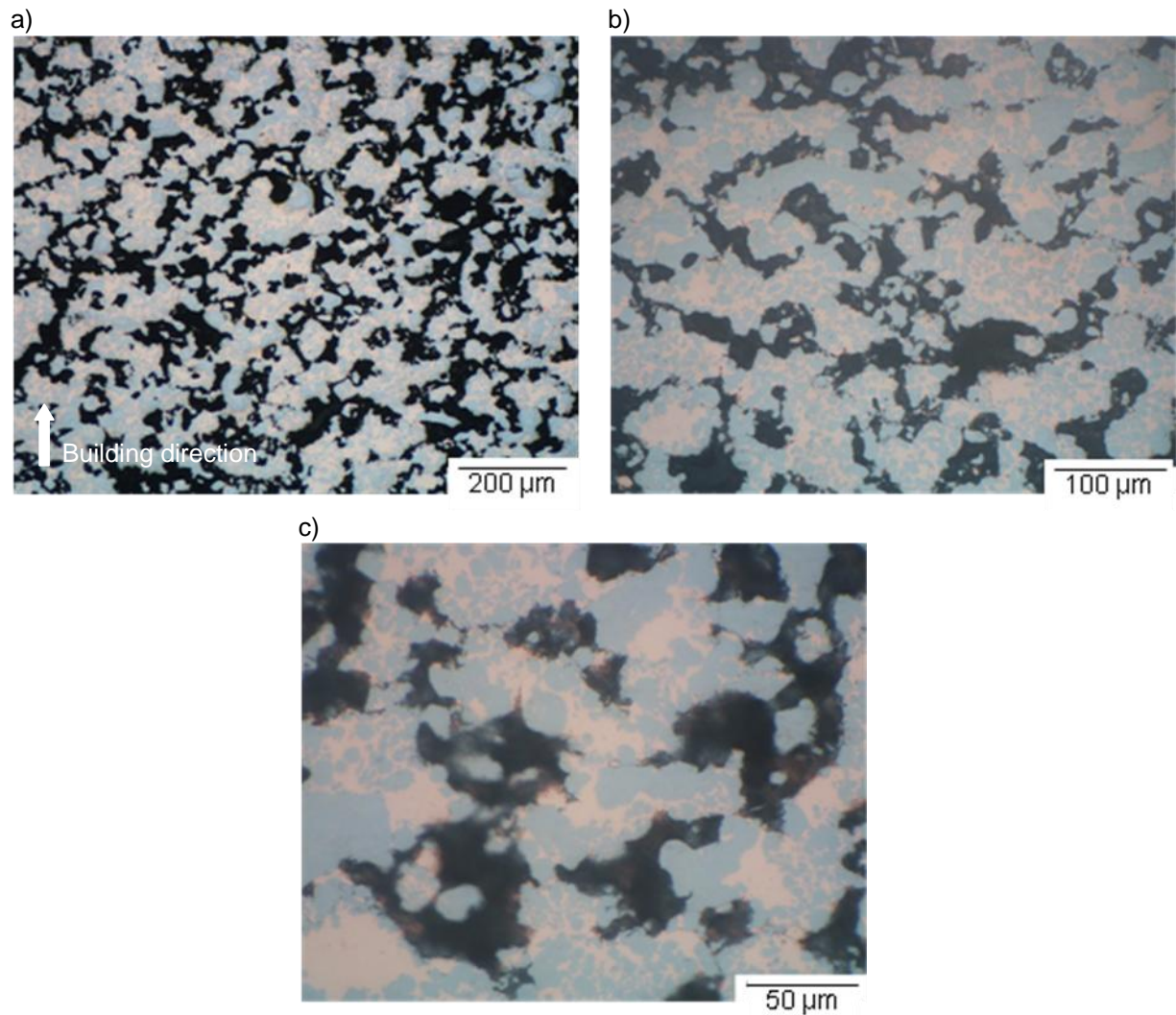


Figure 8.22. Optical micrographs of Mo 63 wt.% - Cu(100) 37 wt.% mixture laser sintered part: a) 12,5x, b) 25x, c) 50x.

Figure 8.23 shows the optical micrographs of polished section of the Mo 63 wt.% - Cu(70)Ni(30) 37 wt.% mixture laser sintered part with the optimized parameters in higher magnification.

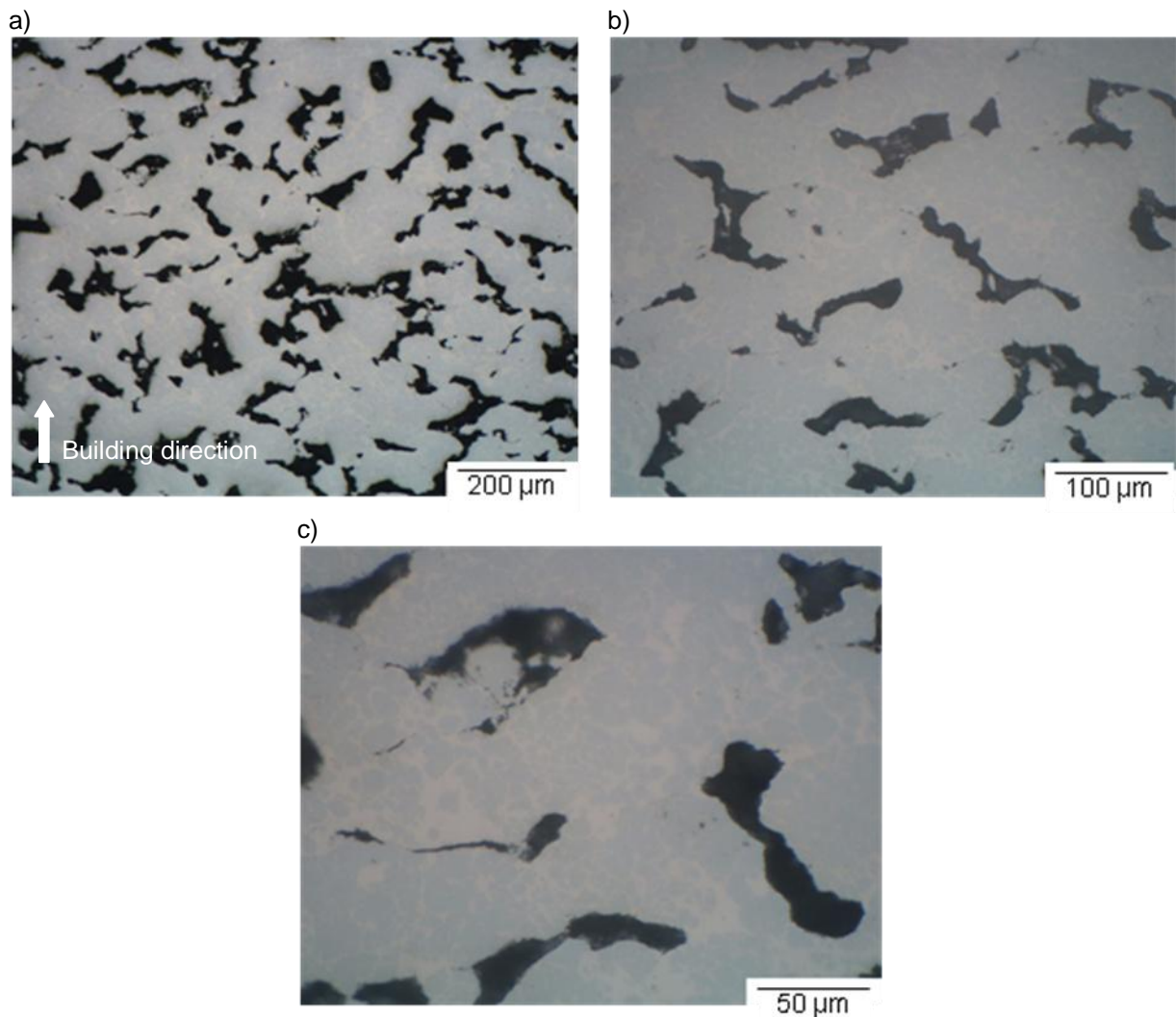


Figure 8.23. Optical micrographs of Mo 63 wt.% - Cu(70)Ni(30) 37 wt.% mixture laser sintered part: a) 12,5x, b) 25x, c) 50x.

Moreover, copper, which is characterized by high thermal conductivity, will increase the heat transfer away from the molten melt pool causing increased solidification rate. With lower Cu content, there is a corresponding decrease in solidification rate and thus prolonged presence of liquid phase (LEONG *et al.*, 2002) as can be seen in Fig. 8.23.

As previously mentioned, the investigation about the production of EDM electrodes by SLS has been carried out by other authors. The porosity is found to be the major problem in the manufacture of the electrodes.

In the work of Dürr, Pilz & Eleser (1999) using Direct Metal Laser Sintering (DMLS) technique and a bronze nickel powder mixture, a minimum porosity of 20 % was achieved. The evaluation of the results showed an increase of the relative electrode wear with rising porosity. An increased porosity means a reduced number of sinter bridges between the bronze coated nickel beads and a smaller firmness of these bridges. The thermal stress by the spark discharge leads during repeated load of the sinter bridges to cracks and thus to a wear of the electrode. The wear increase is larger the smaller the number of sinter bridges and the lower their firmness precipitates. In addition, the analysis of the achieved erosion rates showed a rising material removal rate by a decrease of porosity.

Using a mixture of copper, tin, nickel and phosphorus, Tay & Haider (2001) investigated the EDM electrode production using the DMLS technique. It was concluded that a DMLS electrode without post-treatment could be considered for roughing (although the tool wear rate was high due to the fact that it was soft and with low conductivity, having a low material removal rate), especially where minimal material removal is required and it was found to be unsuitable for finishing operations, as the sintered material was porous and soft.

The material used in the research work of Meena & Nagahanumaiah (2006) was composed by Cu, Ni, Sn and P. Excessive DMLS electrode wear was reported, especially at corners, which limits the use of DMLS tool for EDM machining. The SEM images of DMLS electrode before and after machining indicated that the high porosity (about 20 per cent) was the primary reason for higher electrode wear rate. The corners are subjected to greater wear because more sparks are generated in this area, thus, creating more heat build-up. Another reason could be the low bonding of metal powder particles at the corners (at corners metal powder particles are loosely bonded during laser sintering).

According to Tay & Haider (2001) and Meena & Nagahanumaiah (2006), a DMLS part could become an excellent rapid EDM electrode if some properties of the sintered metal, such as conductivity, surface finish and porosity, can be enhanced. The porosity could be improved by secondary operations like post sintering, infiltration and coating.

Post-treatment can possibly improve the properties of the SLS electrode. For instance, Dürr, Pilz & Eleser (1999) reduced the porosity of the electrodes after the SLS process by infiltration leading to an increase of the relative wear with the increase of the pulse time and/or improving the wear values related to the untreated electrode. In addition, Eubank *et al.* (1998) have developed a new material, ZrB<sub>2</sub>/Cu, to be used as electrodes (the ZrB<sub>2</sub> part was infiltrated with an appropriate copper alloy). The electrodes produced with ZrB<sub>2</sub>/Cu were much superior to pure copper and various graphite's and somewhat better than W-Cu.

Moreover, in the work of Zhao *et al.* (2003) post-treatment was used to improve the strength and density of the part produced with steel, polyester and phosphate material, then the part was infiltrated with copper. The manufactured electrode was not full-dense, but its density was close to that of solid copper and a parametric experiment proved that the wear rate of the electrode approached to that of a general electrode.

In this work, copper-nickel and molybdenum alloy powder material was used in the Selective Laser Sintering process in order to produce electrodes for Electrical Discharge Machining. The minimum porosity achieved was 34 % (estimated porosity), higher than the ones achieved by the other authors. The real value might be less than 34 %, as there is a significant difference when one compares the estimated porosity and the measured porosity. Unfortunately the electrodes have not been tested in an EDM machine yet. After EDM experiments, it will be possible to study the behavior of the copper-nickel and molybdenum alloy sintered electrode regarding material removal rate, surface integrity and electrode wear. After that, a post-treatment might be considered to improve the electrode performance.

## CHAPTER 9

### CONCLUSIONS

In this work, in order to investigate adequate materials to produce EDM electrodes by Rapid Prototyping technology, layer thickness, laser scan speed and hatch distance, as well as metallic matrix composition and percentage of structural material in the mixture were selected as parameters for variation in the experiments.

Selective Laser Sintering was used for the manufacture of a composite system consisting of pre-alloyed Cu-Ni powder, acting as the binder (metallic matrix) and Mo powder, as the structural material. These materials have been chosen due to their characteristics like high thermal and electrical conductivities and high melting point, very interesting to be used as EDM electrodes. The element nickel was added in order to improve densification in SLS process.

Porosity of sintered parts is one of the major problems found when using EDM electrodes manufactured by SLS in terms of electrode wear. In this research work, it was decided to study the effects of variation of SLS process parameters on the porosity of the laser sintered parts.

Microstructures were characterized with the aid of an optical microscope and the following facts can be pointed out:

- Decreasing the layer thickness improved the bonding between sintered layers, decreasing porosity.
- With the decrease of the laser scan speed (higher energy), the porosity slightly decreased.
- Increasing the hatch distance, a more porous part was observed.
- The porosity of the part increased with the increase of Mo in the mixture and a poor sinterability with significant agglomeration of Mo particles was obtained.
- There was an improvement in porosity with the increase of the amount of Ni in the Cu-Ni alloy.

It can be concluded that the SLS process parameters have a great influence on the densification process and that an adequate combination can produce parts with

good quality. The amount of each material in the mixture has a significant influence on the sintered density as well. The energy delivered to the powder bed was enough for liquid phase sintering; still, it was not enough for the melting and connection of all Cu-Ni particles.

## 9.1 DIRECTIONS FOR FUTURE RESEARCH

Other factors that can affect the densification process during SLS could be also investigated:

- Coated particles: the binder material is applied as a coating around the structural material and there is a more effective bonding of the structural particles since the binder material already surrounds all structural particles.
- Particles with different size: in this work the binder material had bigger particles than the structural one. Usually the binder particles are smaller than the structural particles, in order to facilitate their preferential melting.
- Type of laser: the laser absorption of various materials greatly depends on the laser wavelength. Metals absorb much better at short wavelength. This makes Nd:YAG lasers a better choice than CO<sub>2</sub> lasers for metallic materials.

The use of conductive ceramics as structural material for the manufacture of EDM electrodes is very interesting. According to N. Mohri & T. Tani (2006), remarkable innovations have been found in each constituent technology, i.e, electrode materials and structure, target products, gap medium between electrode and workpiece, control system for discharge pulse, and gap servo control. Regarding new materials, the new technologies include: Ti, Si, conductive ceramics, conductive diamond and zinc alloy.

Although the specific properties of most ceramics conflict with technological material requirements for SLS (e.g. low thermal conductivity, high melting point etc.), composites in which ceramic particles are embedded in a metal matrix (binder), can be readily processed by liquid phase SLS using a mixture of ceramics particles that remain

solid throughout the process and metal particles that are melted by the laser (KRUTH *et al.*, 2007).

Finally, post-treatment operations like infiltration and coating could improve the porosity of the sintered parts, as previously discussed in chapter 8.

## 10 REFERENCES

AGARWALA, M.; BOURELL, D.; BEAMAN, J.; MARCUS, H.; BARLOW, J. Direct selective laser sintering of metals. **Rapid Prototyping Journal**, USA, v. 1, n. 1, p. 26–36, 1995.

AgieCharmilles. Available at: [http://www.charmillesus.com/products/edm/When\\_to\\_EDM\\_JULY08.pdf](http://www.charmillesus.com/products/edm/When_to_EDM_JULY08.pdf). Access on: 11 nov. 2009.

AMORIM, F. L. **Tecnologia de Eletroerosão por Penetração da Liga de Alumínio AMP 8000 e da Liga de Cobre CuBe para Ferramentas de Moldagem de Materiais Plásticos**. 2009. 175 f. Tese – Universidade Federal de Santa Catarina, Florianópolis, 2002.

AMORIM, F. L.; LANDIOSI, A. B.; BASSANI, I. A. ELECTRICAL DISCHARGE MACHINING OF TUNGSTEN CARBIDE WITH COPPER-TUNGSTEN ELECTRODES. **Proceedings of COBEM 2009**, Brazil, 2009.

AMORIM, F. L.; WEINGAERTNER, W. L. Influence of Duty Factor on the Die-Sinking Electrical Discharge Machining of High-Strength Aluminum Alloy under Rough Machining. **Journal of the Brazilian Society of Mechanical Sciences**, Brazil, v. XXIV, p. 194-199, 2002.

ARTHUR, A.; DICKENS, P. M.; COBB, R. C. Using rapid prototyping to produce electrical discharge machining electrodes. **Rapid Prototyping Journal**, UK, v. 2, n. 1, p. 4–12, 1996.

BURMAN, R. **Properties and Applications of Molybdenum**. Refractory Metals and Their Industrial Applications. USA: American Society for Testing and Materials, 1984.

CHUA, C. K.; HONG, K. H.; HO, S. L. Rapid Tooling Technology. Part 1. A Comparative Study. **International Journal of Advanced Manufacturing Technology**, Singapore, n. 15, p. 604–608, 1999.

CHUA, C. K.; LEONG, K. F.; LIM C.S. **Rapid Prototyping: Principles and Applications**. 2. ed. Singapore: World Scientific Publishing Co. Pte. Ltd., 2003.

COOPER, K. G. **Rapid Prototyping Technology: Selection and Application**. USA: Marcel Dekker, Inc., 2001.

DAS, S. Physical Aspects of Process Control in Selective Laser Sintering of Metals. **Advanced Engineering Materials**, USA, v. 5, n. 10, p. 701-711, 2003.

DIBITONTO, D. D.; EUBANK, P. T.; PATEL, M. R.; BARRUFET, M. A.. Theoretical models of the electrical discharge machining process I: a simple cathode erosion model. **Journal of Applied Physics**, Texas, v. 66, n. 9, p. 4095-4103, 1989.

DIMLA, D. E.; HOPKINSON, N.; ROTHE, H. Investigation of complex rapid EDM electrodes for rapid tooling applications. **International Journal of Advanced Manufacturing Technology**, UK, n. 23, p. 249–255, 2004.

DOLENC, A. **An Overview of Rapid Prototyping Technologies in Manufacturing**. Helsinki University of Technology, 1994.

DÜRR, H.; PILZ, R.; ELESER, N. S. Rapid tooling of EDM electrodes by means of selective laser sintering. **Computers in Industry**, Germany, n. 39, p. 35–45, 1999.

EL-HOFY, H. **Fundamentals of Machining Processes: conventional and nonconventional processes**. USA: Taylor & Francis Group, 2007.

EOS RP-Tools - Version 4.02. EOS GmbH Electro Optical Systems, 1998.

EUBANK, P. T.; PATEL, M. R.; BARRUFET, M. A.; BOZKURT, B. Theoretical models of the electrical discharge machining process III. The variable mass, cylindrical plasma model. **Journal of Applied Physics**, Texas, v. 73, n. 11, p. 7900-7909, 1993.

EUBANK, P. T.; BRADLEY, W. L.; STUCKER, B. E.; BOZKURT, B.; NORASETTHEKUL, S. A New Electrode Material Resistant to Spark Erosion. Proc. 12th Int. Symp. Electromachining, (ISEM-12), F. Klocke, Ed., Verein Deutscher Ingenieure, Berichte 1405, Dusseldorf, pp. 279-288, 1998.

FREDERICKSON, P. Machining graphite EDM electrodes with high-speed spindles. Nelson Publishing, 2002. Available at: <http://www.entrepreneur.com/tradejournals/article/82756914.html> Access on: 2 sep. 2011.

GEBHARDT, A. **Rapid Prototyping**. Germany: Carl Hanser Verlag, 2003.

GERMAN, R. M. **Liquid Phase Sintering**. USA: Plenum Press, 1985.

GIBSON, I.; ROSEN, D. W.; STUCKER, B. **Additive Manufacturing Technologies: Rapid Prototyping to Direct Digital Manufacturing**. USA: Springer Science+Business Media, 2010.

GRIMM, T. **User's Guide to Rapid Prototyping**. USA: Society of Manufacturing Engineers, 2004.

GU, D; SHEN, Y. Effects of processing parameters on consolidation and microstructure of W–Cu components by DMLS. **Journal of Alloys and Compounds**, China, v. 473, p. 107–115, 2009.

HAGUE, R. **Developments in Rapid Casting**. UK: Professional Engineering Publishing Limited, 2003.

HO, K. H.; NEWMAN, S. T. State of the art electrical discharge machining (EDM). **International Journal of Machine Tools & Manufacture**, UK, n. 43, p. 1287–1300, 2003.

HSU, C. Y.; CHEN, D. Y.; LAI, M. Y.; TZOU, G. J. EDM electrode manufacturing using RP combining electroless plating with electroforming. **International Journal of Advanced Manufacturing Technology**, Taiwan, n. 38, p. 915–924, 2008.

JAMESON, E. C. **Electrical Discharge Machining**. USA: Society of Manufacturing Engineers, 2001.

KARAPATIS, N.P.; GRIETHUYSEN, J.-P.S.; GLARDON, R. Direct rapid tooling: a review of current research. **Rapid Prototyping Journal**, Switzerland, v. 4, n. 2, p. 77–89, 1998.

KECHAGIAS, J.; IAKOVAKIS, V.; KATSANOS, M.; MAROPOULOS, S. EDM electrode manufacture using rapid tooling: a review. **Journal of Materials Science**, Greece, n. 43, p. 2522–2535, 2008.

KERN, R. Sinker electrode material selection. EDM Today Magazine, July/August 2008.

KOENIG, W. Experimental Study of the Basic Process Mechanism for Direct Selective Laser Sintering of Low-Melting Metallic Powder. **Annals of the CIRP**, Korea, v. 46, n. 1, p. 127-130, 1997.

KRUTH, J.-P.; MERCELIS, P.; VAN VAERENBERGH, J.; FROYEN, L.; ROMBOUTS, M. Binding mechanisms in selective laser sintering and selective laser melting. **Rapid Prototyping Journal**, Belgium, v. 11, n. 1, p. 26-36, 2005.

KRUTH, J.-P.; LEVY, G.; KLOCKE, F.; CHILDS, T.H.C. Consolidation phenomena in laser and powder-bed based layered manufacturing. **Annals of the CIRP**, Belgium, v. 56, n. 2, p. 730-759, 2007.

KRUTH, J.P.; WANG, X.; LAOUI, T.; FROYEN, L. Lasers and materials in selective laser sintering. **Assembly Automation**, Belgium, v. 23, n. 4, p. 357-371, 2003.

KRUTH, J. P.; LEU, M. C.; NAKAGAWA, T. Progress in Additive Manufacturing and Rapid Prototyping. **Annals of the CIRP**, Belgium, v. 47, n. 2, p. 525-540, 1998.

KUNIEDA, M.; LAUWERS, B.; RAJURKAR, K. P.; SCHUMACHER, B. M. Advancing EDM through Fundamental Insight into the Process. **CIRP Annals - Manufacturing Technology**, Japan, v. 54, n. 2, p. 64-87, 2005.

LEONG, C.C.; LU, L.; FUH, J.Y.H.; WONG, Y.S. In-situ formation of copper matrix composites by laser sintering. **Materials Science and Engineering A**, Singapore, v. 338, p. 81-88, 2002.

LEPORA, N. **The Elements**: Molybdenum. USA: Marshall Cavendish Corporation, 2007.

LOPES, A.; RICHARDT, N. F. **Normalização de trabalhos técnico-científicos / Sistema Integrado de Bibliotecas da PUCPR**. Curitiba, 2009. Available at:

<[http://www.pucpr.br/biblioteca/sibi/manual\\_normas2009.pdf](http://www.pucpr.br/biblioteca/sibi/manual_normas2009.pdf)>. Access on: 30 nov. 2009.

LÜ, L.; FUH, J.; WONG, Y.-S. **Laser-induced Materials and Processes for Rapid Prototyping**. USA: Kluwer Academic Publishers, 2001.

MatWeb. Available at: <<http://www.matweb.com>>. Access on: 22 nov. 2010.

MEENA, V. K.; NAGAHANUMAIAH. Optimization of EDM machining parameters using DMLS electrode. **Rapid Prototyping Journal**, India, v. 12, n. 4, p. 222–228, 2006.

MOHRI, N.; TANI, T. Recent evolution of electrical discharge machining. **Proceedings of the Second International Conference on Multi-Material Micro Manufacture**, Japan, p. 23-26, 2006.

OZGEDIK, A.; COGUN, C. An experimental investigation of tool wear in electric discharge machining. **International Journal of Advanced Manufacturing Technology**, Turkey, n. 27, p. 488–500, 2006.

PALM, W. Rapid Prototyping Primer. Penn State College of Engineering, 2002. Available at: <<http://www.me.psu.edu/lamancusa/rapidpro/primer/chapter2.htm>>. Access on: 27 may 2010.

PHAM, D. T.; DIMOV, S. S.; BIGOT, S.; IVANOV, A.; POPOV, K. Micro-EDM—recent developments and research issues. **Journal of Materials Processing Technology**, UK, v. 149, p. 50–57, 2004.

RAO, P. N. **Manufacturing Technology: Metal Cutting & Machine Tools**. 2.ed. India: Tata McGraw-Hill Publishing Company Limited, 2009.

RENNIE, A. E. W.; BOCKING, C. E.; BENNETT, G. R. Electroforming of rapid prototyping mandrels for electro-discharge machining electrodes. **Journal of Materials Processing Technology**, UK, n. 110, p. 186-196, 2001.

ROSOCHOWSKI, A.; MATUSZAK, A. Rapid tooling: the state of the art. **Journal of Materials Processing Technology**, UK, n. 106, p. 191-198, 2000.

SCHLESINGER, M. Electrochemistry Encyclopedia. 2002. Available at: <<http://electrochem.cwru.edu/encycl/>>. Access on: 16 jun. 2010.

SEMON, G. A Practical Guide to Electro-Discharge Machining, 2. ed., Ateliers des Charmilles, Geneva, chapter 9, p. 63-76, 1975.

SHAN, Z.; YAN, Y.; ZHANG, R.; LU, Q.; GUAN, L. Rapid Manufacture of Metal Tooling by Rapid Prototyping. **International Journal of Advanced Manufacturing Technology**, China, n. 21, p. 469–475, 2003.

SIMCHI, A. Direct laser sintering of metal powders: Mechanism, kinetics and microstructural features. **Materials Science and Engineering A**, Iran, v. 428, p. 148–158, 2006.

SOMMER, C. EDM electrodes--a matter of choosing wisely: different materials affect machining. (EDM Feature). Tooling & Production. Nelson Publishing, 2001. HighBeam Research. 15 Apr. 2010 <<http://www.highbeam.com>>.

TANG, Y.; FUH, J.Y.H.; LU, L.; WONG, Y.S.; LOH, H.T.; GUPTA, M. Formation of electrical discharge machining electrode via laser cladding. **Rapid Prototyping Journal**, Singapore, v. 8, n. 5, p. 315–319, 2002.

TAY, F. E. H.; HAIDER, E. A. The Potential of Plating Techniques in the Development of Rapid EDM Tooling. **International Journal of Advanced Manufacturing Technology**, Singapore, n. 18, p. 892–896, 2001.

TOLOCHKO, N. K.; LAOUI, T.; KHLOPKOV, Y. V.; MOZZHAROV, S. E.; TITOV, V. I.; IGNATIEV, M. B. Absorptance of powder materials suitable for laser sintering. **Rapid Prototyping Journal**, Belarus, v. 6, n. 3, p. 155-161, 2000.

TOLOCHKO, N.; MOZZHAROV, S.; LAOUI, T.; FROYEN, L. Selective laser sintering of single- and two-component metal powders. **Rapid Prototyping Journal**, Belarus, v. 9, n. 2, p. 68-78, 2003.

VENUVINOD, P. K.; MA, W. **Rapid Prototyping: Laser-based and Other Technologies**. USA: Kluwer Academic Publishers, 2004.

WEISS, L. E. Processes Overview. In: Rapid Prototyping in Europe and Japan - VOLUME I. ANALYTICAL CHAPTERS. p. 5-20, 1997.

WOHLERS, T. Advances in Rapid Technologies Worldwide. 1999. Available at: <<http://www.wohlersassociates.com/euromold.htm>>. Access on: 27 may 2010.

YANG, B.; LEU, M. C. Integration of Rapid Prototyping and Electroforming for Tooling Application. **Annals of the CIRP**, USA, v. 48, n. 1, p. 119-122, 1999.

YARLAGADDA, P. K. D. V.; CHRISTODOULOU, P.; SUBRAMANIAN, V.S. Feasibility studies on the production of electro-discharge machining electrodes with rapid prototyping and the electroforming process. **Journal of Materials Processing Technology**, Australia, n. 89–90, p. 231–237, 1999.

YIH, P., CHUNG, D. D. L. A comparative study of the coated filler method and the admixture method of powder metallurgy for making metal–matrix composites. **Journal of Materials Science**, USA, n. 32, p. 2873–2882, 1997.

ZHAO, J.; LI, Y.; ZHANG, J.; YU, C.; ZHANG, Y. Analysis of the wear characteristics of an EDM electrode made by selective laser sintering. **Journal of Materials Processing Technology**, China, n. 138, p. 475–478, 2003.

ZHU, H.H.; LU, L.; FUH, J.Y.H. Influence of binder's liquid volume fraction on direct laser sintering of metallic powder. **Materials Science and Engineering A**, Singapore, v. 371, p. 170-177, 2004.

## APPENDIX 1. SELECTIVE LASER SINTERING MACHINE

The EOSINT M 250 X<sup>tended</sup> is a Selective Laser Sintering machine that uses a 200 W CO<sub>2</sub> laser, nitrogen atmosphere, works with a temperature of 80°C on the working platform, with a laser spot size of 0,4 mm and a heat affected zone by the laser beam of 0,6 mm. The machine is presented in Fig. A.1.



Figure A.1. EOSINT M 250 X<sup>tended</sup>.

Figure A.2 shows the frontal components in detail of the sintering machine.

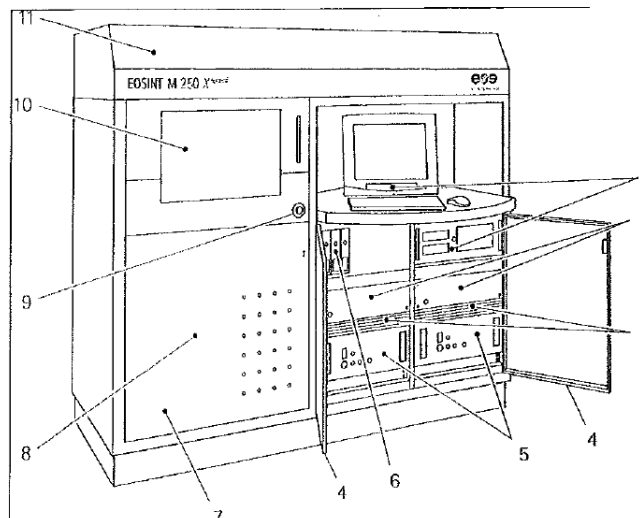


Figure A.2. Frontal components.

- 1 - Computer with CPU, monitor, keyboard and mouse;
- 2 - Laser power source;
- 3 - Directional fans for ventilation;
- 4 - Right frontal door;
- 5 - HF generator for the laser device;
- 6 - Motors-Amplifiers;
- 7 - Left frontal door;
- 8 - Elevation system, dosage platforms and Z axis assembly and storage tank of excess powder;
- 9 - Emergency shutdown button;
- 10 - Processing chamber;
- 11 - Cover that access the laser.

The components in the back of the SLS machine can be seen in Fig. A.3 and A.4.



Figure A.3. Components of the sintering machine.

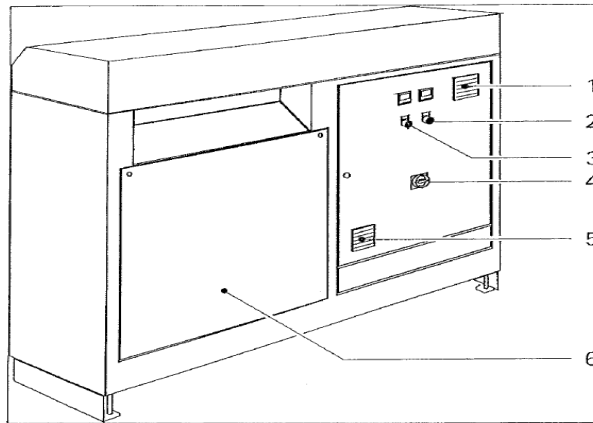


Figure A.4. Components specification.

- 1 - Fan grade;
- 2 - Electrical system shutdown button;
- 3 - Power on electrical system;
- 4 - Main switch;
- 5 - Fan grade;
- 6 - Nitrogen generator rear cover.

Figures A.5 e A.6 show the internal frontal components of the machine.



Figure A.5. Sintering machine internal components.

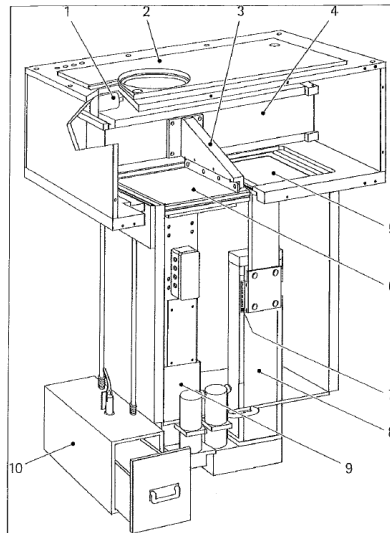


Figure A.6. Sintering machine internal components specification.

- 1 - X axis motor;
- 2 - Optical components refrigeration unit;
- 3 - Sweeper;
- 4 - Band of scrolling cover;
- 5 - Dosage platform;
- 6 - Building platform;
- 7 - Indicator of powder amount;
- 8 - Dosage platform Z axis;
- 9 - Building platform Z axis;
- 10 - Storage tank of excess powder.

The top part of the machine is shown in Fig. A.7 and A.8, where all the laser components are located.



Figure A.7. Sintering machine internal laser components.

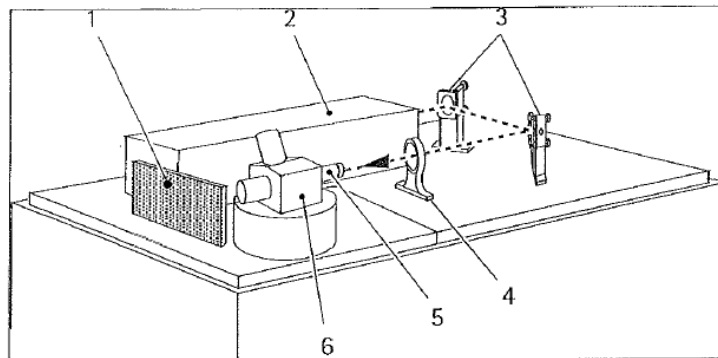


Figure A.8. Sintering machine internal laser components specification.

- 1 - Laser control circuit;
- 2 - Laser with integrated shutter;
- 3 - Deflection mirrors;
- 4 - Diverging lens;
- 5 - Focus lens;
- 6 - Scanner head.

For the laser refrigeration there is an appropriate cooling central, due to the high temperatures reached.

If it's necessary, the finishing machine can be used, in order to reach a better surface quality. Compressed air together with small nutshell spheres is used to decrease the surface integrity. Figure A.9 shows the finishing machine.



Figure A.9. Finishing machine.